

CONTAINS COLOUR PLATES
AT BACK.

I.O.S.

**KING'S TROUGH FLANK: GEOLOGICAL AND GEOPHYSICAL
INVESTIGATIONS OF ITS SUITABILITY FOR HIGH-LEVEL
RADIOACTIVE WASTE DISPOSAL**

BY

**R.B. KIDD, R.C. SEARLE,
P.P.E. WEAVER, C.L. JACOBS, Q.J. HUGGETT,
M.J. NOEL AND P.J. SCHULTHEISS**

REPORT NO. 166

**OCEAN DISPOSAL OF HIGH LEVEL RADIOACTIVE WASTE
A RESEARCH REPORT PREPARED FOR THE DEPARTMENT
OF THE ENVIRONMENT**

**NATURAL ENVIRONMENT
INSTITUTE OF OCEANOGRAPHIC
SCIENCES
RESEARCH COUNCIL**

INSTITUTE OF OCEANOGRAPHIC SCIENCES

Wormley, Godalming,
Surrey, GU8 5UB.
(0428 - 79 - 4141)

(Director: Dr. A.S. Laughton FRS)

Bidston Observatory,
Birkenhead,
Merseyside, L43 7RA.
(051 - 653 - 8633)

(Assistant Director: Dr. D.E. Cartwright)

Crossway,
Taunton,
Somerset, TA1 2DW.
(0823 - 86211)

(Assistant Director: M.J. Tucker)

When citing this document in a bibliography the reference should be given as

KIDD, R.B., SEARLE, R.C., WEAVER, P.P.E., JACOBS, C.L.,
HUGGETT, Q.J., NOEL, M.J. & SCHULTHEISS, P.J. 1983
King's Trough Flank: geological and geophysical
investigations of its suitability for high-level
radioactive waste disposal.
Institute of Oceanographic Sciences, Report,
No. 166, xii + 99pp.

INSTITUTE OF OCEANOGRAPHIC SCIENCES

WORMLEY

King's Trough Flank: geological and geophysical
investigations of its suitability for high-level
radioactive waste disposal

by

R.B. Kidd, R.C. Searle,
P.P.E. Weaver, C.L. Jacobs, Q.J. Huggett,
M.J. Noel and P.J. Schultheiss

I.O.S. Report No. 166

1983

DEPARTMENT OF THE ENVIRONMENT

RADIOACTIVE WASTE MANAGEMENT RESEARCH PROGRAMME 198/8

DoE Report No.: DoE/RW/83.160

Contract Title: DoE selection and evaluation of sites for the disposal of High Level Radioactive Waste

DoE Reference: DGR 481/179

Report Title: King's Trough Flank: Geological and Geophysical investigations of its suitability for high-level radioactive waste disposal.

Authors: KIDD, R.B., SEARLE, R.C., WEAVER, P.P.E., JACOBS, C.L., HUGGETT, Q.J., NOEL, M.J., and SCHULTHEISS, P.J.

Date of submission to DoE: 23 June 1983

Period covered by report: September 1979 to December 1982.

ABSTRACT

The King's Trough Flank study area in the Northeast Atlantic Ocean was chosen in 1979 as a location at which to examine the suitability of pelagic carbonate sequences for sub-seabed disposal of high-level radioactive waste. This report summarises investigations up to the end of 1982; following visits by four research ships to the area during which geophysical data and sediment samples were collected. The region is a characteristically rugged portion of the deep ocean floor with hills and scarps 10 to 30 km apart and slopes around the hills ranging from 18° to 30°. Areas of relatively smooth seafloor occur, however, up to 35 km across, where slopes no greater than 2° are recorded. At this stage an apparent discrepancy between the geophysical and sediment core data leaves some uncertainty regarding the stability of the sediment cover and the likelihood of current erosion in these areas. The general suitability of the area is discussed by comparing our present geological and geophysical data with the set of "desirable characteristics" for a sub-seabed disposal site first outlined in 1979. The difficulties involved in extrapolating findings from presently-sampled depths of up to 10 metres to depths envisaged for shallow waste disposal are emphasised.

Keywords: Disposal under deep ocean bed (94)
Site selection (104)
Geology (110)

This research has been carried out under contract for the Department of the Environment, as part of its radioactive waste management research programme. The results will be used in the formulation of Government policy but, at this stage, they do not necessarily represent Government policy.



CONTENTS		<u>Page</u>
1.	Introduction	1
	(a) Scope of the Report	1
	(b) History of Investigation	1
2.	Regional Setting	8
3.	Geophysical Surveys	14
	(a) Gross Morphology	14
	(b) Sediment Thickness	15
	(c) Microtopography	20
4.	Sedimentology and Stratigraphy	30
	(a) Location of Cores	30
	(b) Lithologies	35
	(c) Micropalaeontology	42
	(d) Oxygen Isotope Measurements	47
	(e) Paleomagnetic Measurements	50
	(f) Stratigraphy	51
	(g) Volcanic Ash Distribution	58
	(h) Glacial Erratics and Ice-rafted Sand Distribution	59
5.	Physical Properties of the Sediments	67
	(a) Consolidation and Permeability Characteristics	67
	(b) Heat Flow Data	70
6.	Discussion	75
	(a) Apparent Conflict between the Geophysical Survey and Sediment Core Studies	75
	(b) General Suitability of the King's Trough Flank Area for Deep or Shallow Disposal	76
	(c) Future Research Needs	81
7.	Conclusions	82
8.	Acknowledgments	82
9.	References	83
10.	Appendices	
	Appendix I Geophysical data charts for the KTF study area held at IOS (to December 1982).	91
	Appendix II Photographs of split sections of the KTF piston cores: 82PCS01, 82PCS02, and 82PCS04.	93
	Appendix III Sub-samples taken from the KTF cores.	97
	Appendix IV Grain-size results from KTF gravity cores analysed at IOS Taunton.	98

FIGURE CAPTIONS

		<u>Page</u>
<u>Figure 1.</u>	Location of the King's Trough Flank (KTF) study area (shaded box); bathymetric contours at 1000-metre intervals.	2
<u>Figure 2.</u>	Geophysical profiling tracks over KTF; thickened track lines represent the three survey cruises since 1979; A and B refer to tracks in Figure 3; B ⁱ to B ⁱⁱ is shown in Figure 41.	3
<u>Figure 3.</u>	Pre-1979 seismic reflection profiles of the KTF study area taken in a NNE-SSW direction; see Figure 2 for locations of tracks.	5
<u>Figure 4.</u>	West to east seismic reflection profiles over KTF taken during Discovery cruise 118 in 1981; see Figure 2 for location; the western area of interest designated after that cruise is marked.	6
<u>Figure 5.</u>	Bathymetry of the KTF study area; contours in 100-metre intervals; outline of GLORIA coverage used for control is shown with a thin box-shaped outline.	9
<u>Figure 6.</u>	Magnetic anomaly chart for KTF, modified from Roberts and Jones (1979); stippled areas represent positive anomalies (>100 gammas); contours in 100-gamma intervals; dashed line is the proposed trace of a transform fault.	10
<u>Figure 7.</u>	Depth-to-basement map (two-way travel time from sea surface to basement) for the KTF study area; isochrons in 200 m/s intervals; thin box outline shows GLORIA coverage; dashed isochrons inferred from bathymetry where seismic profiles are lacking.	16
<u>Figure 8.</u>	Sediment thicknesses on the KTF study area; isopachs in 200 m/s intervals uncorrected two-way travel time; thin box outline shows GLORIA coverage; faults are indicated from sonograph interpretation (Figure 16); rock outcrop is stippled.	17
<u>Figure 9.</u>	Selected graphic seismic reflection profiles projected along track; vertical exaggeration 8.5 to 1; angle of projection is zero degrees; the track represents five secs depth in two-way time; RRS "Shackleton"	19

FIGURE CAPTIONS continued:		<u>Page</u>
	core positions are arrowed.	
<u>Figure 10.</u>	Microtopography at KTF: areas of smooth sediment surface with >10 metres relief (shaded); thickened lines are locations along-track of hyperbolae detected by 10-kHz, 2-kHz and 3.5-kHz profiling; contour line is the 3500 metre isobath; box outlines GLORIA coverage.	21
<u>Figure 11.</u>	Example profiles over areas with smooth sediment surfaces.	23
<u>Figure 12.</u>	Example profiles over locations where open hyperbolae were detected: (a) and (b) open hyperbolae interpreted as side echoes from scarp; (c) open hyperbolae of uncertain origin.	24
<u>Figure 13.</u>	Example profiles over locations where close, overlapping hyperbolae with inflexion points at the sediment surface were detected: (a) profile over suspected sediment slump feature near a steep slope; (b) profile over possible sediment slump or erosion feature (no steep slope nearby).	25
<u>Figure 14.</u>	3.5-kHz profile showing fine-scale relief in a 'smooth area' with a channel-like feature and a small sediment scarp.	27
<u>Figure 15.</u>	Single NNE-SSW track from the GLORIA sonograph coverage of the western KTF study area: TT is the ship's track, R is the seafloor return on either side of the ship.	28
<u>Figure 16.</u>	Full interpretation of the (overlapping) GLORIA survey of the western part of the KTF study area; dashed box outline shows the portion of the sonograph coverage illustrated in Figure 15.	29
<u>Figure 17.</u>	Locations of sampling and the heat-flow station referred to in this report, bathymetry as in Figure 5; box outline locates GLORIA coverage; circles are piston cores, crosses are gravity cores, the triangle is the dredge station and the inverted triangle is the heat-flow station.	31

FIGURE CAPTIONS continued:		<u>Page</u>
<u>Figure 18.</u>	3.5-kHz high-resolution seismic profiles of the M.V. "TYRO" approach to, and departure from, the piston core sites; horizontal scales vary with ship's speed.	32
<u>Figure 19.</u>	North-south Farnella-9 seismic reflection profile showing the locations of two piston cores: note the draped nature of the acoustic horizons.	34
<u>Figure 20.</u>	Lithologies of gravity cores in the King's Trough region, including cores D9806 and D9812 which were taken to the north of KTF.	36
<u>Figure 21.</u>	Lithologies of piston cores of the KTF study area.	37
<u>Figure 22.</u>	Percentage calcium carbonate contents in the three piston cores. Core correlations are based on lithological, coccolith and oxygen isotope data; stippled areas represent glacial intervals.	39
<u>Figure 23.</u>	Mottling and burrow structures in three piston core sections; for location see Appendix II.	40
<u>Figure 24.</u>	Percentage abundance of selected planktonic foraminiferal species in the gravity cores. Correlations based on oxygen isotope, lithological and coccolith data; stippled areas represent glacial intervals. S = slump unit; R = repenetrated unit; NN20 = stratigraphically older units below hiatuses.	44
<u>Figure 25.</u>	Percentage abundance of sinistrally-coiled <u>Globorotalia truncatulinoides</u> , with oxygen isotope measurements and percentage calcium carbonate in the gravity cores. Symbols and stipple as in Figure 24.	45
<u>Figure 26.</u>	Generalized coccolith distributions through the last 500,000 years, showing how each coccolith interval can be defined against a time scale and how the intervals relate to the oxygen isotope stages.	46
<u>Figure 27.</u>	Oxygen isotope values in piston core 82PCS01. Note correlation of high values with marly intervals in the core. Lithological key as on Figure 21.	49
<u>Figure 28.</u>	Percentage abundance of stratigraphically useful coccoliths in the gravity cores; stippled areas represent glacial intervals.	52

FIGURE CAPTIONS continued:		<u>Page</u>
<u>Figure 29.</u>	Percentage abundance of stratigraphically useful coccoliths in the piston cores; stippled areas represent glacial intervals; correlations are thickened lines.	53
<u>Figure 30.</u>	Shaw diagram showing correlations between the piston cores. Points represent lithological boundaries; boxes represent limits of coccolith correlations, defined by the sample intervals. Box 1 = coccolith interval 1/2 boundary; Box 2 = coccolith interval 2/3 boundary; Box 3 = coccolith interval 3/4 boundary; Box 4 = coccolith interval 4/5 boundary. (See text for explanation.)	55
<u>Figure 31.</u>	Shaw correlation diagram showing correlation of cores S8/79/1 to 3 and S8/79/5 to 8 to core S8/79/4. Dots represent lithological changes; boxes represent distance between samples. Correlations represent: (1) oxygen isotope stage 1/2 boundary; (2) minimum value of 18O during oxygen isotope stage 3; (3) oxygen isotope stage 4/5 boundary; (4) interval of sinistrally coiled <u>G. truncatulinoides</u> ; (5) low percentage of <u>G. bulloides</u> , high percentages of <u>G. inflata</u> and <u>G. ruber</u> ; (6) oxygen isotope stage 5/6 boundary; (7) low percentage of <u>G. inflata</u> during oxygen isotope stage 6; (8) oxygen isotope stage 6/7 boundary. Boxes with opposite shading represent coccolith interval boundaries; (9) extinction point of <u>G. aperta</u> ; (10) interval 1/2 boundary; (11) interval 2/3 boundary; (12) interval 3/4 boundary. (See text for explanation).	56
<u>Figure 32.</u>	Selected electron micrographs of volcanic glass shards from the ash layers in S8/79/1 and 2. All, except S8/79/2 (lower), show pumice shards whose outer surfaces are bubble walls; S8/79/2 (lower) is a large plane shard, possibly a large bubble wall shard; scale bars in microns.	60
<u>Figure 33.</u>	Selected electron micrographs of volcanic glass shards	61

FIGURE CAPTIONS continued:	<u>Page</u>
from the ash cores S8/79/3 and 4; pumice shards (upper) and bubble wall shards (lower); scale bars in microns.	
<u>Figure 34.</u> Locations of stations used in the study of ice-rafted material.	63
<u>Figure 35.</u> Grain-size data from rock dredges: log-normal plot of cumulative number of particles against grain size. The cumulative value decreases exponentially as grain size increases; thus the distribution is a negative exponential function: the change in gradient of the lines at 6-cm diameter indicates that there may be two populations being sampled in the same area. For the latitudes so far examined (45°-57°N) there is no change in the relative frequency of different grain sizes; however, the bulk quantity does vary. The two heavier lines denote the stations for which statistical control was good.	65
<u>Figure 36.</u> Normalised rock-dredge grain size data from stations D9756/9 and D9756/14; heavy line A is the cumulative frequency of particles/sq km. From this, estimates of the number of particles greater than 1.5 cm diameter per sq km can be made: for material >6 cm diameter, dotted line B should be used.	66
<u>Figure 37.</u> Downcore percentages of non-carbonate sand in cores V29/177 and 179 against time; stippled zone is the last glacial period; surface sediments were not recovered (after Ruddiman, 1977).	67
<u>Figure 38.</u> Permeability results of a consolidation test on a marl sample, D10333/7.	69
<u>Figure 39.</u> Schematic diagram showing the model GR12 Heat Flow Probe.	71
<u>Figure 40.</u> Results of three penetrations of the heat flow probe at station D10335; the temperature data are corrected for the effects of frictional heating; for explanation, see text.	73
<u>Figure 41.</u> Discovery Cruise 54 seismic profile of the King's	77

FIGURE CAPTIONS continued:

Page

Trough Complex showing the proposed IPOD drill-site "NA-3A"; for location of the track see Figure 2. In the lower profile, the original (upper) record has been photographically reduced in one plane to remove some of its vertical exaggeration. The figure demonstrates that the apparent ruggedness of such seafloor terrains, compared to land areas, is partly a consequence of the scales used during shipboard recording of profiles.

TABLE CAPTIONS		<u>Page</u>
<u>Table 1.</u>	Station data for cores from the KTF study area that have been analysed at IOS.	33
<u>Table 2.</u>	Estimated ages of oxygen isotope stage boundaries and duration of stages for the late Quaternary (from Kominz <u>et al.</u> , 1979).	48
<u>Table 3.</u>	Sedimentation rates in cm/10 ³ yrs computed from piston cores from the KTF area.	57
<u>Table 4.</u>	Location of dredge and core stations used in the study of glacial erratic and ice-rafted sand distributions.	64

1. INTRODUCTION

1(a) SCOPE OF THE REPORT

This report summarises research to date on one of the areas chosen for regional geological and geophysical studies towards selection of sites for radioactive waste disposal below the ocean floor. 'King's Trough Flank', or 'KTF', is situated around 300 miles northeast of the Azores and 600 miles west of northern Spain, in water depths of about 3500 to 4000 metres (Figure 1). Here we present the findings of four research cruises to the area which extended our knowledge of the regional geology beyond that summarised in Kidd et al. (1982). The latter concentrates upon the geology and formation of the King's Trough complex itself, the chain of roughly parallel deep basins and ridges to the north. Our study area, 'KTF', lies on the south flank of this complex.

The reasons for initial selection of the site for study are outlined in Searle (1979). This report is essentially a regional summary dealing with the whole south flank of King's Trough. We show how our research has gradually concentrated into the most suitable areas as more information has become available. We outline all available geophysical, sedimentological and stratigraphical information for the area as of December 1982 and, in addition, attempt to place the site in the context of what is known of sediment physical properties and heat flow in this open ocean environment. We then discuss and compare the geophysical and geological evidence with a view to assessing the general suitability of the area for deep or shallow disposal. Finally, future research priorities for the area are considered.

1(b) HISTORY OF THE INVESTIGATION

When IOS began research into site selection under the DOE's high-level radioactive waste disposal research programme, a review of available geological and geophysical data from the North Atlantic had been carried out with the aim of identifying areas suitable for further study (Searle, 1979). One of the areas that appeared worth studying was King's Trough Flank (KTF). The area chosen for further study extended from 41° to 43°N, 20° to 23.5°W, although it was subsequently extended to about 24.5°W (Figure 2). It was recognised from the beginning that the area's high latitude and possibly its relatively shallow depth (somewhat less than 4000m) made it a marginal choice in terms of the selection criteria outlined in Hollister et al. (1976) and Searle (1979). Nevertheless it was felt that its proximity to the U.K. outweighed these disadvantages, at least

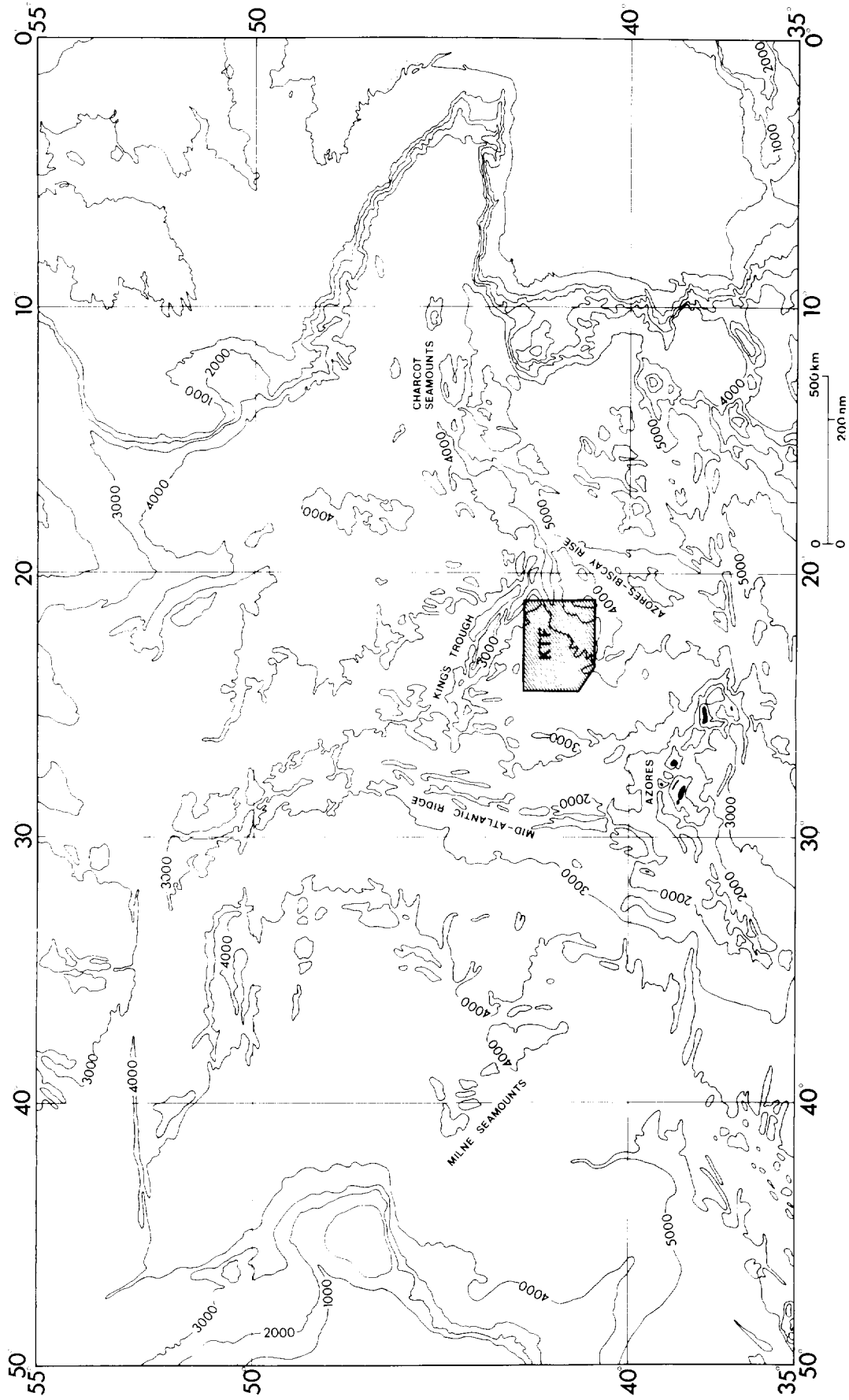


Figure 1. Location of the King's Trough Flank (KTF) study area (shaded box); bathymetric contours at 1000-metre intervals.

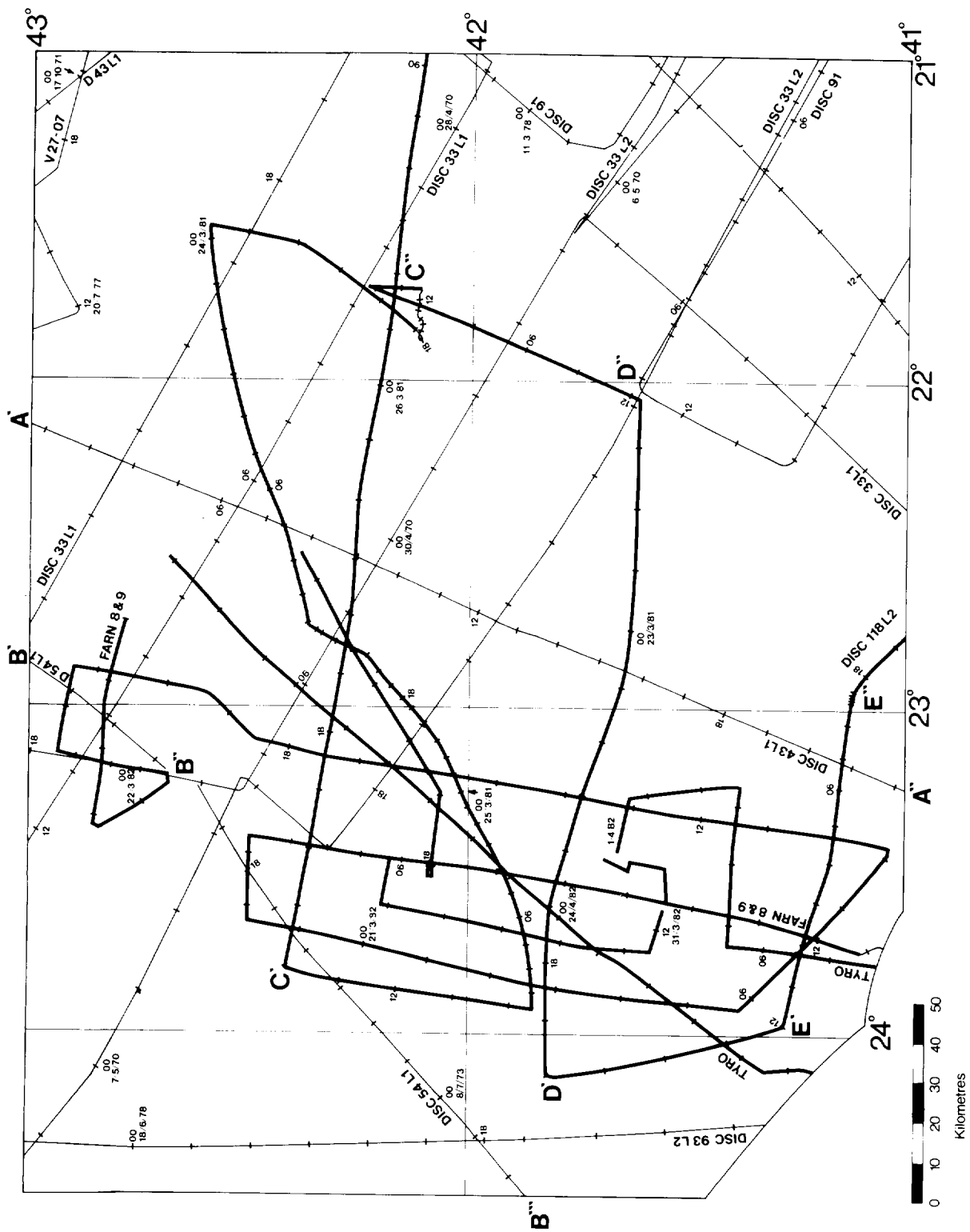


Figure 2. Geophysical profiling tracks over KTF; thickened track lines represent the three survey cruises since 1979; A and B refer to tracks in Figure 3; B1 to B11 is shown in Figure 41.

generic pelagic carbonate sediment environment was concerned.

Seismic reflection and echo-sounder profiles available prior to this study suggested that KTF was an area of extensive sediment cover about a half to one kilometre thick and with major interruptions (scarps or outcrops) on average no closer than 100 km. However, to a large extent these profiles ran parallel to the structural trends so that there was always the possibility that they had missed some major bathymetric features. The few sediment cores in the area consisted of a moderately fine-grained carbonate ooze with a Late Quaternary history of continuous deposition (Buchan et al., 1971; Ruddiman and McIntyre, 1976).

The first sampling undertaken specifically for this project was conducted on Shackleton cruise 8/79 in September 1979 (Francis et al., 1981). Eight gravity cores were taken between 21° and 23°W at sites chosen on the basis of the existing seismic profile coverage. The sites sampled a selection of local environments including topographic highs and lows. In general (though with one or two exceptions) these cores demonstrated a history of uninterrupted sedimentation through the last 200,000 years. This encouraged us to continue investigating the area, the next priority being to extend the coverage of geophysical profiles.

The first opportunity to do this came on Discovery cruise 118 in March 1981 (Francis et al., 1981). Some 600 km of seismic reflection and other geophysical profiles were run, mostly in a WNW-ESE direction perpendicular to the dominant structural trends, between 41.0° and 41.5°N, 20.5° and 24.0° W. These profiles showed a considerably more rugged terrain than had been expected on the basis of the earlier data (Figure 3). The area 41.5° to 42.5°N, 22.0° to 23.0°W proved very rugged, with frequent scarps and outcrops with an average separation of only 10 km (Figure 4, eastern part). There appeared to be a smooth basin approximately 50 km across in the region 41.5° to 42.0°N, 21.5° to 22.0°W, but it was thought this was close enough to the major seamount at 41.4°N, 21.2°W for there to be a risk of sediment instability. The region west of 23°W, therefore, looked the most promising. The new seismic profiles showed a length of over 50 km of seafloor devoid of basement outcrops and with no major seamounts (Figure 4, western part). However, even here there were several sediment-covered ridges and scarps with a relief of around 100m and it was recognised that the stability of the sediment around these features would have to be carefully investigated. A 2-kHz high-resolution seismic profiler was run throughout the Discovery 118 survey and should have enabled a better assessment of the sediment stability to be made. However, the records were so degraded as a result of the bad weather experienced

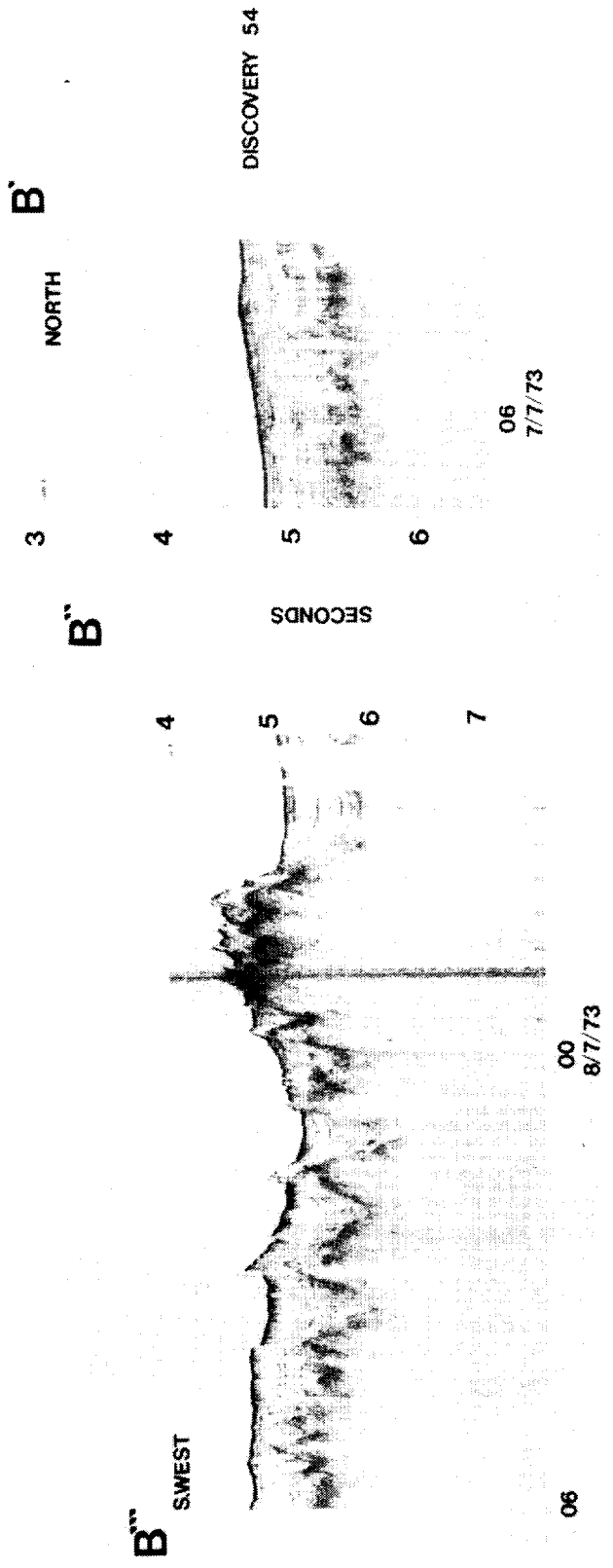


Figure 3. Pre-1979 seismic reflection profiles of the KTF study area taken in a NNE-SSW direction; see Figure 2 for locations of tracks.

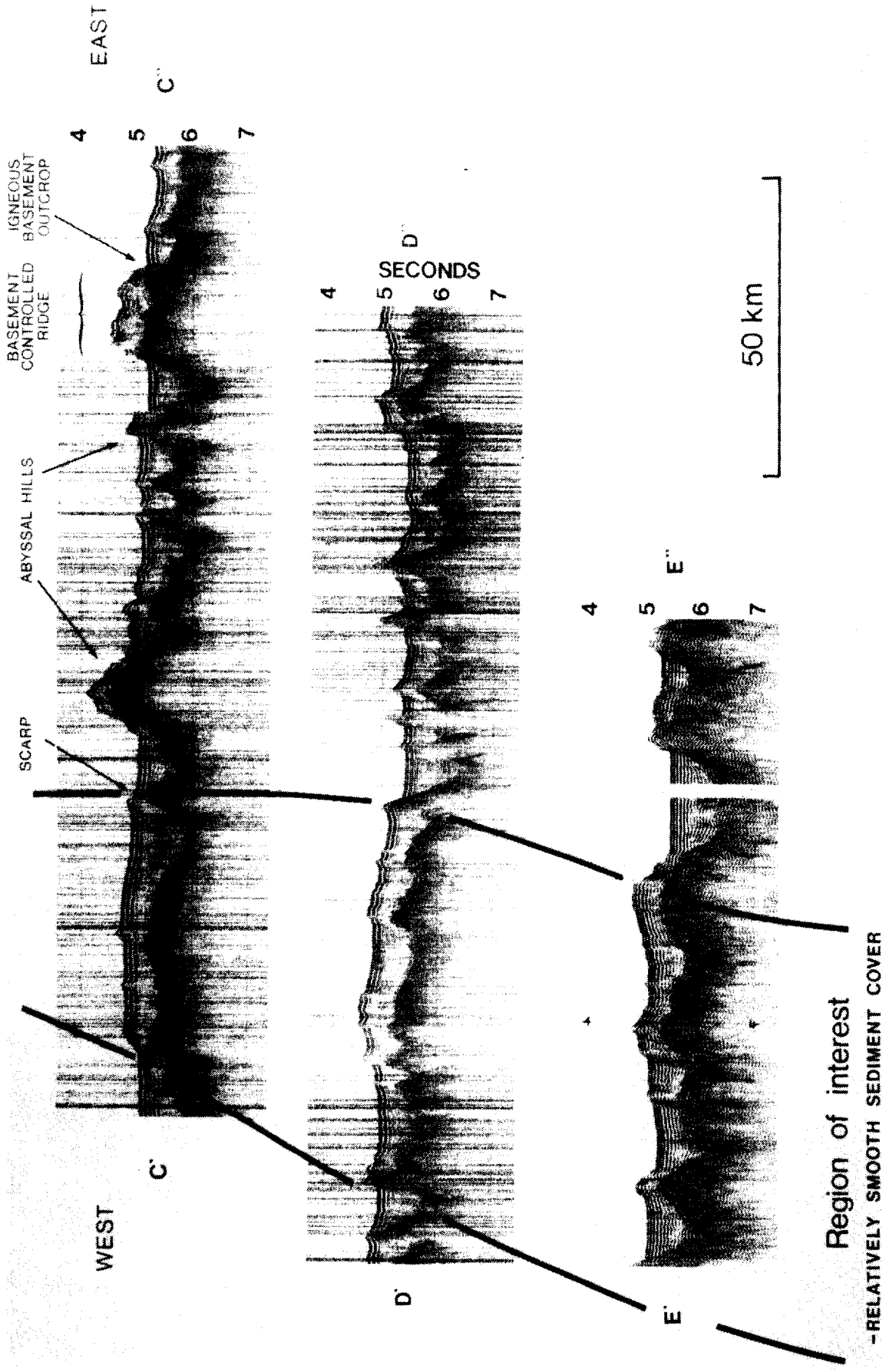


Figure 4. West to east seismic reflection profiles over KTF taken during Discovery cruise 118 in 1981; see Figure 2 for location; the western area of interest designated after that cruise is marked.

during the survey that little additional information could be gleaned from them. The poor weather also prevented most of the planned station work from being carried out, although a Kasten box core was taken for physical properties measurements and a heat flow station was carried out.

In March 1982 the M.V. "Farnella", fitted with the GLORIA long-range sidescan sonar system (Somers et al., 1978; Laughton, 1981) was returning from the Azores to the U.K. The opportunity was therefore taken to run a GLORIA survey over the apparently more promising western part of the Discovery 118 survey area. The sonar results confirmed the presence of scarps and small outcrops with spacings varying from 20 to 50 km throughout the area. Airgun seismic reflection profiles were recorded during the sonar survey and, although the tracks ran parallel to the structural trend, about 50 per cent of the records are characterised by a rather rugged, though sediment-covered, seabed. Much of this rugged topography is associated with the large hill centred near 42.1°N, 23.4°W which lies entirely between the profiles of the Discovery 118 cruise.

The last work covered in this report was carried out in the area by Dutch co-workers aboard M/V "Tyro" en route to and from the Great Meteor East study area in March and April 1982. They collected three piston cores, some watergun seismic reflection profiles and, most important, the first good quality 3.5 kHz records from the KTF study area. These latter records showed still further evidence of rugged topography with frequent small, steep scarps and apparent rock outcrops. The floors of the basins have smoother surfaces but, even there, the seabed rarely extends more than 10 or 20 km without some disturbance by faulting or outcrop.

At this stage it appeared, on the basis of the geophysical evidence (Appendix I), that the KTF area was much less promising as a potential shallow disposal area than had appeared initially in terms of the site selection criteria outlined in Searle (1979). In view of this, it is somewhat surprising that most of the core samples, taken from a variety of different topographic settings within the area, present a story of continuous, undisturbed sediment deposition, at least over the upper ten metres or the last 300 to 400 thousand years. It must be appreciated that the biogenic nature of the calcareous sediments provides the means of determining a very detailed stratigraphy that has a much higher resolution (Weaver, 1981) than any that has currently been achieved in the sediments of the distal abyssal plain study areas (Kuipers, 1981). Some evidence of the sediment instability interpreted from the GLORIA and 3.5 kHz records might be expected in the sediment cores. It was therefore concluded that, in spite of the questions

raised by the geophysical records, more field work is justified to try to reconcile the geophysical and coring results. This detailed work would aim to determine the precise nature and extent of the disturbances (if any) that are suggested by the geophysical profiles.

2. REGIONAL SETTING

The KTF study area is located on the lower eastern flank of the Mid-Atlantic Ridge (Figure 1) in a region characterised by the lineated topography that is typical of such ridge flank environments (Laughton *et al.*, 1975). There is a general regional slope to the south east upon which are superimposed a series of sub-parallel ridges and intervening low areas bounded by scarps and aligned in an approximate 010° direction (Figure 5). The topography to a large extent mirrors the morphology of the acoustic (igneous) basement that was generated at the Mid-Atlantic Ridge (Laughton and Searle, 1980).

This portion of the Mid-Atlantic Ridge flank, however, is not entirely typical. A number of authors have commented upon the symmetrical bulges in the 4000-metre bathymetric contour that occur on either flank of the Mid-Atlantic Ridge between 40° and 47°N. The region is up to a kilometre shallower than would be expected had it subsided normally away from the ridge spreading axis (Searle and Whitmarsh, 1978; Sclater *et al.*, 1975).

The King's Trough Flank study area is located on oceanic crust of predominantly Eocene age (Kidd *et al.*, 1982). An analysis of the magnetic profiling data suggests that one small transform fault may disrupt the igneous basement of the area. Along the southern edge of the area at 41°N, magnetic anomaly 18 (41 Ma, Priabonian stage, on the time-scale of Lowrie and Alvarez, 1981) can be recognised near 24°W, and anomaly 25 (56 Ma Thanetian) passes just to the east of 21°W (Figure 6, modified from Roberts and Jones, 1979). These magnetic anomaly identifications are in agreement with those published by Searle (1977) and Whitmarsh *et al.* (1982). Along the northern edge of the area (43°N), the sequence of anomalies traditionally recognised (e.g. Searle and Whitmarsh, 1978) has been: number 17 (40 Ma, Priabonian) at 23.5°W, number 18 at 23.3°W and numbers 20 to 24 running continuously through the area to terminate between 22.7°W and 21.0°W at 43°N. On this interpretation, anomaly 19 is missing. However, a re-examination of the anomalies, with the addition of new data from Discovery Cruise 118, suggests that a possibly better interpretation is to accept the presence of a small transform fault, with a dextral offset of between 30 and 50 km running WNW-ESE between 42.7°N, 23.4°W, and 42.2°N, 21.3°W. The offset shows up

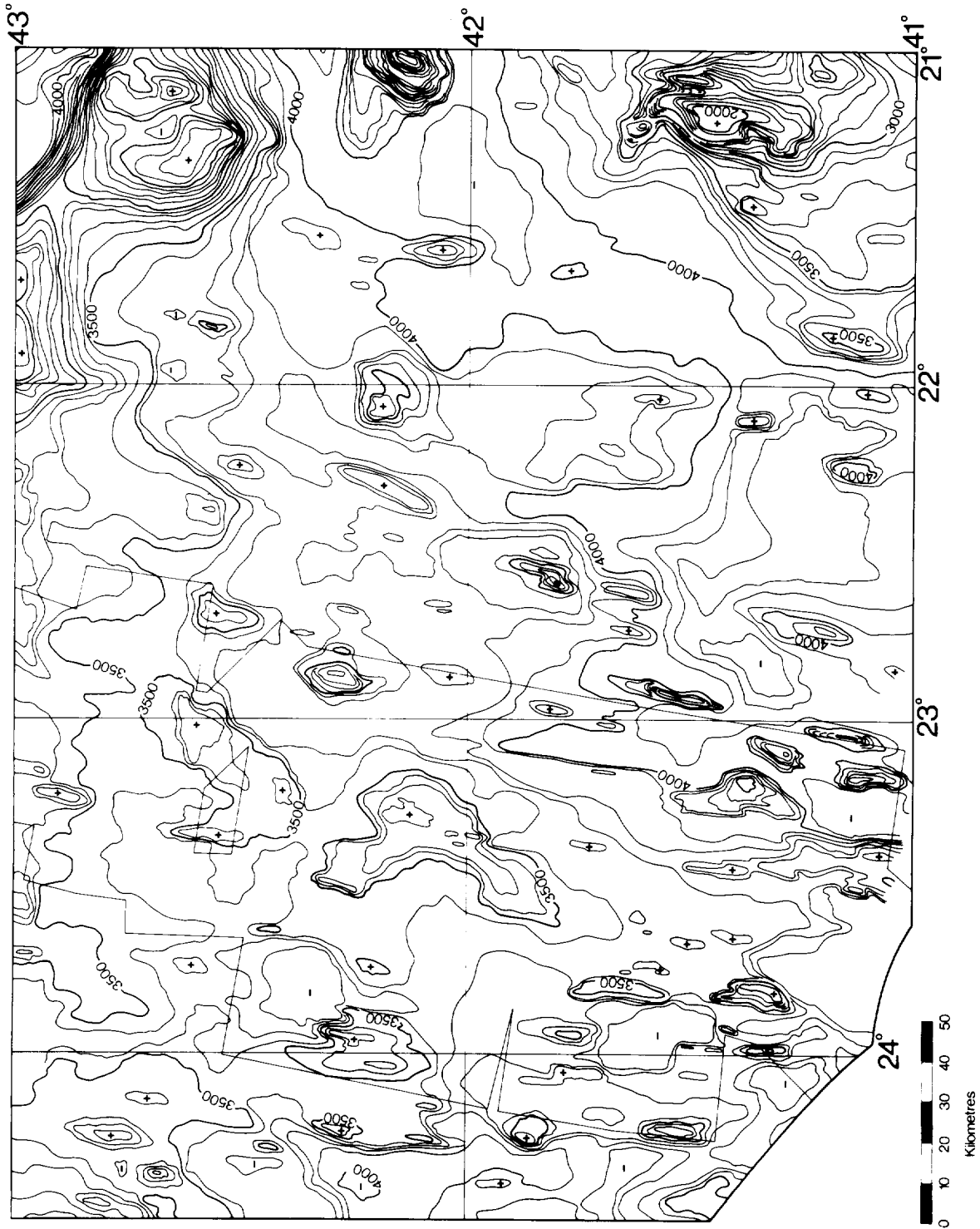


Figure 5. Bathymetry of the KTF study area; contours in 100-metre intervals; outline of GLORIA coverage used for control is shown with a thin box-shaped outline.

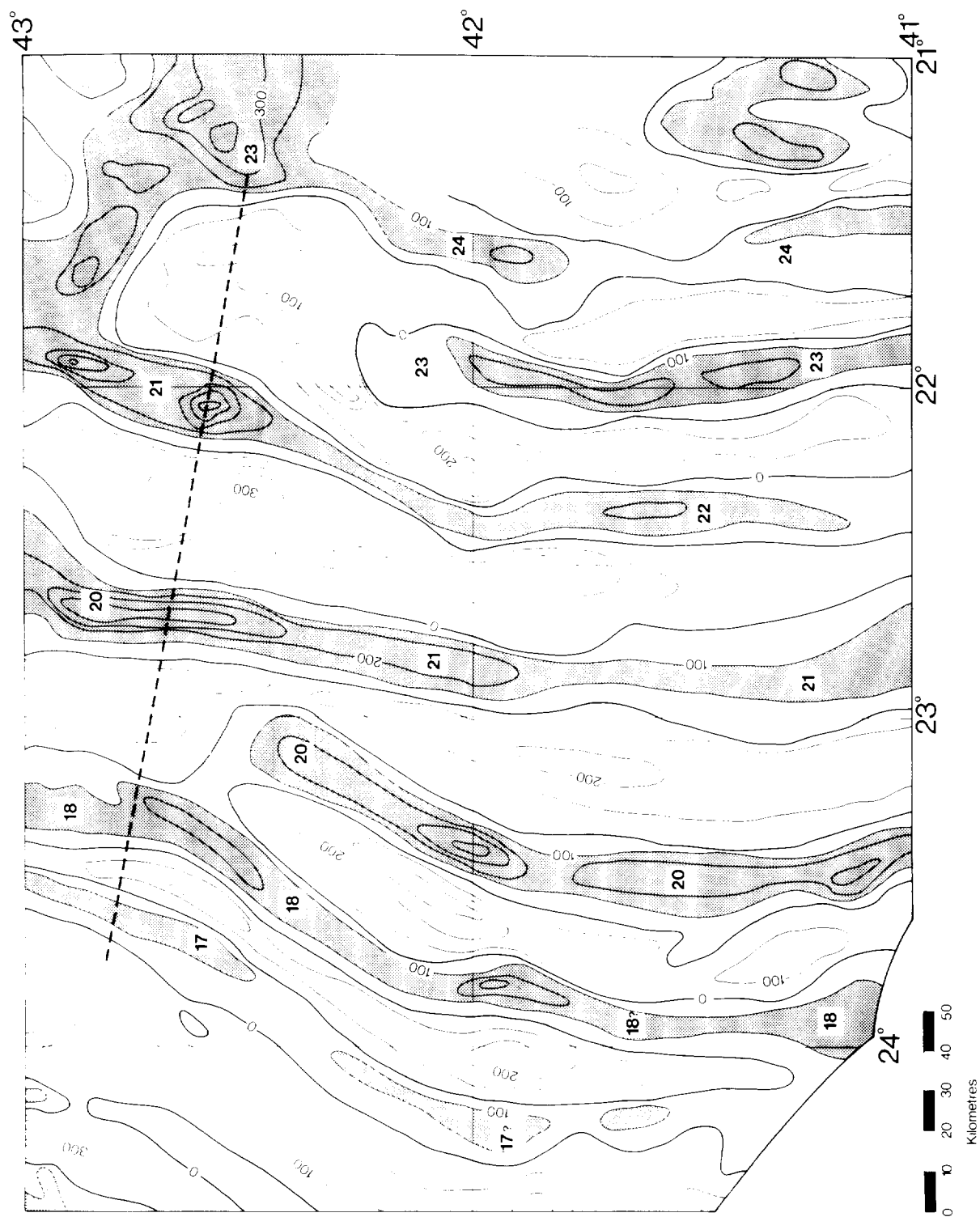


Figure 6. Magnetic anomaly chart for KTF, modified from Roberts and Jones (1979); stippled areas represent positive anomalies (>100 gammas); contours in 100-gamma intervals; dashed line is the proposed trace of a transform fault.

best as a bend in anomaly 18 but is also recognisable in anomalies 20 to 24. Although the magnetic directions appear continuous, anomaly 21 south of the fracture zone (22.8°W) is offset 50 km to the east (22.0°W) north of it. The positive anomaly due north of 21 on the northern side of the fracture zone is actually anomaly 20 (Figure 6). Apart from this one instance, the area appears to be completely free of transform fault zones.

The study area is bounded on three sides by a number of unusual bathymetric features of the Northeast Atlantic Ocean (Figure 1). To the north is the King's Trough Complex itself (Matthews *et al.*, 1969; Searle and Whitmarsh, 1978; Kidd *et al.*, 1982), the Azores Biscay Rise is to the south east (Whitmarsh *et al.*, 1982) and the Azores Platform (Searle, 1977) lies to the southwest. All are anomalously shallow when related to normal subsidence curves for oceanic crust and a number of hypotheses for their individual origins and for the development of this part of the Northeast Atlantic as a whole have been proposed. The scope of these hypotheses extends to the European continental margin, implicating also the anomalously shallow Charcot and Biscay Seamounts (Grimaud *et al.*, 1982) and the North Spanish Trough (Sibuet and Le Pichon, 1971). It has been suggested that a compressive plate boundary may have existed off Northern Spain in Eocene times and that this extended westward via an Azores-Biscay Rise transform fault and a King's Trough compression zone (Vogt and Avery, 1974; Grimaud *et al.*, 1982).

Searle and Whitmarsh (1978) found no evidence of compression nor of significant transform motion at King's Trough and they suggested that this feature, formed from fracturing or rifting along the crest of an aseismic ridge, developed from a hot spot on the Mid-Atlantic Ridge (MAR). A later GLORIA survey along with sampling operations at King's Trough led Kidd *et al.* (1982) to confirm this origin showing that the hot spot began building the aseismic ridge at the MAR prior to 56 million years ago. The ridge was uplifted about 2 km around 32 million years ago and its crest became rifted 16 to 20 million years ago to form the down-dropped central trough, which is presently at a depth of around 4500 metres. Whitmarsh *et al.* (1982), in proposing an origin for the Azores-Biscay Rise (ABR), suggested that it too is an aseismic ridge with a hot-spot origin. The ABR lies opposite a rise feature on the western side of the MAR that includes the Gauss and Milne seamounts. Their model suggests that a regional 'King's Trough High' existed during the development of both the Azores Biscay Rise and King's Trough aseismic ridges. This would explain the overall shallowness of the intervening KTF study area. Conclusions in both Kidd *et al.* (1982) and Whitmarsh

et al. (1982), the most recent regional studies of the area, indicate that the area has been free of major regional tectonic movements since the middle Miocene; that is, the last 11 to 15 million years. What is not clear, however, is whether any local tectonic movements have occurred in the recent geological history of the area such as small-scale movements on basement-controlled faults. Searle (1977) recognised the problem of identifying recent faulting in seismic profiles in an area closer to the Azores, since pelagic, draped sediments will often mirror basement topography in such a way as to make identification of faults in the sediment cover uncertain. This problem was recognised in IOS Report No. 77 (Anonymous, 1978) but, as yet, no deep-towed geophysical surveys and precise core or dredge sampling have been carried out in the KTF study area. Recent reviews of intraplate earthquake activity, which could give an indication of such latent fault movements, suggest that seismicity within the North-east Atlantic region is generally low. Only two earthquake events with magnitudes > 4.5 on the Richter Scale were detected over the period 1964-1969 and a further two over the period 1913-1963 (Lilwall, 1982). One historical event has no assigned magnitude but was located by Lilwall to the northwest of the KTF study area at 44.29°N , 24.86°W .

The KTF study area underlies the present-day northern edge of the Bermuda-Azores high pressure atmospheric system and there is a parallel anti-cyclonic oceanic flow over the area of the southern parts of the North Atlantic Current, the downstream extension of the Gulf Stream (Crowley, 1981). Part of this Current turns northeastwards and part returns as the eastern boundary Portugal and Canary currents. An area of positive temperature anomaly overlies the KTF area, reflecting poleward advection of warm North Atlantic current waters. The trace of the sub-tropical convergence lies close to the area (Sverdrup et al., 1942).

Bottom water circulation over the KTF area is generally considered to be very weak. Data derived from CTD and long-term tide gauge stations suggest average bottom current flows of the order of 1-2 cm per second (Saunders, 1982). Unpublished data from two current meter stations in the southwest of the area measured mean scalar speeds 50 metres above bottom of only 4.1 and 4.7 cm/sec respectively but also maximum hourly speeds of 13.9 and 18.8 cm/sec; values which might be much more significant in terms of sediment erosion at the seafloor (R. Dickson, personal communication).

The oceanographic picture presented above has changed considerably through the glacial cycles of the Pleistocene. McIntyre et al. (1976), through their climate-oriented micropalaeontological studies, showed that the dominant feature

of the North Atlantic winter ocean 18,000 years ago was a steep thermal gradient nearly coincident with latitude 42°N. Its northern boundary (constituting the Polar Front) lay just north of King's Trough along 45°N. The position of the Polar Front remained unchanged during the glacial summers and the surface currents of the subpolar sea exhibited a weakly counter-clockwise rotation. Present day areas of deep water formation in the Norwegian and Labrador Seas were ice-bound and large volumes of deep water for circulation southward were simply not formed. Little exchange of surface with deep water is thought to have occurred around the Polar front so deep circulation over the KTF area is thought to have been sluggish.

Certain features of the KTF study area can now be explained in terms of the recent studies of the region's tectonic and palaeoenvironmental history that were referred to earlier. The area has remained anomalously shallow for a ridge-flank region such that it has never been below the regional carbonate compensation depth (CCD: the depth at which carbonate supply from the surface matches carbonate dissolution and there is no net accumulation of calcareous sediment). Also the 'King's Trough High' has been effectively isolated from any long-range gravity-controlled, turbidite or other bottom-transported sediment supply from the Azores archipelago (Searle, 1978). However, supply of volcanic tephra carried in the prevailing winds from this island chain could be an important sediment source. Overall sediment thickness (see section 3c) is somewhat greater than is typical of similar pelagic carbonate platforms. The regional geological history of the area suggests a number of possible explanations for this:

1. Back-tracking along subsidence curves shows that both the King's Trough and Azores-Biscay rise aseismic ridges were subaerial at some time in their history (Kidd et al., 1982; Whitmarsh et al., 1982), so allowing for a terrigenous, probably volcanoclastic, sediment supply. For example, sediments could have been shed from an exposed Antialtair seamount to the KTF area in the late Oligocene;

less important might be:

2. Higher productivity of carbonate around shoal areas due to local upwelling.
3. Increased supply of ice-rafted sediment, since the polar front lay close to the King's Trough area during the maxima of the Pleistocene glaciations (Ruddiman and McIntyre, 1976; Weaver, 1983).

3. GEOPHYSICAL SURVEYS

3(a) GROSS MORPHOLOGY

The contour chart (Figure 5) presents an up-to-date bathymetry, based upon 10-kHz echo soundings and modified in the west for morphologic trends visible on long-range sidescan sonar (GLORIA) records.

The eastern boundary of the area is dominated by three large seamounts. The large seamount in the northeast quadrant forms a boundary of the southern basin of King's Trough and rises above the regional depth of 3900-4000m, to shallower than 2200m. Seismic reflection profiles show that the seamount is a basement high, draped by a thin sediment cover (approximately 360 metres thick), although on parts of its flanks igneous basement is occasionally exposed. The large seamount in the south-east quadrant forms part of the northern flank of the Azores-Biscay Rise. This, too, rises from a regional depth of 3900-4000m to less than 2000 metres and is draped by a thin sedimentary cover (between 180-540 metres thick). The third seamount, on the eastern boundary of the area, is conical in shape (above 3500m) and rises from a regional depth of more than 4000m to less than 2300m. Seismic reflection and 2-kHz profiles over this seamount show that in depths shallower than 3700m its sedimentary cover is extremely thin or absent altogether. These seamounts generally have slopes of 8-10° (the steepest is 18° at 41.5°N, 21.25°W) and are surrounded by more gently sloping sedimented areas (<2°). The seamounts may have been constructed by Paleogene off-axis volcanism within the 'King's Trough High', such as occurred at King's Trough around 32 million years ago (Kidd et al., 1982).

At ~22°W is a structural high which can be traced from 41.4°N to 42.4°N. This is a major feature which mirrors a basement high. Acoustic (presumed igneous) basement crops out along scarps on its steepest slopes (Figure 4). According to Figure 6 it is within magnetic anomaly 23, indicating a crustal age of 52 million years (Early Eocene).

The maximum depth of over 4300m occurs in the southern part of the area, between 22-23°W, while the shallowest parts are the three large seamounts, noted above. The majority of the study area has a depth range from 3500m to 4000m, deepening towards the southeast, but abyssal hills rising above 3500m occur most frequently in western parts of the study area.

There is a strong linear element to the abyssal hill topography. They strike in a 005° direction subparallel with the trend of the Mid-Atlantic ridge.

The regions situated between and around the abyssal hills have a gently

sloping sediment cover with gradients generally less than 3°. The spacing of the abyssal hills is consistently between 10 and 30 km in a north-south direction. In an east-west direction, the spacing varies greatly from 10 km upwards tending to be further apart with increasing distance from the Mid-Atlantic ridge axis.

The majority of the abyssal hills appear, from the seismic reflection profiles, to be sediment-covered basement highs and vary considerably in size, from less than 10 km² to greater than 100 km² in areal extent and stand 100m to 500m above their surrounding areas.

Should the scarps making up the sides of abyssal hills represent fault locations, their vertical height differences would indicate throws up to 700m. These major scarps are mainly confined to the south western portion of the area. There is some indication in the bathymetry of the proposed transform fault (which offsets the magnetic anomalies horizontally at around 42°30'N) in the form of a steep slope between the 3500 and 3800 metre contours.

3(b) SEDIMENT THICKNESS

Depth-to-basement and sediment thickness maps for the KTF study area, shown in Figures 7 and 8 respectively, have been derived from seismic reflection profiles obtained by IOS since 1970. The depth-to-basement map (Figure 7) was constructed by plotting, at six-minute intervals along track, values of the total two-way travel time; that is, the time for sound to travel from source through the water and sediment cover to the acoustic (igneous) basement and back to the ship. The chart was contoured conventionally, using the bathymetric chart (Figure 5) as a guide and, in the western sector, the GLORIA sonographs helped to define areas of probable igneous basement outcrop.

The sediment thickness map (Figure 8) was constructed in a similar way to the depth-to-basement map, with the values being plotted every six minutes along track. Sediment thickness is taken as the travel time from the surface of the sea bed to the igneous basement and back again to the surface of the sea-bed. No measurements of seismic velocity have been made in the area but, where necessary in the text, a mean velocity of 1.8 km/sec has been assumed to convert travel time to sediment thickness.

Sediment thickness within the area varies greatly. It is thickest in the south-east, on the flank of the Azores-Biscay Rise, with values of between 0.9-1.2 seconds (approx. 800-1200 metres thick) that in places on the flanks reach in excess of 1.6 seconds. This area of thick sediments is contoured in Figure 8. It forms a 40 km-wide basin around 41.6°N, 21.7°W which widens further south as

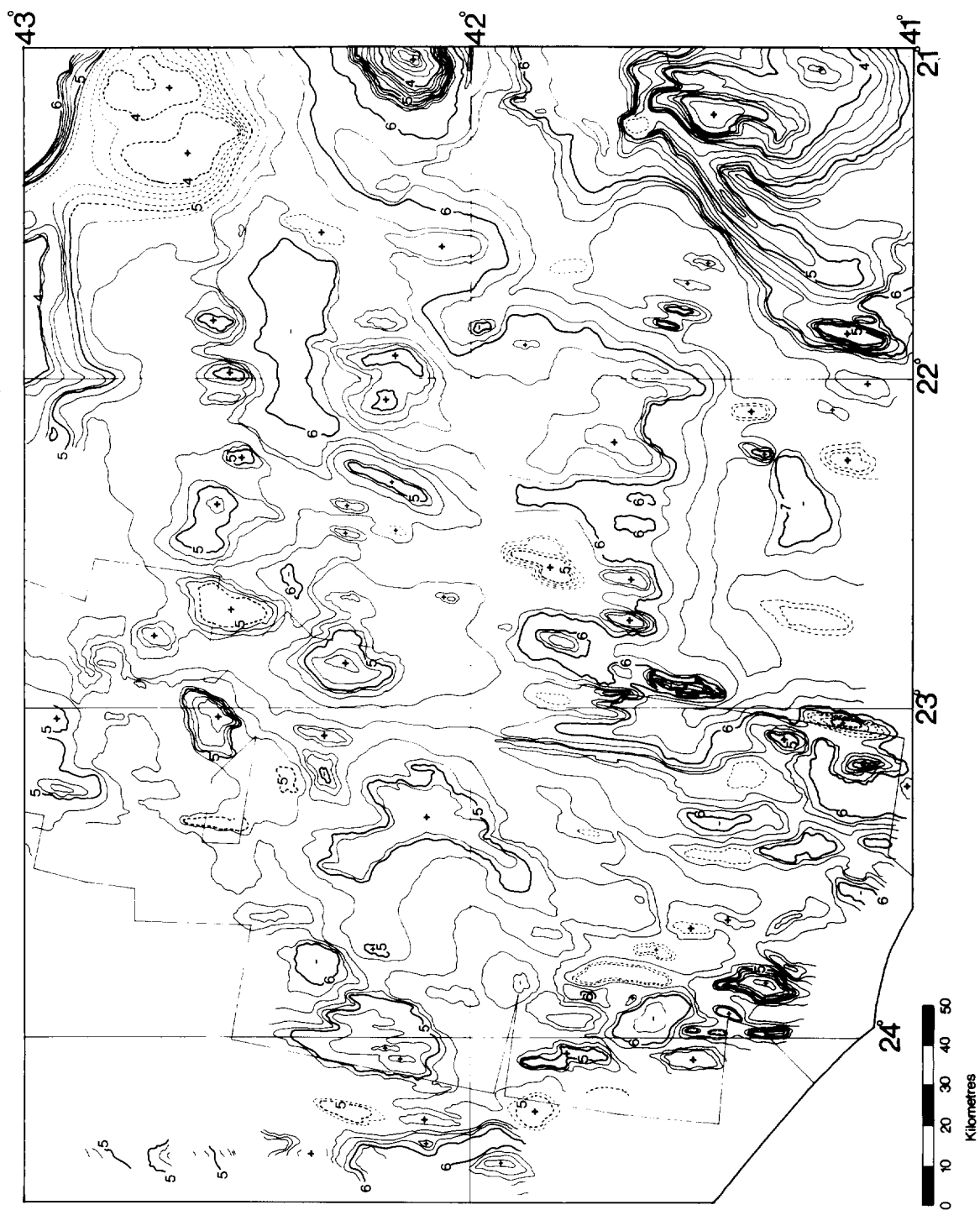


Figure 7. Depth-to-basement map (two-way travel time from sea surface to basement) for the KTF study area; isochrons in 200 m/s intervals; thin box outline shows GLORIA coverage; dashed isochrons inferred from bathymetry where seismic profiles are lacking.

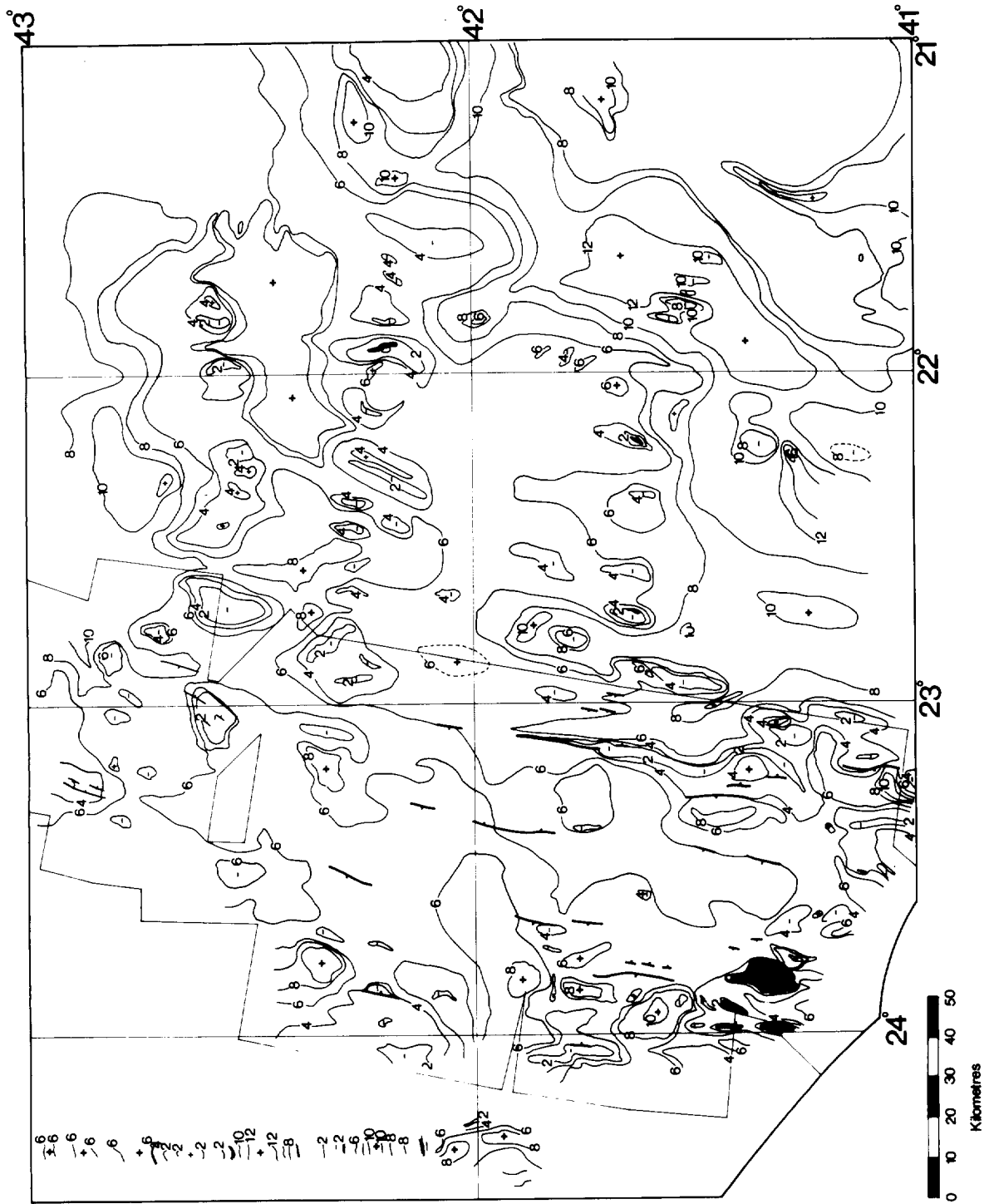


Figure 8. Sediment thicknesses on the KTF study area; isopachs in 200 m/s intervals uncorrected two-way travel time; thin box outline shows GLORIA coverage; faults are indicated from sonograph interpretation (Figure 16); rock outcrop is stippled.

much as 80 km as it extends westwards. It is bounded there by a series of basement highs along 23°W. Within this basin between 41° to 41.5°N and 22° to 23°W, the basement reaches its greatest depth of more than 1.6 seconds below the seafloor.

The thick southeastern sediment sequence, close to the flanks of the Azores-Biscay Rise, is characterised by a prominent mid-sediment reflector with a mean depth of 0.5 secs (approx. 400m) below the seafloor. This reflector smoothly drapes the basement but is occasionally truncated by basement highs (Figure 9).

Over the remainder of the KTF study area, the sediment is similarly draped over the igneous basement, mirroring the gross basement morphology (Figure 9). Sediment thicknesses vary from nil (outcrop) on the flanks and summits of some abyssal hills, to 1.0 seconds in areas of low gradients (<3°). Over most of the area the sediment cover on basement lies in the range 360-900 metres.

Throughout the KTF area, the sedimentary sections appear to be of a draped, pelagic type with little evidence from the seismic reflection profiles of extensive, ponded, turbidite-type deposits (see Figure 19, Section 4a). The profiles show no evidence either of major sediment slides (Embley, 1982) or sediment drifts (Hollister et al., 1978; Roberts and Kidd, 1979).

North and west from the thick sediment sequence near the Azores-Biscay Rise, two prominent mid-sediment reflectors characterise the seismic profiles, forming discontinuous, although easily correlatable horizons. These two reflectors appear always to be sub-parallel and they either both follow the basement morphology, or are both unconformable with it. Over most of the area, the upper reflector is found between 0.2-0.4 seconds depth and the lower between 0.4-0.6 seconds depth below seafloor. They have a uniform separation of 0.2 seconds. Where basement highs and associated abyssal hills are present, the two reflectors are often truncated. One explanation for these regional mid-sediment reflectors is that they represent volcanoclastic sediments shed from the ridges bounding the KTF area during periods when those ridges were subaerial. Another is that they represent hiatuses caused by periods of intensified deep ocean circulation.

Two types of rock outcrop occur in the study area: the first are outcrops of igneous basement, as evidenced by the seismic reflection profiles; the second are outcrops of semi- or completely-consolidated sediments now exposed on the crests of or on the scarps bounding the abyssal hills. For GLORIA interpretation (Section 3c, Figure 13) one has to interpret an area of strong, well-defined

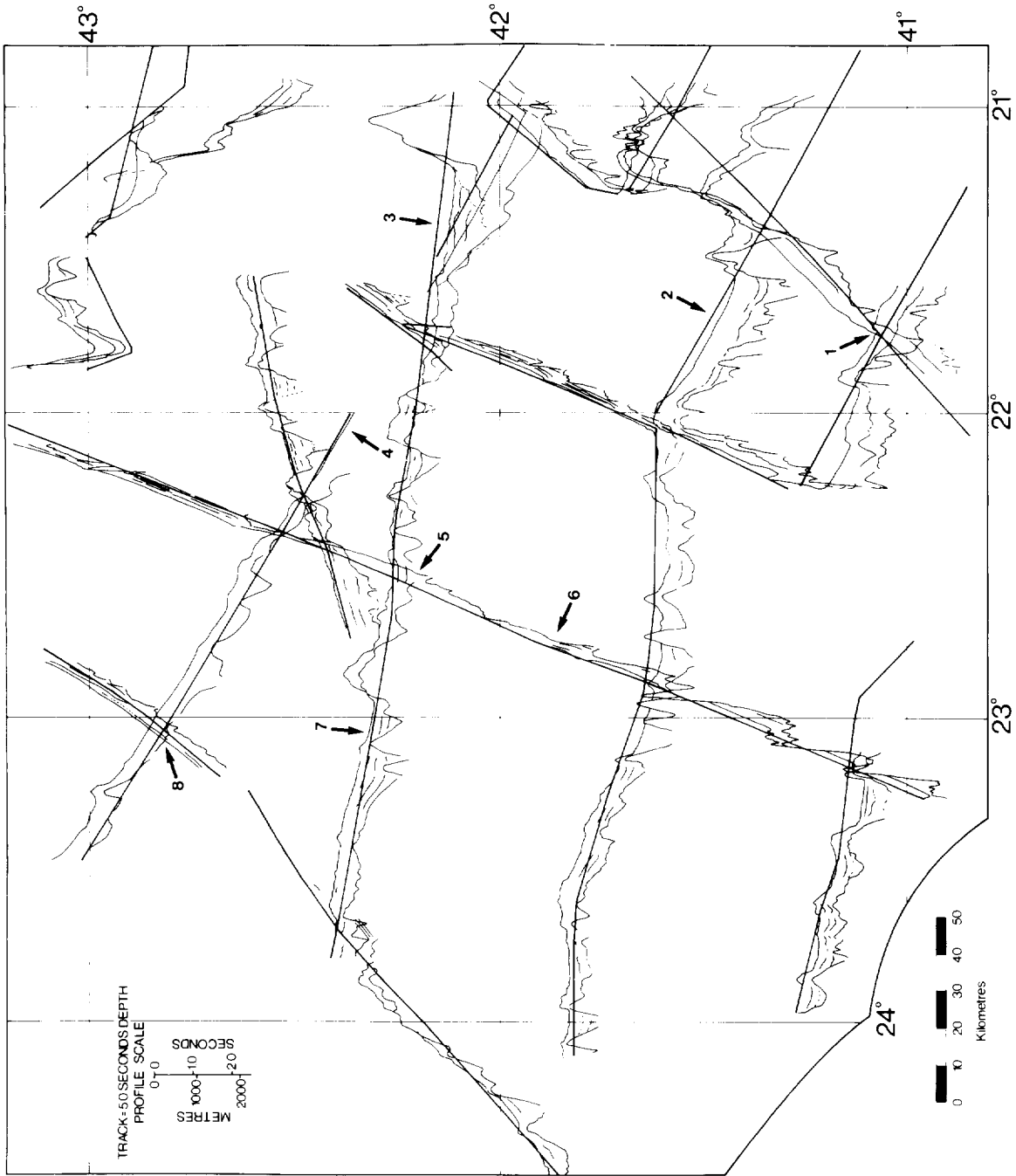


Figure 9. Selected graphic seismic reflection profiles projected along track; vertical exaggeration 8.5 to 1; angle of projection is zero degrees; the track represents five secs depth in two-way time; RRS "Shackleton" core positions are arrowed.

backscattering simply as a hard rock outcrop, with no soft sediment cover. We can only assume that it is an igneous basement outcrop when this is clear from seismic reflection profiles over or near the feature. Confirmed igneous basement outcrops occur mainly in the western part of the area, as would be expected from the westward decrease in the age of the crust and overall sediment thickness.

Frequent basement lows with an approximate azimuth of 010° , between the abyssal hills are apparent in Figure 7. Here the sediments are locally thicker. The lows are between 40-50 km apart in an east-west direction. Between 42.3° - 42.5° N and 21° - 22.8° W are located two particular basement lows trending 100° with two-way travel times to basement in excess of 6.0 seconds. They are bounded to the north and south by highs, mostly less than 5.0 seconds. These aligned basement depressions correlate with the location of the proposed dextral transform fault interpreted in an earlier section from the magnetic anomalies.

3(c) MICROTOPOGRAPHY

The microtopography chart (Figure 10) was produced from along-track identification of small-scale relief on 10 kHz echo-sounder records and from the interpretation of echo character on 2 kHz, 3.5 kHz and 10-kHz records. Most of the echo-character interpretation depended upon 10-kHz echo-sounder records because very few high-resolution seismic profiles (3.5 kHz and 2 kHz) were available. Figure 10 shows the frequency of occurrence of areas having a smooth sediment surface (<10 metres relief) as opposed to those areas having an irregular or hummocky sediment surface. Smooth areas are mapped in irrespective of overall bathymetry so that, although smooth sediment surfaces generally occur in topographic depressions, some smooth areas are apparent in hill regions. Also noted, are locations where hyperbolae were recorded that could suggest redeposition of sediment (Damuth, 1980). The long-range sidescan sonar (GLORIA) survey of the western part of the KTF study area also provides information on microtopography through its detection of backscattering increases over rough ground (Kidd and Roberts, 1982). Interpretations from the sidescan data sometimes conflict with those from the profiling.

'Smooth' areas: Smooth sediment surface are usually found at least 2-3 km from the steeper slopes ($>5^\circ$) and scarps, and away from the more hilly sectors of the KTF area. They comprise between 10-15% of the total study area, representing in excess of 9000 km^2 of smooth sediment cover. However, based upon our existing profiler coverage (Figure 2), no area of smooth, uninterrupted ground is greater



Figure 10. Microtopography at KTF: areas of smooth sediment surface with >10 metres relief (shaded); thickened lines are locations along-track of hyperbolae detected by 10-kHz, 2-kHz and 3.5-kHz profiling; contour line is the 3500 metre isobath; box outlines GLORIA coverage.

than 35 km wide. The smooth areas lie within generally rugged terrain between abyssal hills in the northwestern part of the area while, in the south and east, they are found mainly in broader basins. No obvious correlation exists between the areas of smooth sediments and the total thickness of sediment on basement.

On the 10-kHz records, which only rarely show sub-bottom penetration, most of the smooth sedimented areas are characterised by a single, strong echo, with no sub-bottom echoes. From the few good quality 2-kHz and 3.5 kHz records available it appears that the smooth areas are, in general, acoustically well-laminated to the penetration limit which is generally less than 50 metres (Figure 11a, b, c). Sub-bottom penetration to 75 metres is occasionally achieved and continues to show uniform layering. These upper parts of the sediment sequences generally have a draped style rather than a ponded character, which suggests that gravity-controlled turbidite deposition does not dominate the sedimentary regime. As indicated previously by the air-gun records, pelagic sedimentation prevails over most of the KTF area.

'Hummocky' areas: The areas displaying hummocky relief show many variations in echo character. The most common types of echo are large, open hyperbolae, found along the bases of scarps and in hill regions of very rough topography. These are best displayed on the 3.5 kHz records (Figure 12a) but can also be seen clearly on 10-kHz records (Figure 12b). Hyperbolic echoes are generated by rough topography because the wide-beam of the echo-sounder (whether 3.5 or 10 kHz) allows echoes to be received from any reflecting surface over a wide range of angles as the ship passes by. Other large, open hyperbolae are not associated with nearby scarps and often show relatively ordered, internal layering on the 3.5 kHz records (Figure 12c). These may result from sedimentary features or faulting rather than simply from side echoes as above.

Another echo-character type within the hummocky sedimented areas occurs where the seabed is made up of many close, overlapping hyperbolae, with their inflexion points at the sediment surface (Figure 13a, b). Almost always these areas of hyperbolae are in topographically low areas or near the bases of slopes. Based upon the observations of Damuth (e.g. 1980), Embley (e.g. 1976), Jacobi (e.g. 1976), Flood (1978) and our own experience with high-resolution seismic profiling in other areas, we recognise that this echo-type could represent an area of slumped sediment transported from nearby slopes, or a field of erosional sedimentary furrows. In view of the weak present-day bottom water circulation over the area we recognise that current erosion features of this type would be a

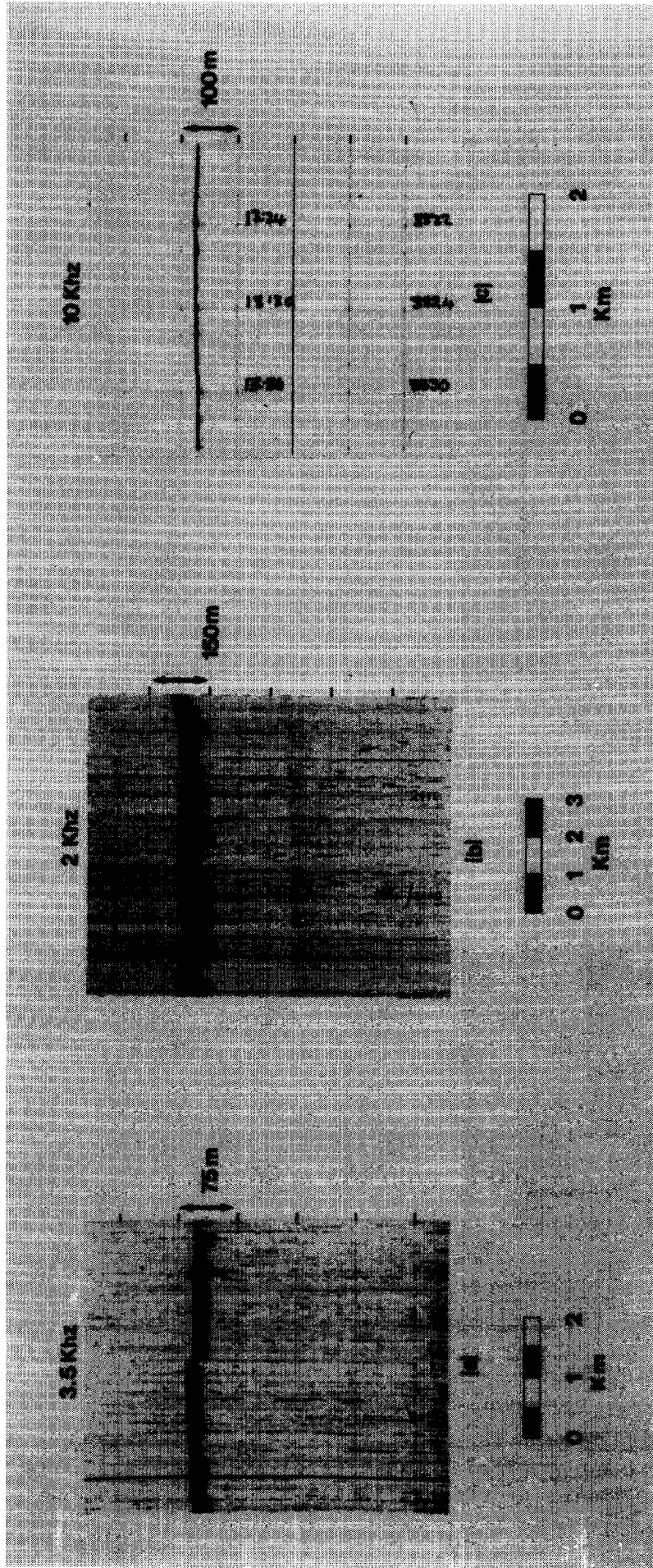


Figure 11. Example profiles over areas with smooth sediment surfaces.

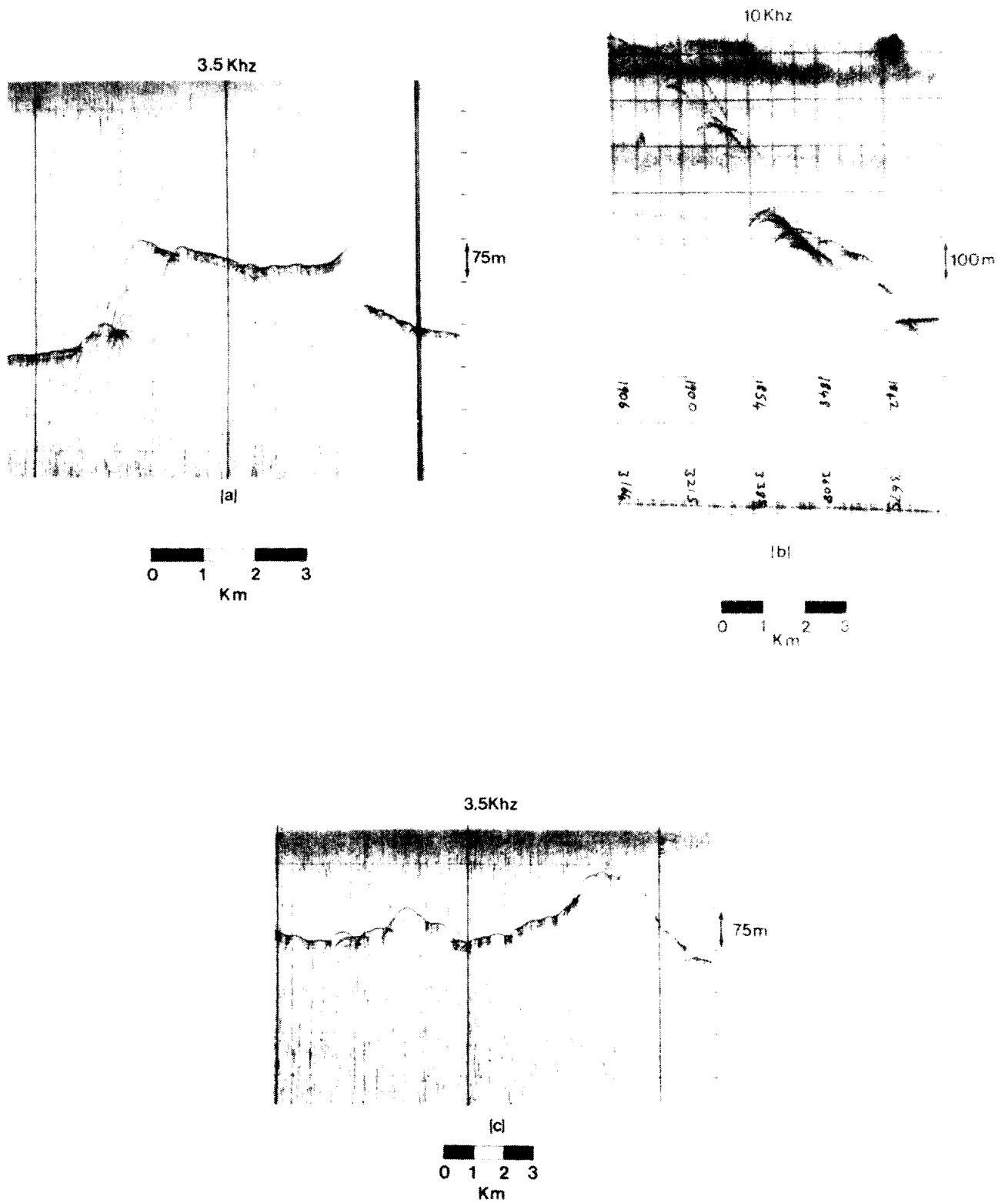


Figure 12. Example profiles over locations where open hyperbolae were detected: (a) and (b) open hyperbolae interpreted as side echoes from slarp, (c) open hyperbolae of uncertain origin.

surprising discovery. They cannot be entirely ruled out because of the maximum hourly current speeds detected in the recent bottom current meter experiments referred to earlier. Near-bottom surveys and samples are required to make a real distinction but for the present we follow the former interpretation and regard these features as due to slumping.

Some occurrences of hyperbolae are within areas of "smooth" sediment cover (Figures 10 and 13b). Also, within the areas of smooth sediments channel-like features and small sediment scarps occur with depth changes of the order of 10 metres (Figure 14). Again, because of the lack of 3.5 kHz and 2 kHz seismic coverage, the majority of these small features are seen only on 10 kHz profiles. At present, it is not possible to interpret their origin or mode of formation.

GLORIA interpretation

Comparisons of the along-track profiles with the GLORIA sonograph records are inconclusive at present. In other areas of the North Atlantic, features detected on 3.5 kHz profiles match changes in backscattering intensity on GLORIA sonographs so that the areal extent of, for example, sediment slumps or debris flows can be mapped (Kidd, 1982; Kidd and Roberts, 1982; Simm and Kidd, in press). The main features of the GLORIA mosaic of the western part of KTF (Figures 15 and 16) in terms of areal coverage, are subtle variations in the amount, or intensity, of backscattering from the seafloor. Unfortunately, these are not crossed by 3.5 kHz profiles. More striking are linear areas of very high backscattering that denote scarps and other outcrops of hard rock (probably, but not necessarily, igneous basement). The subtle changes in backscattering, on the other hand, produce a diffuse mosaic of 'lobate' features and lineations of differing intensities. The differences in the backscattering strength represent subtle changes in topography, slope angle and/or changes in bottom roughness (Kidd and Roberts, 1982; Kidd and Searle, in press). Bottom roughness may be caused by sedimentary bedforms, changes in sediment grain-size, lithification or bioturbation, or a variety of features caused by mass movement such as slumps, slides and debris flows. Specific possibilities for this area would be patches of ice-rafted pebble and/or boulder debris and rock outcrop thinly covered by soft sediment. A number of the 'lobate' areas of relatively high backscattering on the GLORIA interpretation (Figure 16) are closely related to abyssal hills or scarps e.g. at 41.5°N, 23.25°W and 42.1°N, 23.1°W. These we interpret tentatively as slumping of sediment away from the upstanding feature. Other similar 'lobate' areas, e.g. at 42.05°N, 23.9°W, show no clear relationship to

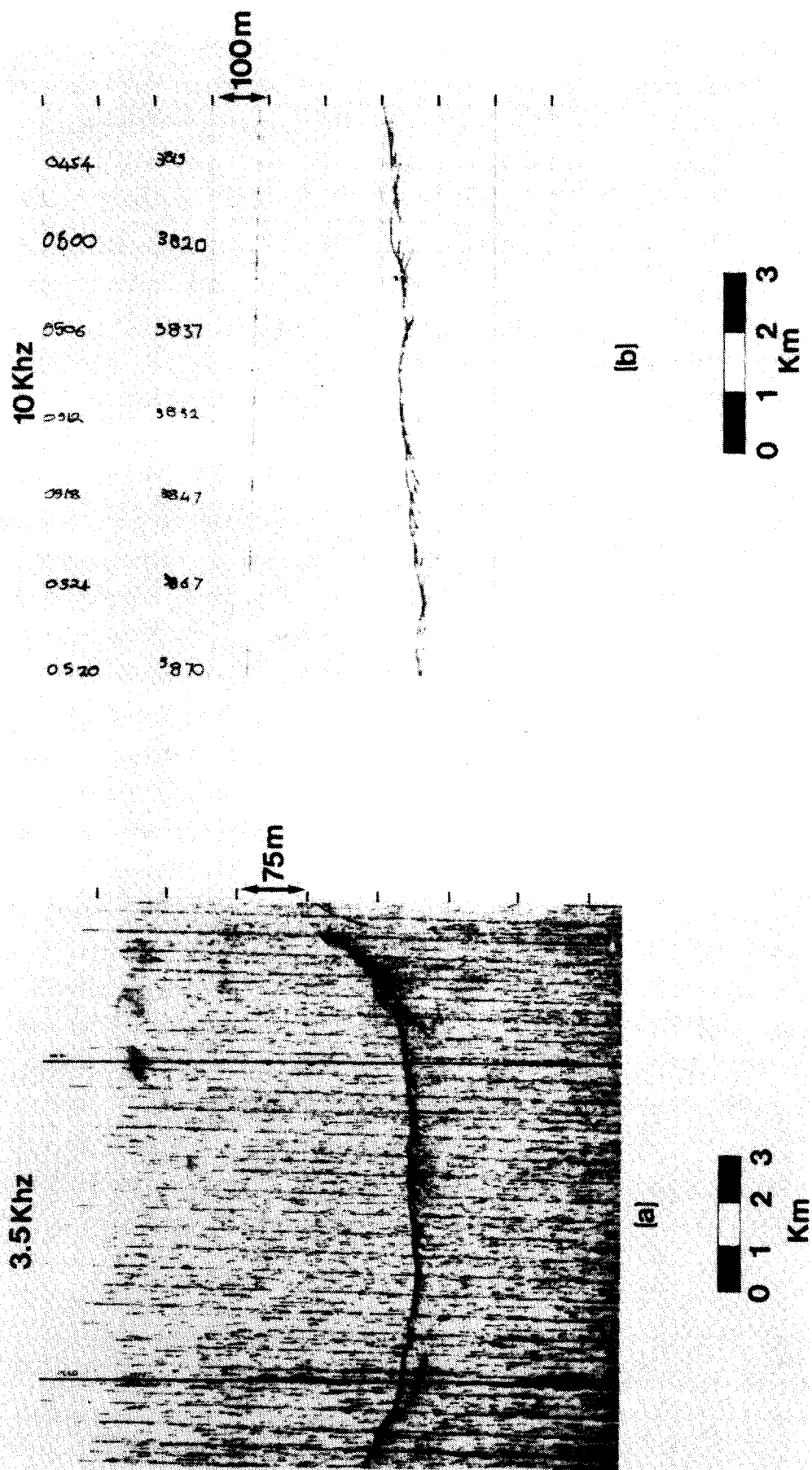


Figure 13. Example profiles over locations where close, overlapping hyperbolae with inflexion points at the sediment surface were detected: (a) profile over suspected sediment slump feature near a steep slope; (b) profile over possible sediment slump or erosion feature (no steep slope nearby).

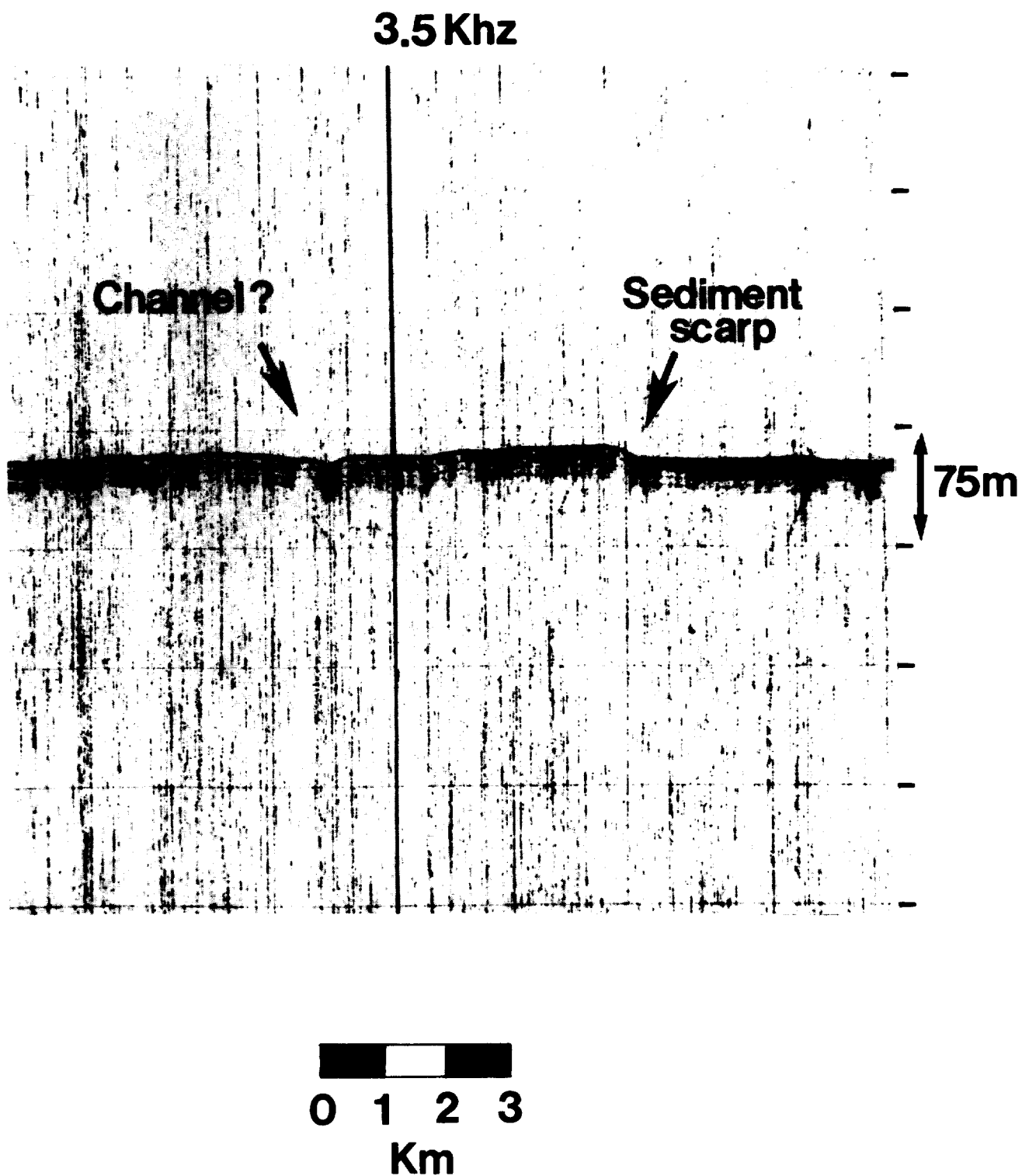


Figure 14. 3.5-kHz profile showing fine-scale relief in a 'smooth area' with a channel-like feature and a small sediment scarp.

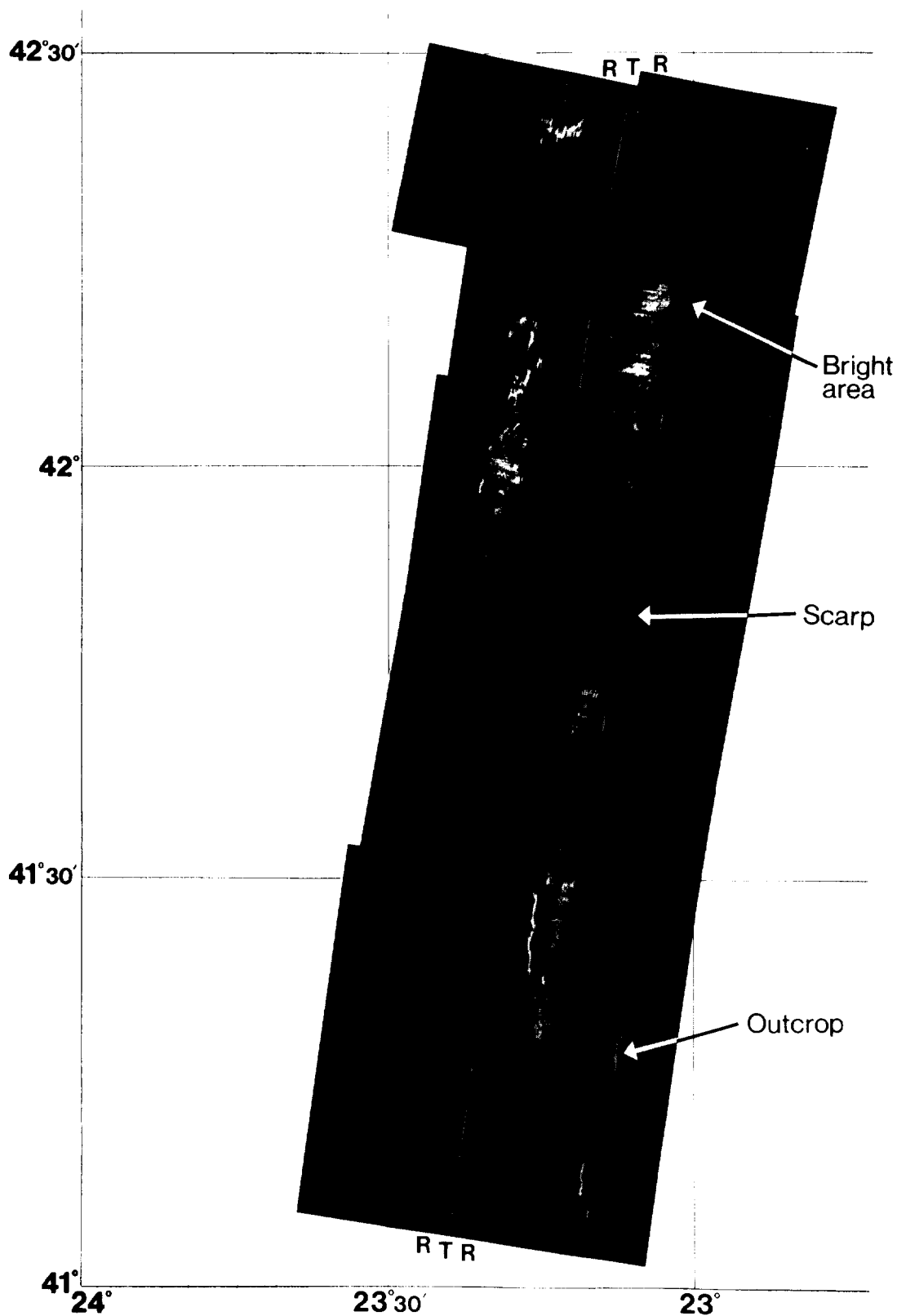


Figure 15. Single NNE-SSW track from the GLORIA sonograph coverage of the western KTF study area: TT is the ship's track, R is the seafloor return on either side of the ship.

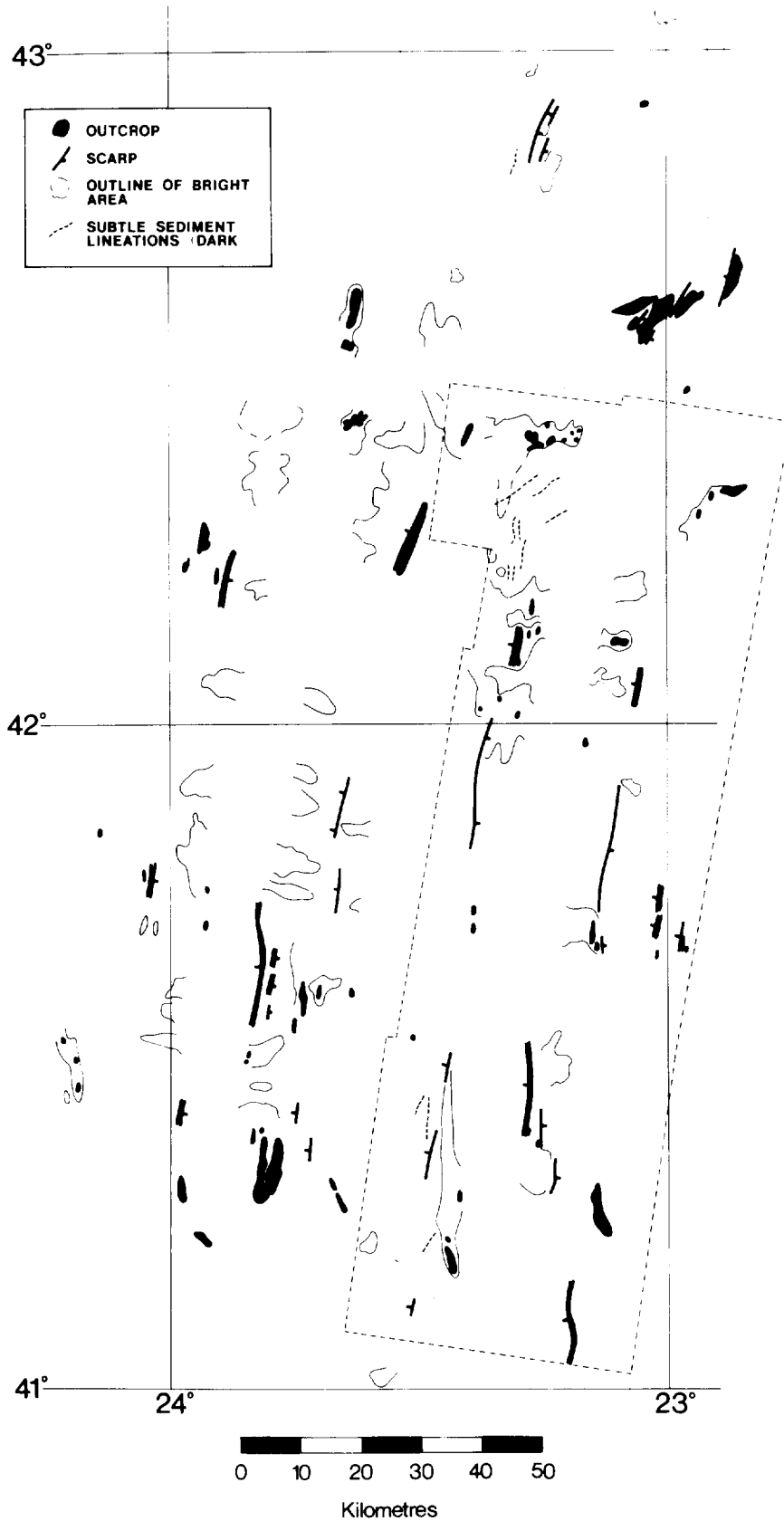


Figure 16. Full interpretation of the (overlapping) GLORIA survey of the western part of the KTF study area; dashed box outline shows the portion of the sonograph coverage illustrated in Figure 15.

hills or tectonic features.

Comparison of Figure 10, constructed from the profiling tracks, with Figure 16, the GLORIA interpretation, shows that the lobate areas of relatively high backscattering strength occasionally occur within the smooth sedimented regions and are not confined to hummocky areas. Some patches of high backscattering, mapped from the sonographs, clearly cross well-controlled boundaries between the "smooth" and "hummocky" sediments mapped from the profiling. Further data is required to calibrate the GLORIA interpretation. Even within those areas mapped as "smooth" sediment surfaces there are small rough patches that could have resulted from sediment instability, erosion or glacial debris; all of importance to site assessment. Precise sampling and near-bottom camera and profiling surveys over these features is required to clear up these uncertainties, and extension of the 3.5 kHz profiling coverage in and around the smoothly-sedimented areas would confirm their limits and sub-bottom continuity.

4. SEDIMENTOLOGY AND STRATIGRAPHY

4(a) LOCATION OF CORES

Sediment sampling in the study area for HLRWD work has so far been limited to nine gravity cores and three piston cores. Core positions are given in Table 1 and shown on Figure 17. Those which lie on seismic profiles are shown in Figures 9, 18 and 19. The area consists of a wide range of sedimentary environments but the extent of this variability was only appreciated after completion of the seismic surveys. Consequently, many more cores are required to determine the extent of localised slumping and sediment redistribution in the area. Cores S8/79/2, 3, and 4 were taken on relatively flat areas of seabed (Figure 17) whereas cores S8/79/1 and 6 lie adjacent to major hills (Figure 9). The other cores are from settings somewhere between these two extremes. Core D10333 was taken in the deepest part of the area.

Cores S8/79/1, 2, 5, 7 and 8 were taken along tracks displaying hyperbolic reflections on the 10 kHz echo sounder record. Most of the other cores were recovered from areas without hyperbolae. Cores 82PCS02 and 4 were taken along 3.5 kHz tracks that showed hyperbolic reflections on the approach to the core sites (Figure 18). Core S8/79/3 was taken in an area where horizontal sub-bottom layering to 35m was visible on a 3.5 kHz profile. Four cores (S8/79/3, 6, 7 and D10333) are from areas mapped as 'smooth' from the profiling tracks. When these various locations are considered with respect to the stratigraphies of the cores

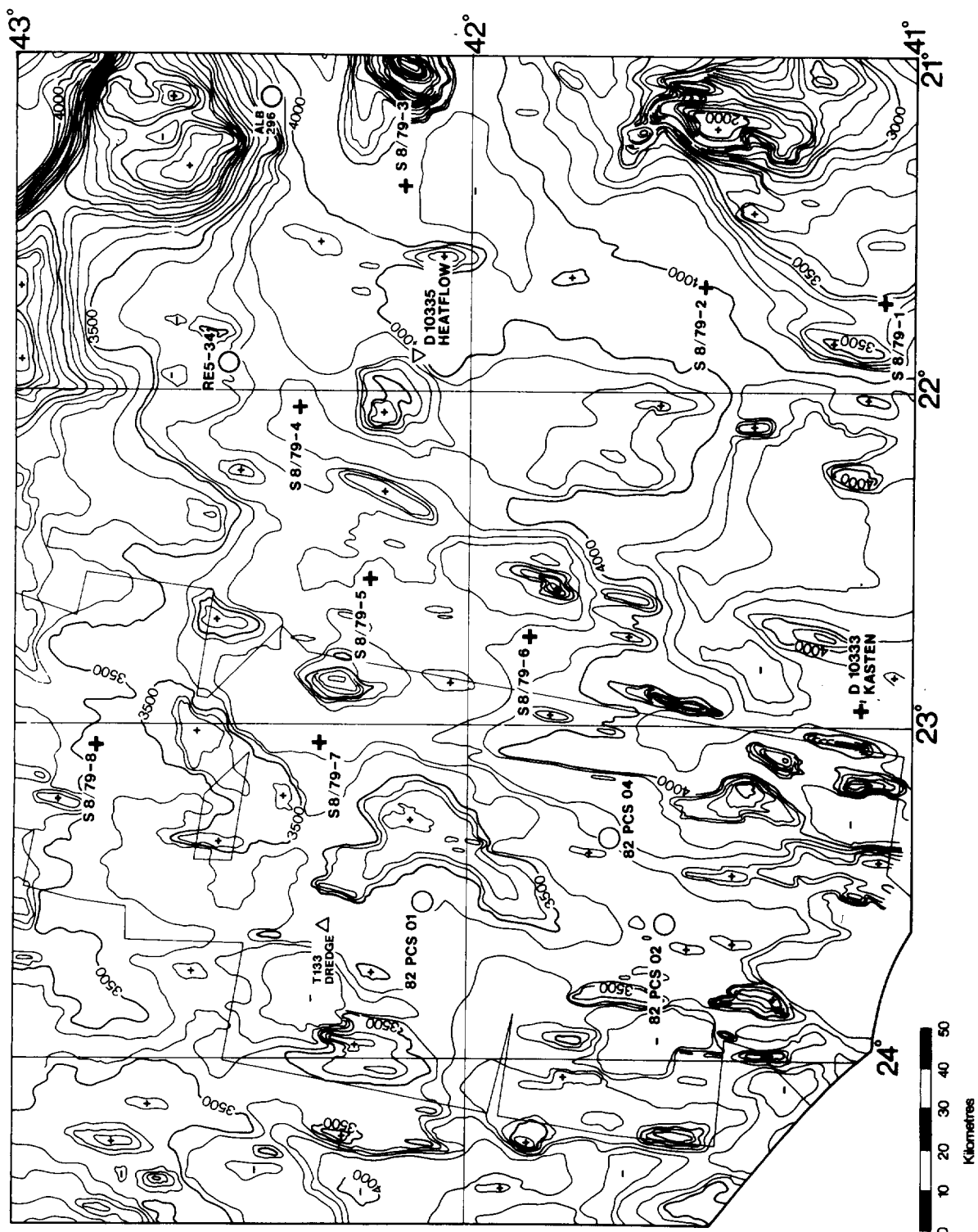


Figure 17. Locations of sampling and the heat-flow station referred to in this report, bathymetry as in Figure 5; box outline locates GLORIA coverage; circles are piston cores, crosses are gravity cores, the triangle is the dredge station and the inverted triangle is the heat-flow station.

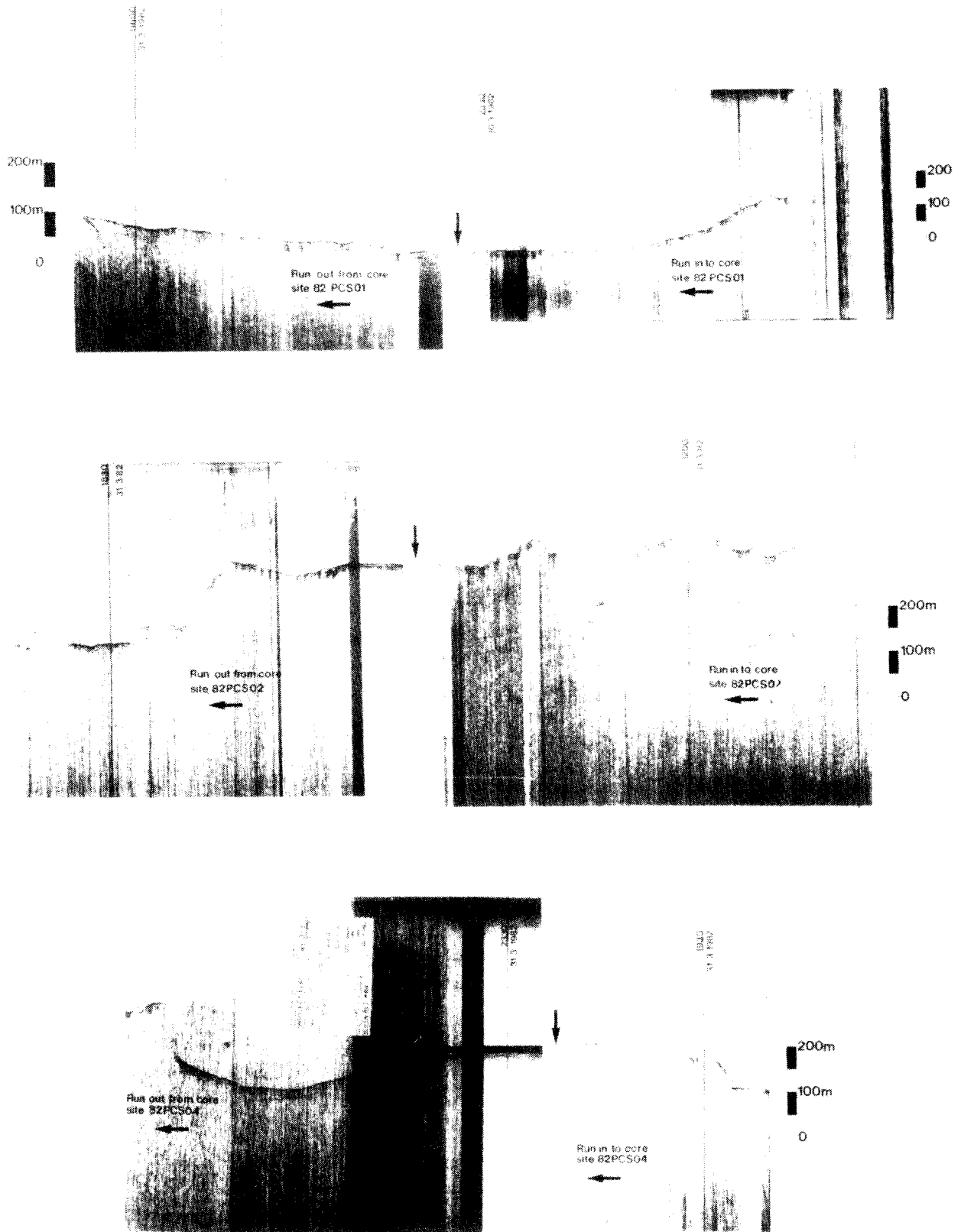


Figure 18. 3.5-kHz high-resolution seismic profiles of the M.V. "TYRO" approach to, and departure from, the piston core sites; horizontal scales vary with ship's speed.

TABLE 1 - Station data for cores from the KTF study area that have been analysed at IOS.

Core No.	Latitude	Longitude	Depth (m)	Core Length (m)
S8-79-1	41°04'.3N	21°44'.2W	3687	2.46
S8-79-2	41°28'.5N	21°41'.4W	4003	2.54
S8-79-3	42°08'.7N	21°23'.6W	4095	3.60
S8-79-4	42°22'.6N	22°03'.1W	3877	2.53
S8-79-5	42°13'.5N	22°33'.9W	3785	2.44
S8-79-6	41°51'.9N	22°44'.2W	3819	1.96
S8-79-7	42°19'.9N	23°03'.5W	3768	2.98
S8-79-8	42°49'.6N	23°03'.8W	3520	2.60
D9806	43°32'.5N	17°53'.5W	3594	0.62
D9812	45°14'.4N	22°25'.8W	3898	1.19
D10333	41°07'.3N	22°57'.1W	4133	1.74
82PCS01	42°05'.9N	23°31'.0W	3540	8.80
82PCS02	41°33'.1N	23°36'.9W	3622	8.81
82PCS04	41°40'.8N	23°21'.0W	3685	9.75

(section 5f) there is no obvious connection between the occurrence of hyperbolae and sediment disturbance.

When interpreting gravity cores two problems relating to the coring method must be considered. These are shortening of sedimentary layers and corer repenetration (Richards, 1961; Weaver and Schultheiss, 1983). Cores S8/79/3 and S8/79/4 both show repenetration features while all the S8/79 cores show severe shortening of lithological intervals. Overall, there is an estimated 40-50% reduction in the length of cored material compared to in-situ thicknesses of units. The reduction of length, however, is not constant along the length of the core. Weaver and Schultheiss (1983) have shown that the amount of shortening is dependent upon the length of core recovered and the sediment type. Marls and clays are shortened more readily than oozes. This means that sedimentation rates based on gravity cores are likely to be inaccurate, particularly if the core contains a sequence of oozes and marls. Piston cores (Figure 19) do not suffer from either of these problems but, where they do not completely penetrate, they can mis-sample the upper layers or produce flow-in structures at the base of the core (Burns, 1963; Kuipers, 1981). No flow-in structures were found in the

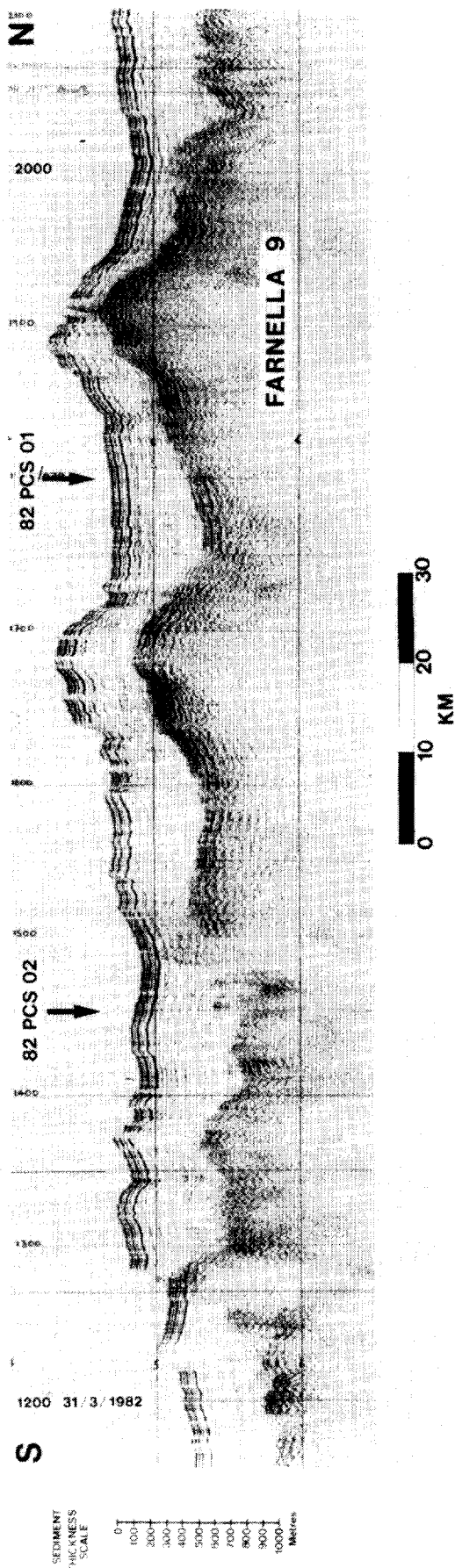


Figure 19. North-south Farnella-9 seismic reflection profile showing the locations of two piston cores: note the draped nature of the acoustic horizons.

three piston cores recovered from the study area (Appendix II), but core 82PCS02 has omitted to sample the upper 1.5 metres (see Section 4f, Figure 29).

The only other cores available for study in the general area were two short gravity cores taken on Discovery cruise 93 in 1978. These both come from north of King's Trough and are consequently of limited value to this study. Some published information is available on two other cores taken in the KTF area (ALB-296 of Olausson, 1953; RES-34 of Ruddiman and McIntyre, 1976). Locations of these are shown in Figure 17.

4(b) LITHOLOGIES

The sediment cores studied at IOS were split, described and analysed sedimentologically using methods adapted from those used by the Deep Sea Drilling Project. Similarly, a modified form of the DSDP sediment classification was employed for sediment terminology (see Hsu, Montadert *et al.*, 1978, pp. 10-17). Two major differences in procedure, however, were adopted: (1) sample depth was consistently measured from the top of the sediment surface in the core; (2) an electro-osmotic knife was used to split the sediments in order to expose the best possible surfaces for visual description (Schultheiss *et al.*, in preparation).

The cored sediments are composed of a series of carbonate ooze layers interbedded with marl and marly ooze layers (Figures 20 and 21). The oozes are firm and white and the marls are softer and buff to yellowish-brown in colour; they are easily distinguished visually. In broad terms, the oozes represent deposition during interglacial intervals of Quaternary earth history, whereas the marls represent glacial intervals. The explanation for the lithologic distinction is suggested to be a greater input of terrigenous non-carbonate material associated with ice-rafting and increased erosion of continental shelves during lowered sea levels corresponding to glacial periods (Ruddiman and McIntyre, 1976). The ice-rafting is particularly important near King's Trough as the polar front lay just to the north during glacial maxima (McIntyre *et al.*, 1972). The effects of the oceanographic changes clearly affected sedimentation on the KTF study area (see Section 5h). Small glacial erratic pebbles have been found in the cores as well as dispersed ice-rafted quartz sand (Figure 20).

Downcore variations in the proportion of carbonate to non-carbonate material were determined either by 'carbonate bomb' (Müller and Gastner, 1971; Dunn, 1980) for the "Shackleton" cores (Figure 25, Section 4c and Appendix III) or 'LECO' carbon analyser (Boyce and Bode, 1972) for the 82PCS cores (Figure 22). Total carbonate values lay in the range 40% to 98%. No organic carbon values are

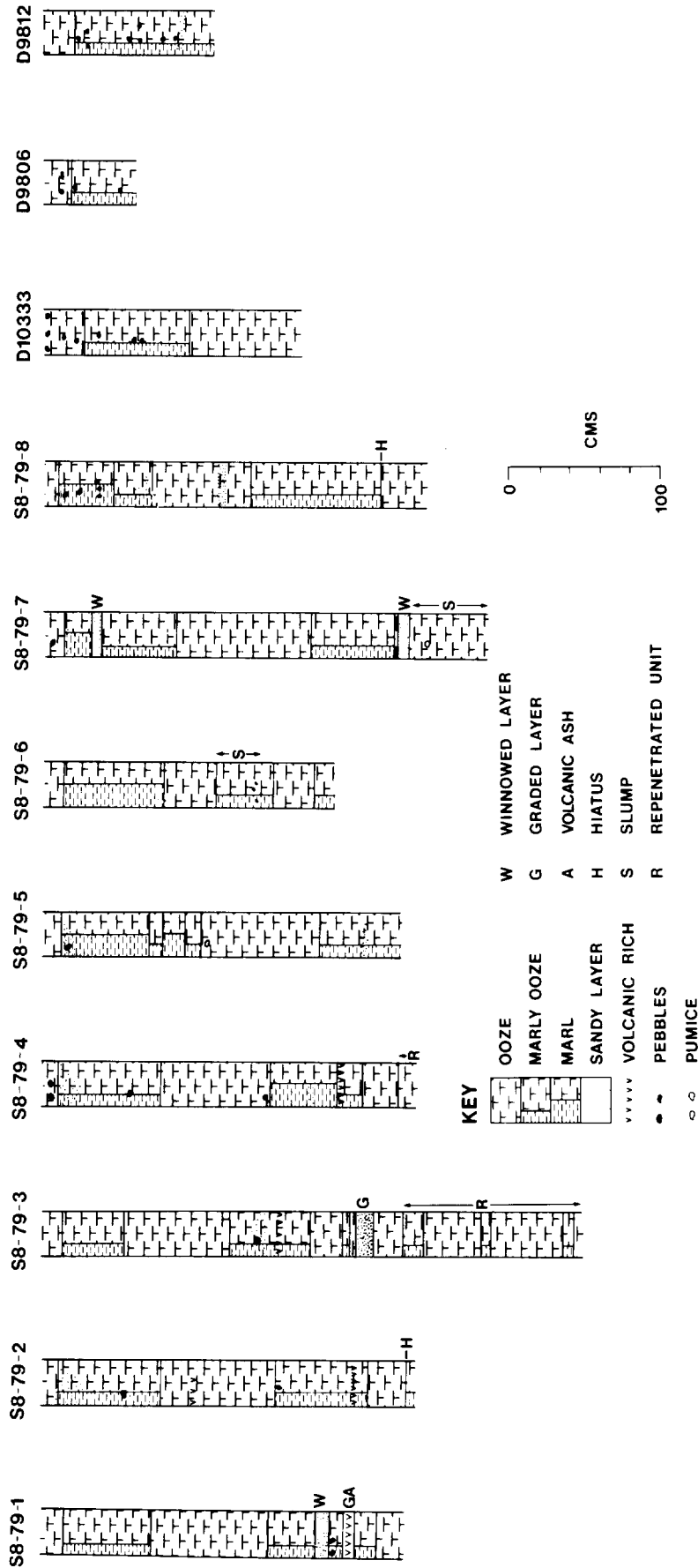


Figure 20. Lithologies of gravity cores in the King's Trough region, including cores D9806 and D9812 which were taken to the north of KTF.

82 PCS 01

82 PCS 02

82 PCS 04

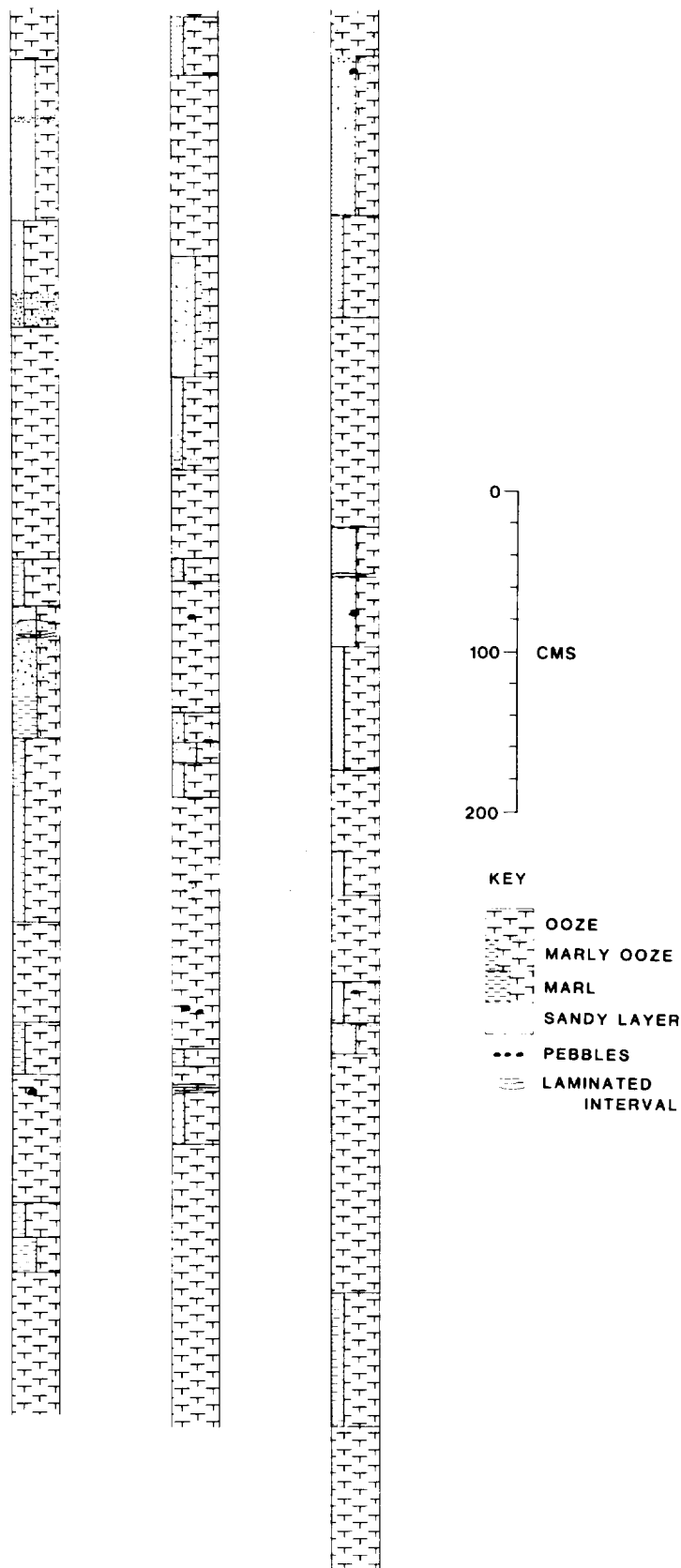


Figure 21. Lithologies of piston cores of the KTF study area.

available from the cores but values would be expected generally to be less than 0.2% (Litzitzin, 1972).

To substantiate the visual subdivisions and to determine the constituents of each layer, sediment smear slides have been examined from each lithological unit under a petrological microscope. These semi-quantitative estimates of biogenic and mineral components were supported by selective X-ray diffraction studies for bulk mineralogy. The calcium carbonate fraction of the KTF study area sediments is composed of calcareous nannoplankton and foraminiferal skeletons. The non-carbonate fraction is mainly composed of detrital clay with occasional siliceous microfossils such as radiolaria, diatoms and sponge spicules. Minor non-biogenic components are fine-grained quartz and volcanic glass shards, along with fine-grained rock and isolated mineral fragments (feldspars, pyroxene, amphibole, zeolites and iron oxides) occurring occasionally in the glacial intervals or associated with volcanic ash layers (Section 4g).

X-ray diffraction analyses confirm the smear-slide observations and show the detrital clays of the KTF study area to be dominated throughout by illite and smectite, with only minor kaolinite or chlorite abundances. Zimmerman (in press) has differentiated between the clay mineral abundances of glacial and interglacial periods in a core, RE5-34 (Figure 17) taken on the study area. He recognises the dominance of illite and smectite in the present day sediments and shows that illite becomes even more abundant during the glacial periods. Chlorite becomes less abundant during the glacial periods than at present. Zimmerman concludes that the general increase in detrital clay and quartz input to this latitudinal zone (~45°N) during the glacials must be related to increased ice-rafting near the glacial polar front.

Evidence of bioturbation is very common in the cores and shows up as a mottling of one sediment type into another. Consequently, bioturbation is most apparent around lithological boundaries where two sediment types are juxtaposed (Figure 23). However, it is safe to assume that an equal amount of bioturbation has occurred in the middle of each lithological unit, but the dominance of one sediment type here means that the structures cannot be so easily seen or detected on X-radiographs. Other sedimentary structures are relatively rare. Occasional winnowed foraminiferal sand-rich layers are found, generally about 5-10 centimetres thick, representing short periods of localised current activity during which fine-grained material was removed. Volcanic tephra-rich layers have also been detected (see Section 4g) and one tephra layer in core S8/79/1 shows grading indicative of localised redeposition. X-radiography of the core sections using

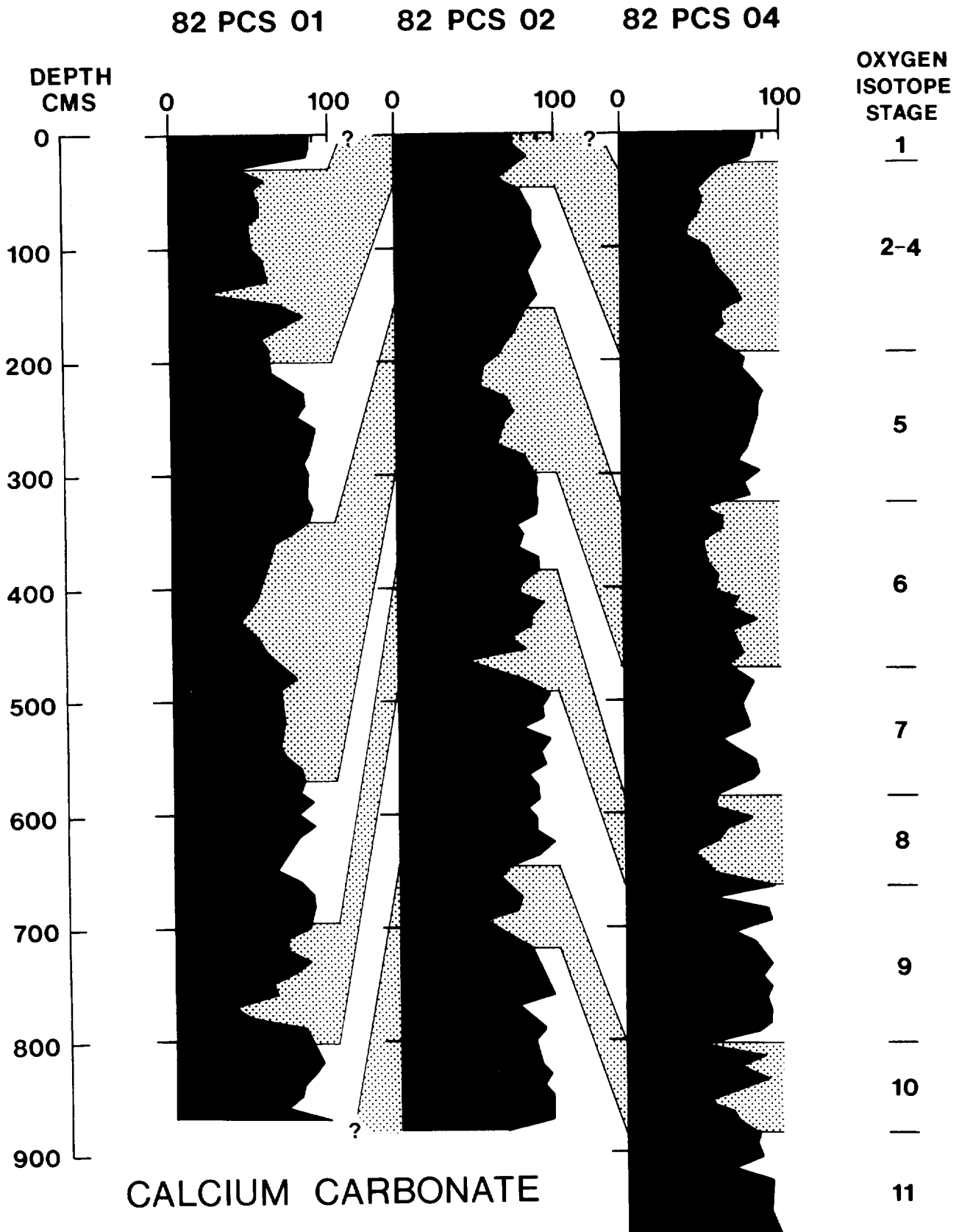


Figure 22. Percentage calcium carbonate contents in the three piston cores. Core correlations are based on lithological, coccolith and oxygen isotope data; stippled areas represent glacial intervals.

82 PCS 01/7

82 PCS 01/9

82 PCS 02/5



Figure 23. Mottling and burrow structures in three piston core sections; for location see Appendix II.

the methods outlined in Bouma (1969) and visual examination of sediment surfaces cut by an electro-osmotic knife have revealed a few thin laminated layers indicative of redeposition and also some more major slump structures. The slumps occur in cores S8/79/6 and S8/79/7. In core S8/79/6 the slump is 26 centimetres thick. It is not associated with any erosion (Section 5f and Figure 20). Unfortunately, the corer did not fully penetrate the slump in core S8/79/7. Thus its total thickness is not known; neither is it known whether its formation was associated with erosion. Evidence of erosion can be found in cores S8/79/2 and S8/79/8 (see Section 4f) but in neither case is it apparent as a distinct lithological change and it was only revealed by micropalaeontological techniques.

Grain-size analyses were carried out on gravity core samples at IOS Taunton using standard sieve and pipette techniques. Routinely, each major lithological unit was measured. Size-frequency distributions have been plotted conventionally in phi units ($\phi = -\log_2 D$, the particle diameter in mm; Krumbein, 1936) in order to obtain statistical measures such as sorting and skewness (Trask, 1932). At this stage, our interest is primarily (1) in median grain diameters, through which to assess generally the likely adsorption properties of the sediment, and (2) in content of sand grade ($>63 \mu\text{m}$; $<2 \text{ mm}$; Inman, 1952) or coarser material that might have some effect on waste emplacement. Appendix IV lists percentages in the sand, silt and clay grades along with median grain diameters in phi units. (Further grain size data for the samples listed are on file at IOS Wormley).

Median grain diameters range from 9ϕ (approx $2\mu\text{m}$) to 7ϕ ($\sim 8\mu\text{m}$) for both oozes and marls. No significant difference in grain size exists between the (cold) glacial and (warm) interglacial deposits. They reach 2.6ϕ (approx. $165\mu\text{m}$) in the thin winnowed layers rich in foraminifera. These microfossil concentrations represent the coarsest sediment in the cores, if one excludes ice-rafted material; sand percentages at winnowed horizons can be over 80%. Graded layers are generally less well-sorted such that the layer in core 3, for example, has a median diameter of only 3.9ϕ (or $73 \mu\text{m}$) even though it is made up of over 54% sand size material. The ice-rafted sand that is dispersed through the cores causes only a slight increase in sand grade percentages in temperate areas such as KTF, if one compares it with pelagic carbonate sequences in lower latitudes (Lizitzin, 1972; see Section 4h and Figure 37).

The alternations of ooze and marl layers, so apparent during the last 400,000 years, are probably likely to be less pronounced or absent altogether at depth in the KTF sediment sequences. The glacial/interglacial extremes in ice volume were not as large in the early Quaternary (Pisias and Moore, 1981). Rock coring,

dredging and drilling near here, and in similar environments within the Atlantic, indicate that in pre-Quaternary times this area was unaffected by ice-rafting. IOS cores recovered from rock outcrops north of the area on the King's Trough complex (Kidd et al., 1982), and to the south on the Azores-Gibraltar fracture zone, contain Pliocene sediments consisting of very pure carbonate ooze with no marly intervals. Extrapolating late Pleistocene sedimentation rates, this type of sediment would be expected at depths greater than about 40 metres on the KTF study area. We emphasise later in this report the urgent need for deep sampling, such as hydraulic piston coring from a drilling vessel, to obtain information on the sedimentary medium at these levels; well below those attainable by our conventional piston coring.

4(c) MICROPALAEONTOLOGY

The two dominant microfossil groups found in the cores are planktonic foraminifera and calcareous nannoplankton. Both have both been examined in detail and are the basis of a high-resolution stratigraphy. Work on planktonic foraminifera from cores 82PCS01, 02 and 04 has not yet been completed. Studies of the microfaunas and -floras enable a series of horizons to be identified which can then be correlated from core to core; thus giving a temporal breakdown of sediments in the area. Changes in sedimentation between intervals and within intervals across the area can then be examined. The ages of certain horizons, such as glacial/interglacial boundaries, are known (see Piasias and Moore, 1981) and consequently sedimentation rates can be determined. The resulting stratigraphic picture will be limited by the number of cores and their areal distribution and is restricted to the time interval represented by the cores.

Planktonic Foraminifera: Planktonic foraminifera were analysed from samples taken at 10-cm intervals. This interval gives good resolution while avoiding most of the problems caused by bioturbation. The washed residues are sieved through a 180 μ sieve and splits of 300 individuals are divided into species and counted. The stratigraphy derived from such counts reflects the changing surface water masses in the area since individual species of planktonic foraminifera are associated with particular water masses. During the late Quaternary such changes have been particularly severe in this area due to the fluctuations from glacial to interglacial conditions.

Globorotalia truncatulinoides, a well-known subtropical species (Kipp, 1976), varies in abundance in the King's Trough area from absent during glacial periods

to about 10% of the planktonic foraminiferal fauna during interglacial periods (Figure 24). *Neogloboquadrina pachyderma* (sinistral), a very cold, low-salinity water indicator, shows an inverse distribution with high percentages during glacial periods (Ruddiman and McIntyre, 1981). Thus, glacial and interglacial intervals can be easily recognised in the cores. The boundaries of these intervals tie in very closely with the lithological (calcium carbonate) changes, with the higher carbonate intervals representing interglacials.

Other species of planktonic foraminifera show more subtle changes. Oxygen isotope sub-stage 5e is characterised by increased percentages of *G. inflata* and *G. ruber* and a reduction in the percentages of *G. bulloides*. This reflects the warmer temperatures experienced during stage 5e (Shackleton, 1969) and gives a useful correlation point. A further correlation point is provided by a coiling direction change in *G. truncatulinoides* (Figure 25). This species is dominated by the dextral form in the King's Trough area today (Kipp, 1976). However, during oxygen isotope sub-stage 5d there was a short-lived pulse dominated by the sinistral form. The reasons for this short pulse are unclear but it has also been recorded by Pujol (1980) in a core taken near the King's Trough study area. Pujol has shown that coiling direction changes are a common phenomenon in *G. truncatulinoides* but in different areas of the North Atlantic they occur at different times. Therefore, they can only be relied on for intra-regional correlation, such as within the King's Trough area.

Calcareous Nannoplankton: In the Quaternary coccoliths are the chief constituent of the calcareous nannoplankton. These are small (2-20 μ) plates derived from calcareous algae. They are represented by a large number of species but not all of them are stratigraphically useful. In the King's Trough area a stratigraphy can be produced for the last 450,000 years using just four commonly-occurring species (Figure 26). Species of coccoliths evolve rapidly and so the stratigraphy produced by them is based on evolutions and extinctions and does not rely on identifying water mass changes. This method is, therefore, independent of the planktonic foraminiferal stratigraphy.

Only four species (*Emiliana huxleyi*, *Gephyrocapsa muelleri*, *Gephyrocapsa aperta* and *Gephyrocapsa caribbeanica*) are routinely counted although an examination is made for other species which may indicate older or reworked sediments. About 300 specimens from each sample are counted from random traverses under the light microscope. *E. huxleyi* is sometimes difficult to distinguish by this method and so S.E.M. analyses have been used to corroborate

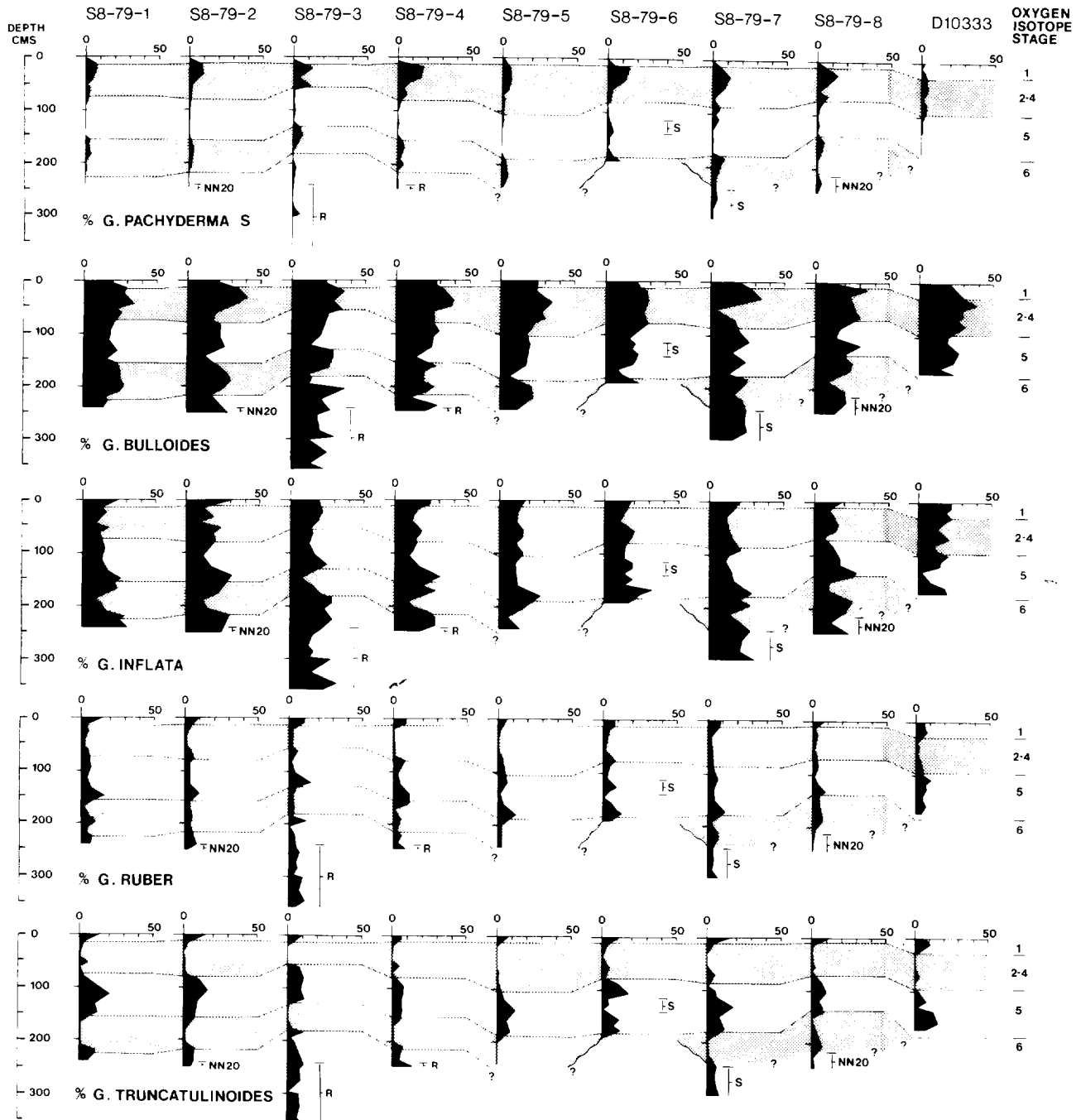


Figure 24. Percentage abundance of selected planktonic foraminiferal species in the gravity cores. Correlations based on oxygen isotope, lithological and coccolith data; stippled areas represent glacial intervals. S = slump unit; R = repenetrated unit; NN20 = stratigraphically older units below hiatuses.

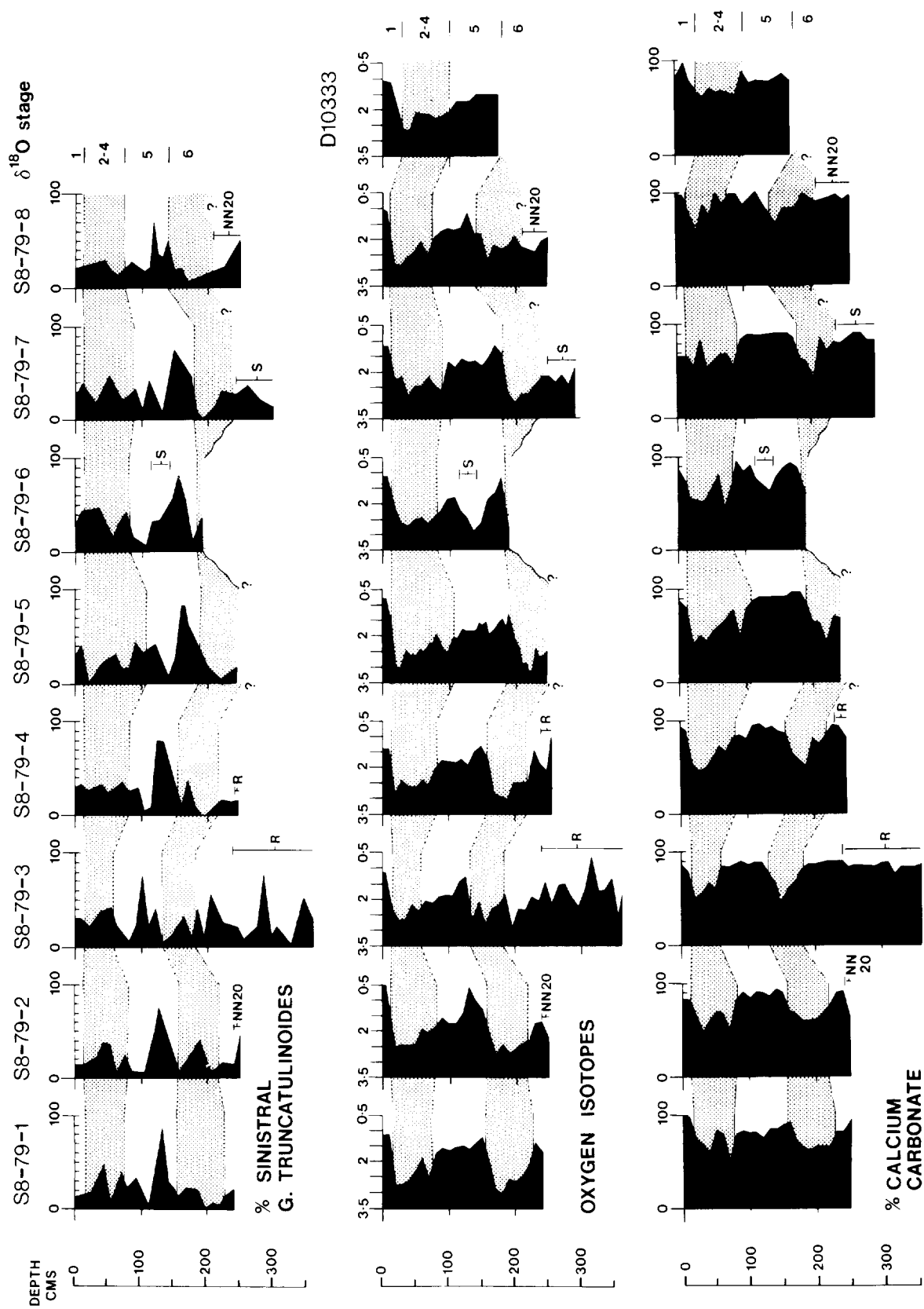


Figure 25. Percentage abundance of sinistral Globorotalia truncatulinoides, with oxygen isotope measurements and percentage calcium carbonate in the gravity cores. Symbols and stipple as in Figure 24.

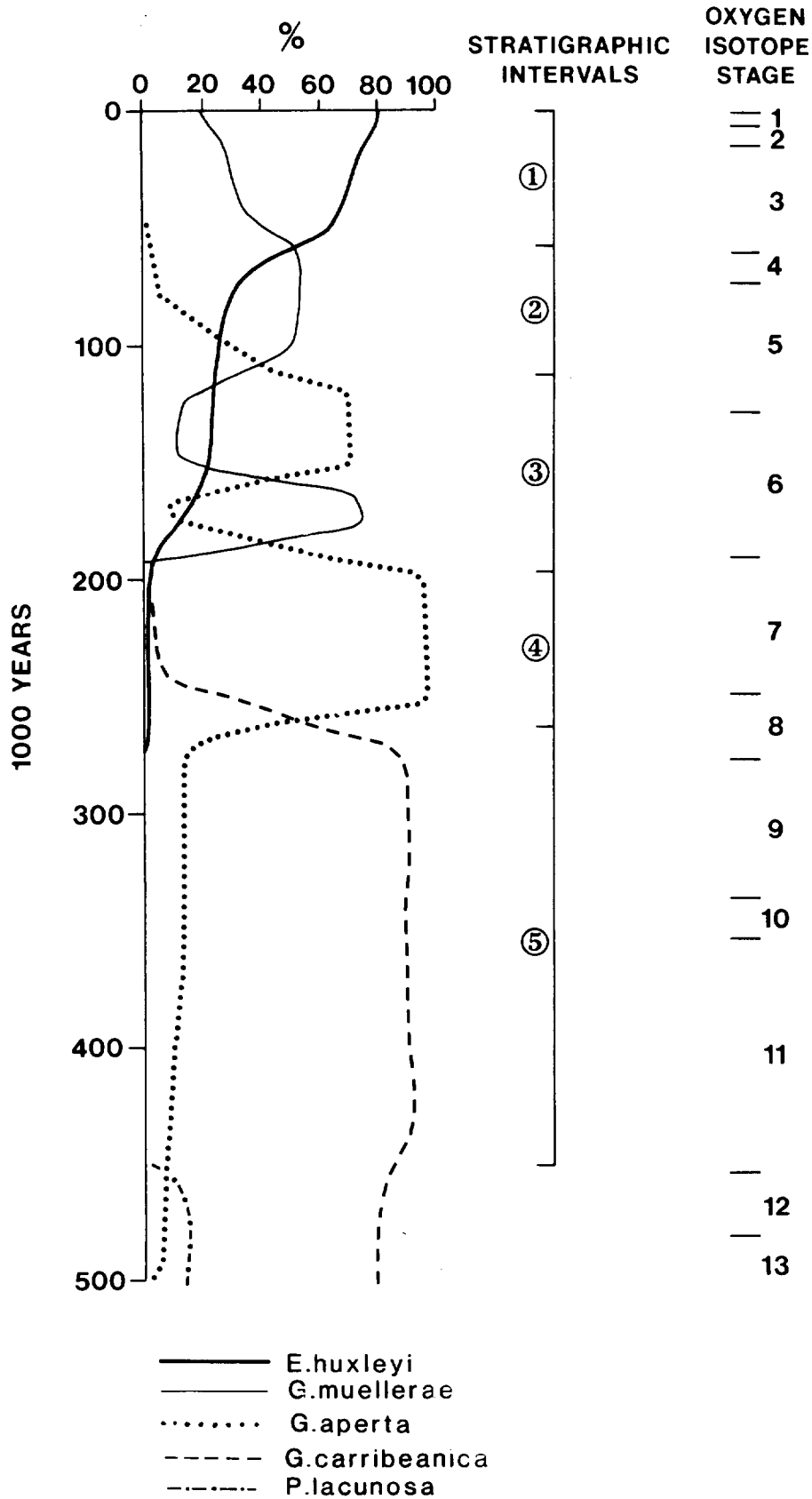


Figure 26. Generalized coccolith distributions through the last 500,000 years, showing how each coccolith interval can be defined against a time scale and how the intervals relate to the oxygen isotope stages.

some of the E. huxleyi counts, particularly when small numbers of this species were encountered.

The following stratigraphic intervals, beginning with the youngest, have been recognised:

1. An interval of dominant E. huxleyi. Base taken at the reversal of dominance between G. muelleræ and E. huxleyi. This interval continues to the present day and is known as the E. huxleyi acme zone (Gartner and Emiliani, 1976). This interval occupies Isotope stages 1, 2 and most of stage 3.
2. An interval where G. muelleræ is dominant over G. aperta and E. huxleyi. Base marked by the last reversal of dominance between G. aperta and G. muelleræ. Top marked by a reversal of dominance between G. muelleræ and E. huxleyi. This interval occupies Isotope stage 4 and most of stage 5.
3. An interval mainly dominated by G. aperta. Base marked by a reduction in its percentage to less than 90%. Top marked by the last reversal of dominance between it and G. muelleræ after which G. aperta declines rapidly. A correlation point within this interval is a short-lived dominance of G. muelleræ over G. aperta. E. huxleyi makes up about 10-20% of the coccolith flora in this interval. This interval occupies the lower part of Isotope stage 5 and most of Isotope stage 6.
4. An interval of dominant G. aperta. Base marked by a reversal of dominance between G. caribbeanica and G. aperta. Top marked by a reduction in the percentage of G. aperta to less than 90%. E. huxleyi evolved near the base of this interval but is rare throughout. The interval occupies the lowest part of Isotope stage 6, all of stage 7 and the upper half of stage 8.
5. An interval of dominant G. caribbeanica. Base not penetrated but defined elsewhere to be the point at which Pseudoemiliana lacunosa becomes extinct. Top marked by a reversal in dominance between G. caribbeanica and G. aperta. This interval occupies the lower half of Isotope stage 8, together with stages 9, 10 and 11.

4(d) OXYGEN ISOTOPE MEASUREMENTS

Oxygen isotope measurements provide a very reliable method of determining glacial and interglacial intervals. Some stages such as oxygen isotope stage 5 also have characteristic plots of downcore values. These enable us to positively identify units even if there has been some erosion or redeposition. Oxygen isotope determinations were made at the University of Cambridge by Dr. N.J.

TABLE 2 - Estimated ages of oxygen isotope stage boundaries and duration of stages for the late Quaternary (from Kominz et al., 1979).

Isotope stage boundary	Age (Kyr. B.P.)	Isotope stage	Duration (Kyr. B.P.)
1/2	11	1	11
2/3	29	2	18
3/4	61	3	32
4/5	73	4	12
5/6	127	5	54
6/7	190	6	63
7/8	247	7	57
8/9	276	8	29
9/10	336	9	60
10/11	352	10	16
11/12	453	11	101

Shackleton on specimens of G. bulloides. These were routinely taken at the appropriate 10-cm intervals on all the RRS "Shackleton" cores (Figure 25) and also on core 82PCS01 (Figure 27). The records clearly show oxygen isotope stage 5 in each of the cores but the relatively slow deposition rates in the RRS "Shackleton" cores (partly an artefact produced by core shortening (see Weaver and Schultheiss, 1983) obscures the fine detail and makes it difficult to distinguish between stages 2-4. Anomalously-high ¹⁸O values during stage 5 in core S8/79/6 are the result of a slump in this core.

At stages older than stage 5, oxygen isotopes can only be used to indicate glacial or interglacial conditions. Independent verification is required to be certain that there has been no erosion or duplication of complete cycles. This verification is obtained from the calcareous nannoplankton and, using the two methods in conjunction, a very precise stratigraphy can be produced. Thus, we know that core 82PCS01 extends back into late oxygen isotope stage 9 since both oxygen isotope and coccolith data agree, but cores S8/79/2, S8/79/7 and S8/79/8 contain older sediments at their bases detected from the coccolith data alone.

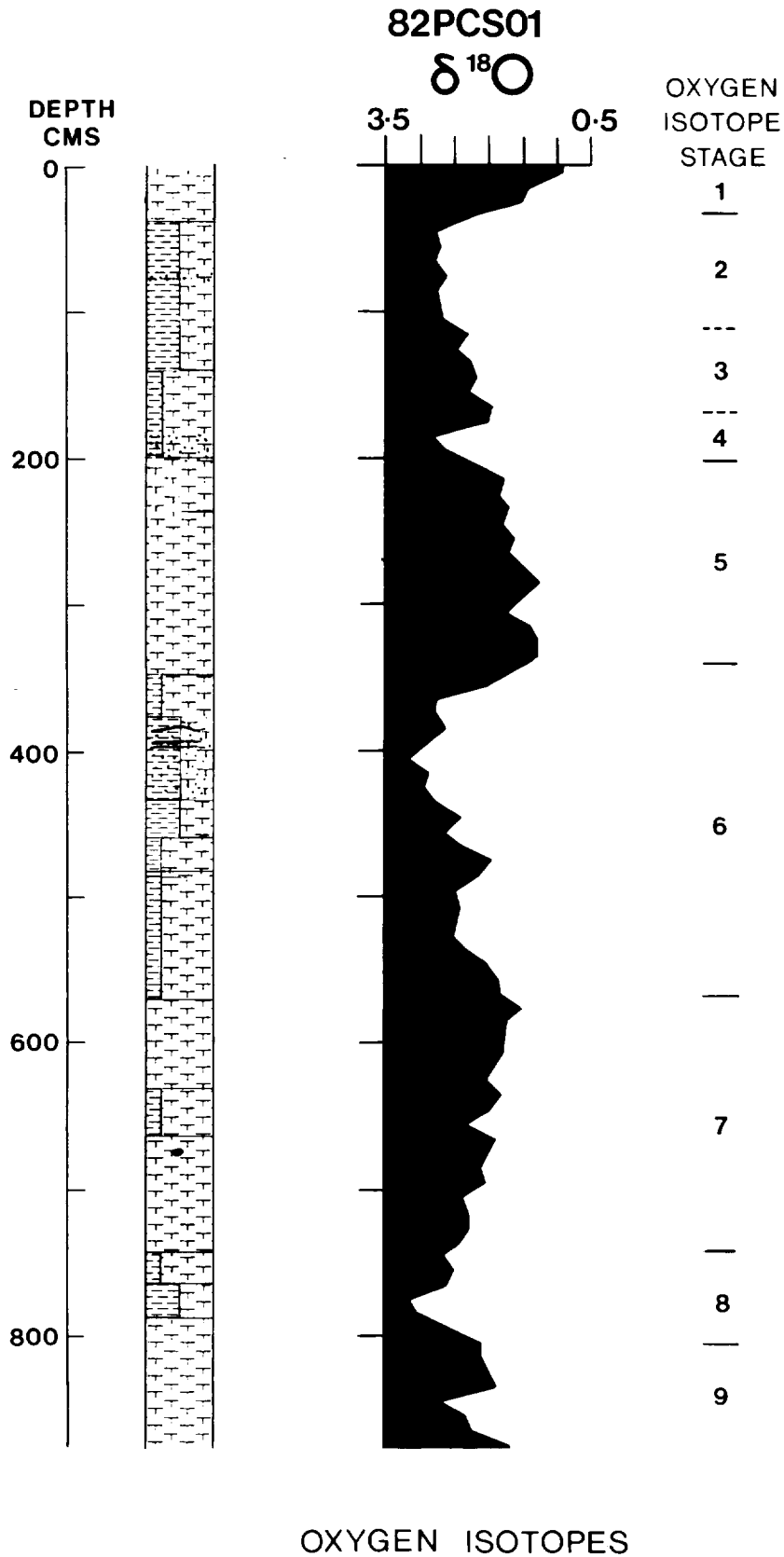


Figure 27. Oxygen isotope values in piston core 82PCS01. Note correlation of high values with marly intervals in the core. Lithological key as on Figure 21.

The ages of oxygen isotope stage boundaries are known (Table 2) and deposition rates can consequently be calculated for each oxygen isotope stage (Section 4f, Table 3).

4(e) PALAEOMAGNETIC MEASUREMENTS

A variety of magnetic parameters were measured on the eight RRS "Shackleton" cruise 8/79 cores and they have been useful in providing additional evidence for stratigraphic correlation of the cores. Along-core scans for magnetic susceptibility have been run both by IOS and by S. Robinson of Liverpool University. In addition, a large number of individual samples has been measured, again at Liverpool University (see Appendix II), as part of a thesis project aimed at recognising atmospheric particulate flux to the North Atlantic. Parameters measured at Liverpool included magnetic susceptibility, anhysteretic and saturation isothermal remanent magnetisation (ARM and SIRM respectively). One of the cores, S8/79/5, was the subject of a pilot study by Dr. E.A. Hailwood at Southampton University to examine whether any systematic variation in magnetic remanence direction existed that could be attributable to geomagnetic secular variation. Magnetic intensity, susceptibility and susceptibility anisotropy were also measured at Southampton.

In a stratigraphic sense it was clear at the outset that the period covered by these cores was unlikely to extend to the last major reversal (~700,000 years B.P.). A number of short-lived polarity reversals have occurred since that time but generalised estimates of North Atlantic sedimentation rates suggested that only the last of these, the Blake Event at ~200,000 years B.P. (Rampino, 1981), which is itself poorly defined, could conceivably have come within the range of the "Shackleton" cores. The longer Dutch piston cores, however, may, following our micropalaeontological investigations, warrant a search for the last reversal and the other short excursions.

Downcore variations in magnetic remanence were measured on the S8/79/5 core that extends into isotope stage 6 and were shown to be surprisingly stable and strong. Systematic fluctuations in direction with depth occur that could conceivably result from palaeosecular variation (E.A. Hailwood, personal communication).

Of greater significance in establishing long-range correlation of our cores were the measurements of magnetic susceptibility and "SIRM". Both the along-core scans and individual sample measurements of magnetic susceptibility provided excellent core-to-core correlations that match well the glacial/interglacial

micropalaeontological and oxygen isotope divisions. High values of "SIRM" match marl and marl-ooze deposits of glacial periods and conversely low values are measured in the interglacial ooze deposits. In other areas further south (Francis *et al.*, 1981b) we have recognised a correspondence of magnetic susceptibility peaks with volcanic tephra layers. Magnetic susceptibility peaks in the "Shackleton" cores, however, relate most strongly to occurrences of ice-rafted sand and pebbles; the regional volcanic ash at ~165,000 years B.P. that was located in cores in the eastern part of the study area (see Section 4g) cannot be seen in the susceptibility plots.

Magnetic anisotropy measurements (Rees, 1965) were made in order to examine the nature of the sedimentation and post-depositional processes. In sampling core S8/79/5 for this work attempts were made to avoid sections showing obvious bioturbation. Samples were taken from three intervals: 3-15 cm, 138-150 cm, 150-165 cm. Only the upper interval (latest Pleistocene) has a primary magnetic fabric which correlates with apparently undisturbed laminations visible on the cut surface of the core. The other samples were considered to have a weak anisotropy probably due to burrowing (E.A. Hailwood, personal communication) although this was not visible on the cut core surface or in X-radiographs. It was considered that, in view of the extensive bioturbation, the cores did not warrant further magnetic fabric measurements.

4(f) STRATIGRAPHY

An accurate stratigraphic breakdown of the cores is provided by a combination of oxygen isotope and calcareous nannoplankton data. The oxygen isotope data divides the cores into glacial and interglacial intervals and the calcareous nannoplankton indicate whether the sequence is in the correct order without any hiatuses (Figures 28 and 29). Once this framework has been set up other correlation points such as lithological changes, planktonic foraminiferal datum points and any useful palaeomagnetic data can be added to give as many correlations as possible. Thus, the cores can be divided into geologically very small time units of the order of 10 to 20 thousand years and small changes in sediment supply or localised erosional events can be identified.

Before we consider sedimentation rates, it is important to emphasise again the relationship between a core and the sediment it was taken from. Sedimentary intervals in cores are not always directly comparable to the in-situ thicknesses of the intervals, because of the way in which corers operate (see section 4a) (Weaver and Schultheiss, 1983). Gravity cores do not produce reliable

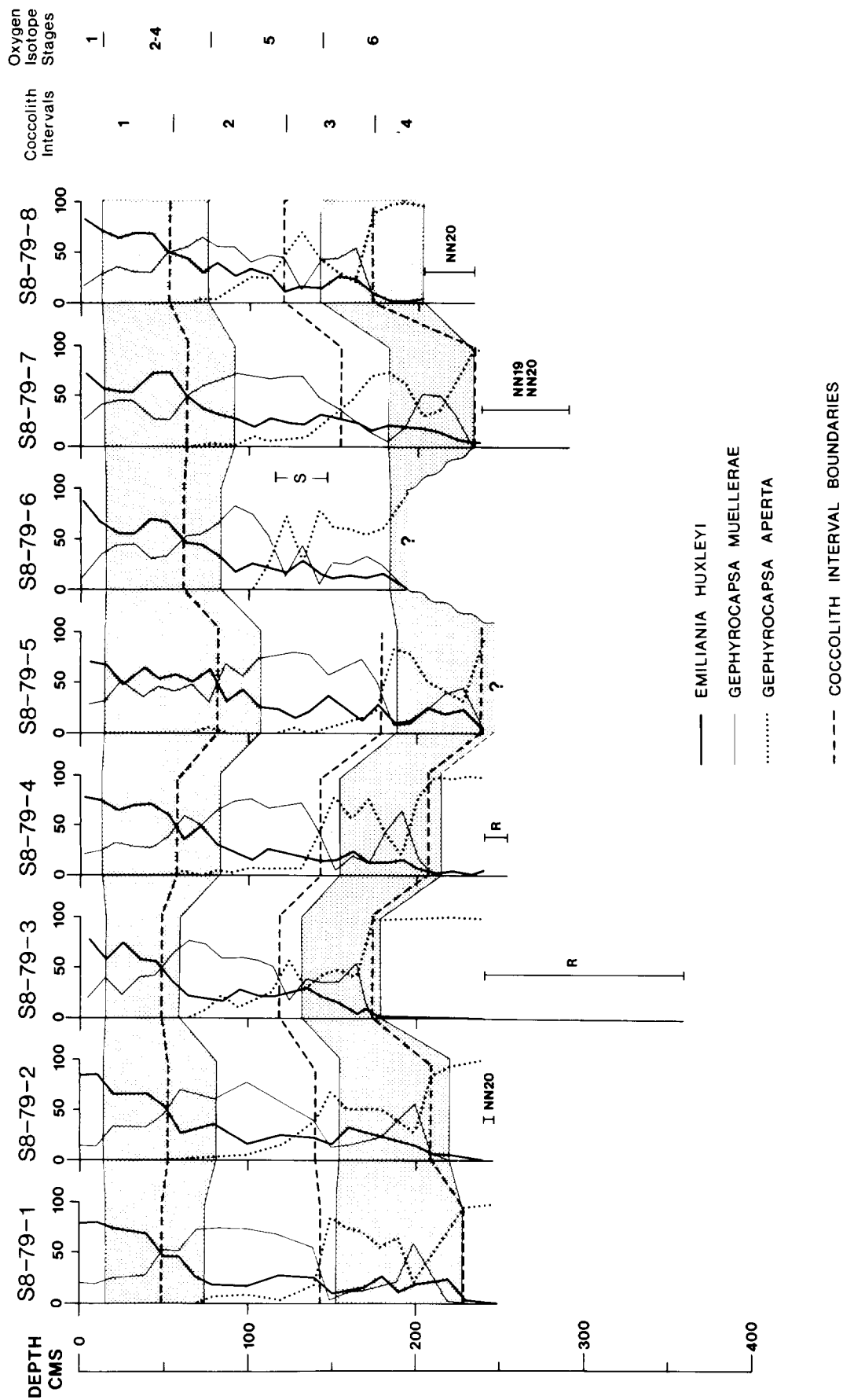


Figure 28. Percentage abundance of stratigraphically useful coccoliths in the gravity cores; stippled areas represent glacial intervals.

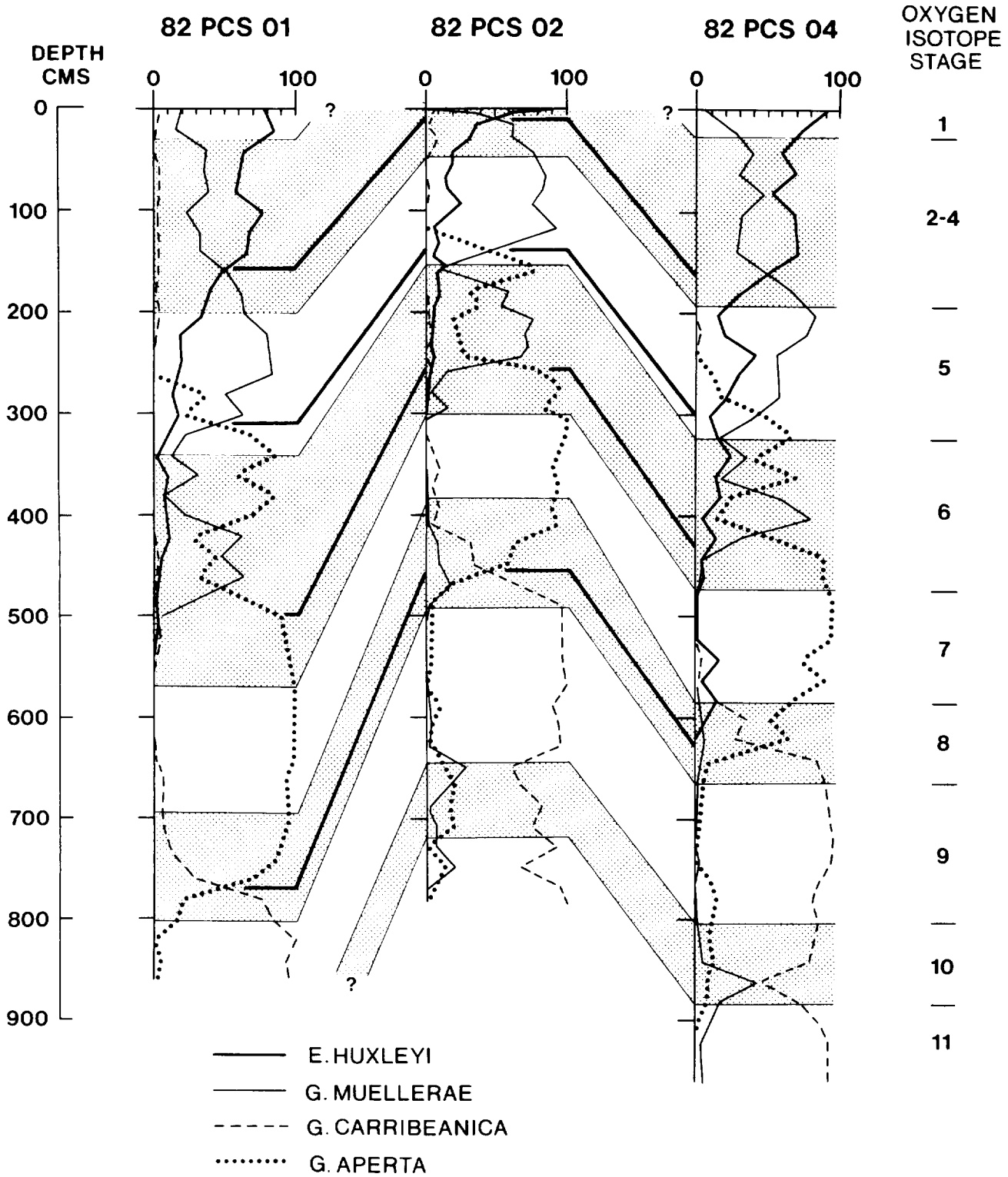


Figure 29. Percentage abundance of stratigraphically useful coccoliths in the piston cores; stippled areas represent glacial intervals; correlations are thickened lines.

sedimentation rates, whereas piston cores usually do.

To assist with the stratigraphic interpretation, Shaw diagrams have been used (Figures 30 and 31). In this type of diagram the distances between the top of the core and each correlation point are compared between one selected core and each of the others. Thus, cores with equal sedimentation rates will produce straight regression lines at 45° to the axes. The deviation from a 45° slope is a measure of the dissimilarity between the two cores, which reaches its maximum when a line parallel to one of the axes is produced by an additional amount of sediment or removal of an amount of sediment in one core. Because the gravity corer shortens the cores and piston corers do not, cores taken by different instruments must be plotted separately. In these diagrams the boxes represent the distance between samples. The actual correlation point can lie anywhere between two samples and so the constraint on the line is for it to pass through the box and not through the specific point. An exception to this is the lithological boundaries which can be accurately defined and consequently are plotted as points.

The piston cores show very good correlation with each other (Figure 30). They contain no sedimentary disturbances and have average sedimentation rates of 2.5-3 cms/1000 years. The sedimentation rates vary from as low as 1.6 cms/1000 years during interglacial stage 8 to as high as 3.6 cm/1000 years during glacial stage 6 presumably related to the general increase in terrigenous input in the glacials (Section 4b). These three cores contain a complete record of sedimentation over the last 400,000 years and provide the longest available records from the KTF study area. The only evidence of current deposition in these three cores is the laminated intervals during oxygen isotope stage 6 in cores 82PCS01 and 82PCS04. Only 82PCS01 shows an increased sedimentation rate during this interval (Table 3). Laminations of this type within fine sediments could result from either turbidity current or bottom current deposition. If the former, the laminations are formed during the waning phase of a sudden incursion of turbid water and sediment and usually form part of a graded sequence (Bouma, 1962). In these piston cores no addition of sediment is recognised (Figure 30) nor is there any grading present (Figure 21). Deposition in a steady near-bottom current regime is, therefore, a more likely origin for the lamination (Bouma and Hollister, 1973). Thus, there appears to have been a period of increased bottom current activity in the west of the area between 127 and 190 thousand years ago (Table 2). Since Figure 30 also shows no net removal of sediment during this period we know that the bottom currents, at least at the locations of the piston

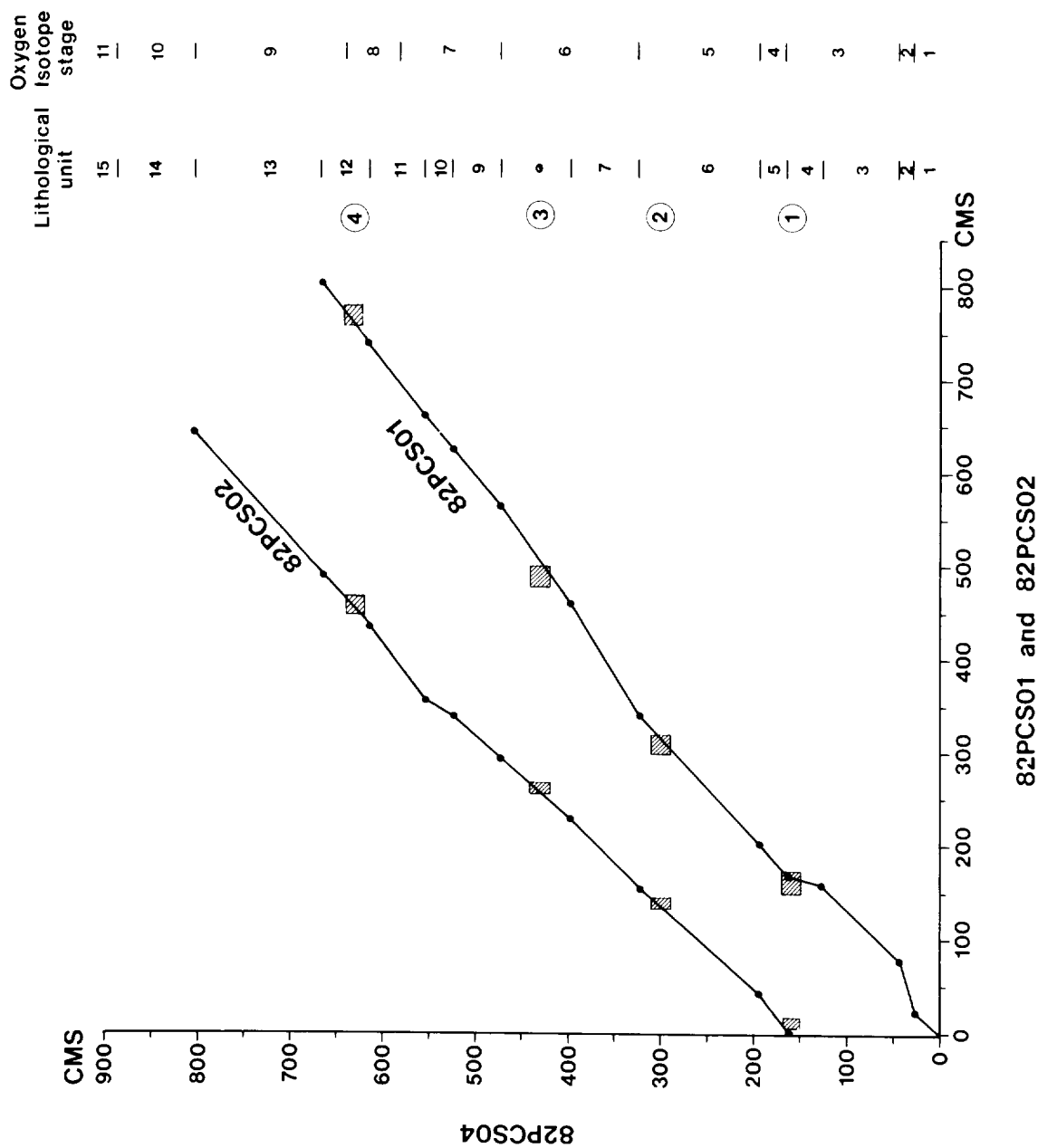


Figure 30. Shaw diagram showing correlations between the piston cores. Points represent lithological boundaries; boxes represent limits of coccolith correlations, defined by the sample intervals. Box 1 = coccolith interval 1/2 boundary; Box 2 = coccolith interval 2/3 boundary; Box 3 = coccolith interval 3/4 boundary; Box 4 = coccolith interval 4/5 boundary. (See text for explanation.)

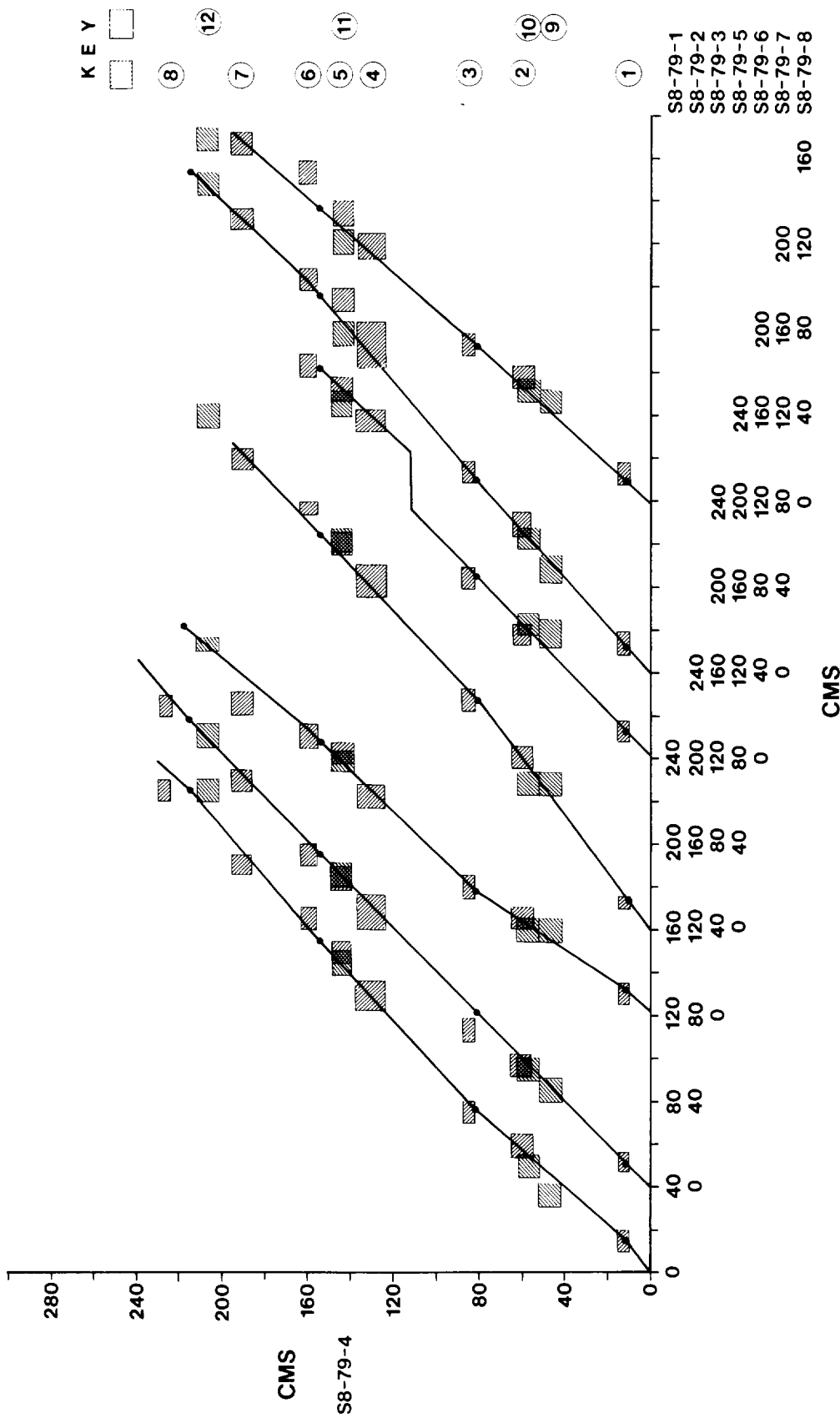


Figure 31. Shaw correlation diagram showing correlation of cores S8/79/1 to 3 and S8/79/5 to 8 to core S8/79/4. Dots represent lithological changes; boxes represent distance between samples. Correlations represent: (1) oxygen isotope stage 1/2 boundary; (2) minimum value of 180 during oxygen isotope stage 3; (3) oxygen isotope stage 4/5 boundary; (4) interval of sinistrally coiled *G. truncatulinoides*; (5) low percentage of *G. bulloides*, high percentages of *G. inflata* and *G. ruber*; (6) oxygen isotope stage 5/6 boundary; (7) low percentage of *G. inflata* during oxygen isotope stage 6; (8) oxygen isotope stage 6/7 boundary. Boxes with opposite shading represent coccolith interval boundaries; (9) extinction point of *G. aperta*; (10) interval 1/2 boundary; (11) interval 2/3 boundary; (12) interval 3/4 boundary. (See text for explanation).

TABLE 3 - Sedimentation rates in cm/10³ yrs computed from piston cores from the KTF area.

Oxygen Isotope Stage	82PCS01	82PCS02	82PCS04
1	2.8		2.6
2-4	2.7		2.6
5	3.2	2.0	2.4
6	3.6	2.2	2.4
7	3.0	2.6	2.5
8	2.0	1.6	1.6
9		2.6	2.3
10		3.3	3.9
Average	2.9	2.4	2.5

cores, were not erosive.

In the gravity cores there is evidence of slumping in cores S8/79/6 and S8/79/7. In core S8/79/6 the slump occurs within oxygen isotope stage 5. It was first picked out by the coccolith data but can also be seen as an anomaly on the oxygen isotope and planktonic foraminiferal plots. This slump represents the addition of 26 cms of sediment (length uncorrected for core shortening). The Shaw diagram (Figure 31) shows an offset of 26 cms in the regression line for core S8/79/6, which indicates that erosion did not accompany this event. The base of the slump in core S8/79/7 was not penetrated (Figure 19) and so its total thickness is unknown, as is any association it may have with erosion.

Hiatuses have been identified in cores S8/79/2 and S8/79/8, but neither core is long enough to establish the amount of missing sediment. By analogy to the coccolith occurrences in core 82PCS02, it is clear that all of oxygen isotope stage 7 is missing in core S8/79/8 which in core 82PCS02 comprises 1.5 metres of sediment. Similarly, about 1m of sediment is missing in core S8/79/2. Neither core shows development of a hardground at this level. This we interpret to indicate a removal of sediment (erosion) rather than cessation of supply (non-deposition).

The hiatuses in cores S8/79/2 and 8 and the slump in S8/79/7 all occur at the top of oxygen isotope stage 7. This could indicate a regional event at around 190,000 years B.P.; for example, an earthquake, or an interval of changed sedimentation conditions, such as a period of bottom current erosion. All three

cores occur in topographically low areas rather than on or near steep slopes. It is not possible, at present, to suggest which type of activity is more likely.

With a few exceptions, therefore, the cores show evidence of relatively quiet deposition and the core-to-core correlations appear to demonstrate good horizontal continuity. No major slumps or hiatuses have been recorded. Sedimentation rates across the area are reasonably constant when corrections are made for shortening in the gravity cores. Cores taken so far at locations displaying hyperbolae on the seismic profiles show little evidence of sediment disturbance. On the other hand, the sampling to date has been limited to the top 10 metres of sediment, representing the last 400,000 years. There may be major undetected sediment disturbances or significant changes in sediment type below this depth (Section 4b). Furthermore, coring has so far been concentrated on the flatter areas whereas the areas adjacent to fault scarps and at the base of some of the hills have been avoided. Almost certainly these areas will show significant sediment disturbances. Should there be any areas of major erosion, such as a large slump, then Pliocene chalk might outcrop and lead to easy lateral pathways for pore water migration.

4(g) VOLCANIC ASH DISTRIBUTION

When the 'Shackleton' gravity cores were first described and X-radiographed, a volcanic ash layer (sediment containing more than 15% volcanic glass) was identified in one of them. The 5 cm thick graded layer was found in core S8/79/1, at a depth in the sequence corresponding to an age of approximately 165,000 years. The same layer was not immediately apparent in the other ten cores from KTF, nor did Ruddiman and Glover (1972) report any ash layers in RE5-34, the 5-metre long piston core taken by Lamont Doherty Geological Observatory. It was suspected that equivalent occurrences of the layer might exist in the other KTF cores as increases in the background level of the fine volcanic material that is generally disseminated through the marl and ooze intervals. As noted in section 4e, magnetic susceptibility measurements, which on other study areas had proved useful in this context, were inconclusive when run on the KTF cores because of the effects on the instrument of ice-rafted debris.

The micropalaeontological stratigraphy was used to identify zones up to 50-cm thick within each of the cores that were the age equivalents of the layer in core S8/79/1. Smear slide sampling was carried out in the zones at four, two and finally one centimetre intervals. Three cores, S8/79/2 to 4, were found to contain volcanic ash concentrations at the relevant levels in the sequence. The

equivalents of the 5-cm thick graded layer in S8/79/1 then were 0.4 cm thick laminae.

Sediment samples from the laminae and the layer were treated with HCl to remove the carbonate material, mounted on gelatin slides and tested using Rayner fluids for refractive index determination. The refractive index (R.I.) of the glass in S8/79/1, 3 and 4 was 1.515 (± 0.005) while that in S8/79/2 was 1.525 (± 0.005). This difference possibly indicates separate volcanic sources but could also result from varying volcanic glass devitrification (Müller, 1961). The latter explanation now seems likely since electron microscope analysis of the ash samples showed up no systematic morphological differences between their component volcanic glass shards. All four samples contained both reticular and plane shards, varying in size from 60 μm to 360 μm (Figures 32 and 33).

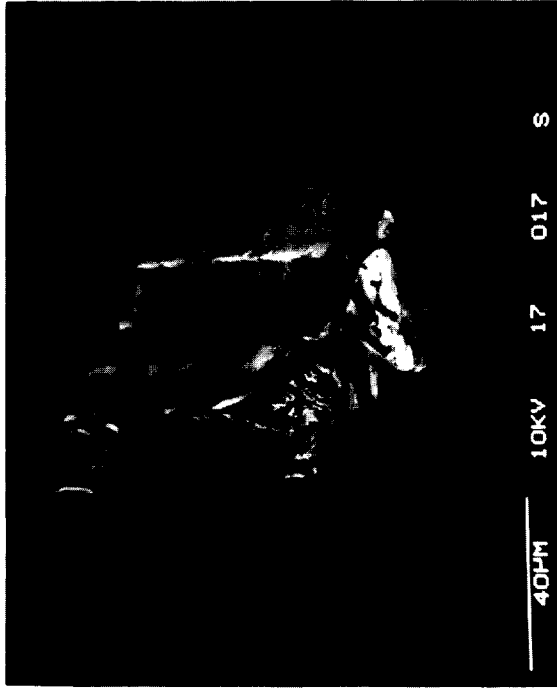
Because of the time coincidence of the layers we conclude that they represent a single volcanic eruption, although the grading of the layer in S8/79/1 and its apparent patchiness over the area suggests that it has undergone redeposition.

The most likely source of the ash layer is the Azores. Sigurdsson and Carey (1981) described ash from a Caribbean eruption which had travelled up to 790 km from source so it would not be unusual for the ash identified at KTF to have travelled with the prevailing winds the 660 km or so from the Azores. Ice rafting of volcanic material from the north, recognised by Ruddiman and Glover (1972) was ruled out as a possible source for this ash because their 9000-year-old ice-rafted ash, so prevalent in northern cores, is not present in the tops of those from KTF.

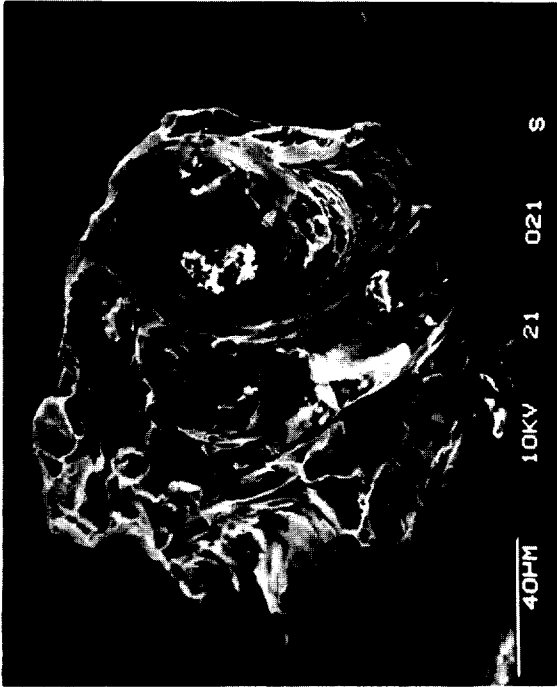
4(h) GLACIAL ERRATIC AND ICE-RAFTED SAND DISTRIBUTIONS

A glacial erratic is defined as "a rock fragment carried by glacial ice deposited some distance from the outcrop from which it was derived" (Bates and Jackson, 1980). The occurrence of glacial erratics in the King's Trough region was first reported by Edwards (1883). Since then, glacial erratics have been commonly found in other dredge hauls from sites around the area (Cann and Funnell, 1967; Ramsay, 1970; Stebbins and Thompson, 1978; Kidd *et al.*, 1982) giving cause for concern that ice-rafted material might be present in sufficient quantity to hinder some of the marine disposal methods being considered for high-level radioactive waste. Present-day iceberg movements and sightings are collected by the U.S. Navy (USN00, 1968) which has records of iceberg sightings at and somewhat south of the KTF area.

The findings reported in this section are based upon a study of the



S8/79-1



S8/79-2

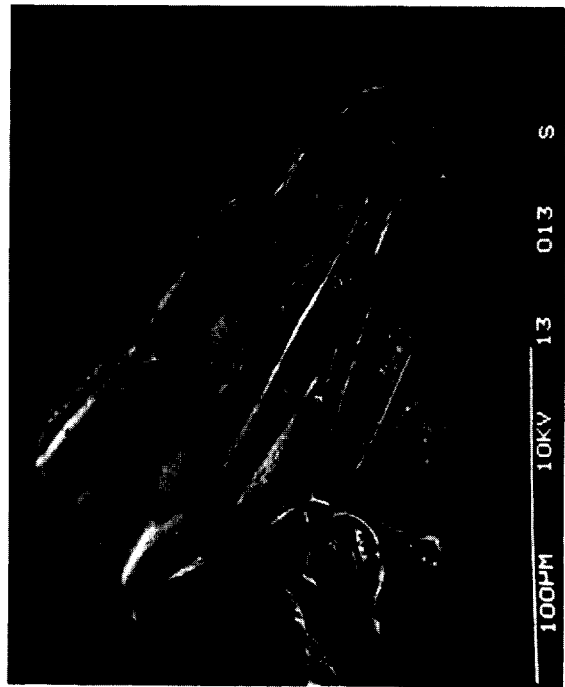
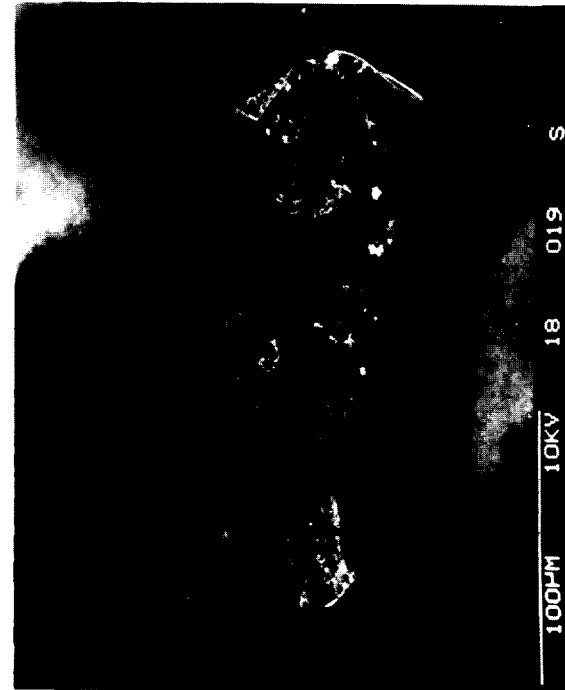
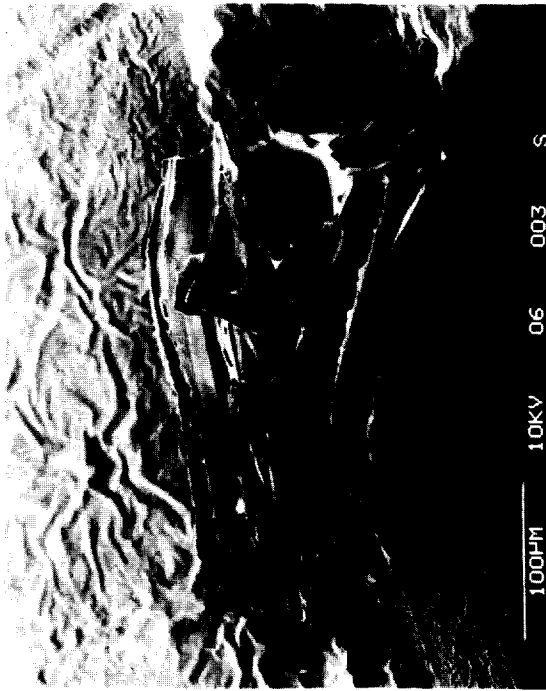
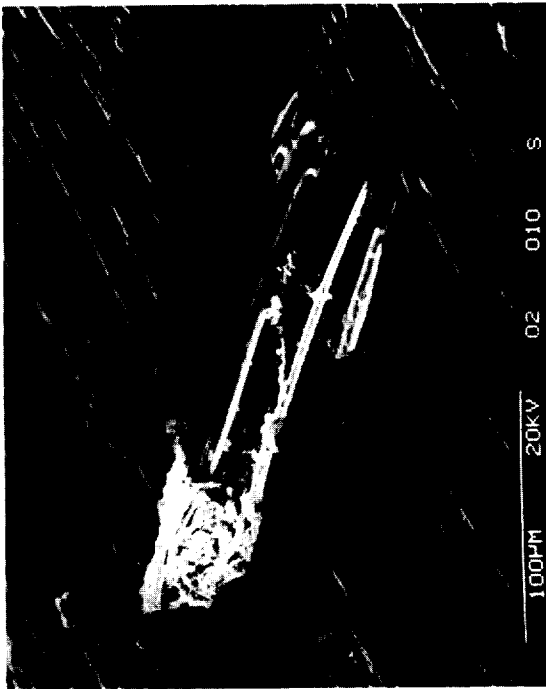
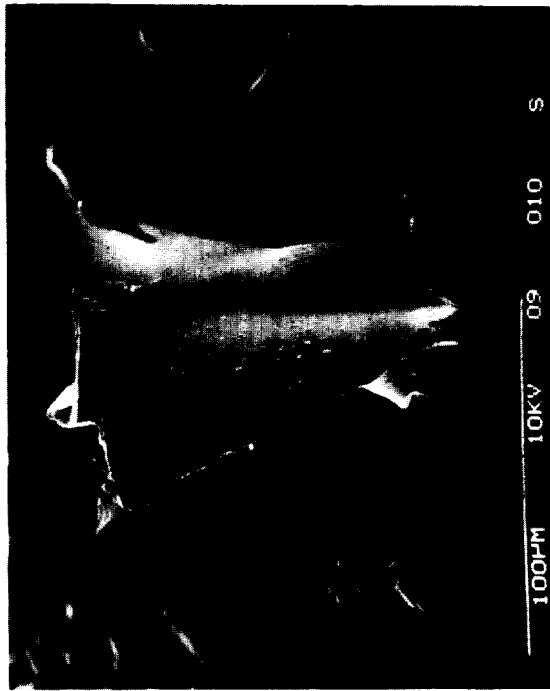


Figure 32. Selected electron micrographs of volcanic glass shards from the ash layers in S8/79/1 and 2. All, except S8/79/2 (lower), show pumice shards whose outer surfaces are bubble walls; S8/79/2 (lower) is a large bubble wall shard, possibly a large bubble wall shard; scale bars in microns.



S8/79-4



S8/79-3



Figure 33. Selected electron micrographs of volcanic glass shards from the ash cores S8/79/3 and 4; pumice shards (upper) and bubble wall shards (lower); scale bars in microns.

distribution of ice-rafted material over the whole of the Northeast Atlantic seafloor. Rock dredge collections examined in the UK and abroad included material from eleven stations in the general vicinity of KTF (Figure 34, Table 4). Regrettably, many of the samples had been split during their initial examination and, with the exception of material recovered at V27 Dr. 8, none of the samples could be used for grain-size analysis.

Studies of glacial material from eight stations, collectively with a wide latitudinal spread in the Northeast Atlantic (Table 4), indicate that grain size follows a negative exponential distribution; the finest material being most abundant (Figure 35). To the north of KTF at 50°N, 14°W a frequency of 100,000 particles per square kilometre has been determined for material larger than 1.5 cm (maximum diameter) lying on or within 3 cm of the sediment surface (Figure 36). This estimate is for material deposited during the last 1000 years and represents only 0.04% of the total time over which ice-rafting has taken place in the North Atlantic. Geotechnical review studies suggest that boulders in excess of 25 cm diameter would become buried when dropped because of their higher terminal velocities in the water column (Anonymous, 1982). This would explain the apparent lack of large material in dredge hauls over sediment surfaces and indicates that further work requires use of a deep-towed high-resolution seismic profiler if distributions of the larger material within the sediment are to be examined.

The largest boulder to have been dredged from the vicinity of KTF has a maximum diameter of 50 cm. This is the largest size single rock fragment that it is possible to recover using conventional rock-dredging equipment. This particular boulder was recovered from an area of rock outcrop (Station D9564). The only real limitation on boulder size is iceberg size. Direct observations (USNOO, 1968) and studies of iceberg plough marks (Belderson *et al.*, 1973) show that icebergs of 300 metres draft are not uncommon in the Northeast Atlantic. Such an iceberg could potentially transport boulders up to 78-metres diameter; calculated on the basis that an iceberg may carry up to 7.5% by volume of rock.

Studies of ice-rafted sand in sediment cores have shown that the rate of ice-rafting varies synchronously with the climate as it changes to and from glacial conditions (Ruddiman and McIntyre, 1981). Two cores close to the study area (Figure 34) indicate that present-day input of ice-rafted material is between 12% and 38% of input rate during the last glacial interval (Ruddiman, 1977; Figure 37). Such variations will be taken into consideration in future work involving detailed assessments of both the distribution and the volume of ice-rafted material in the North Atlantic.

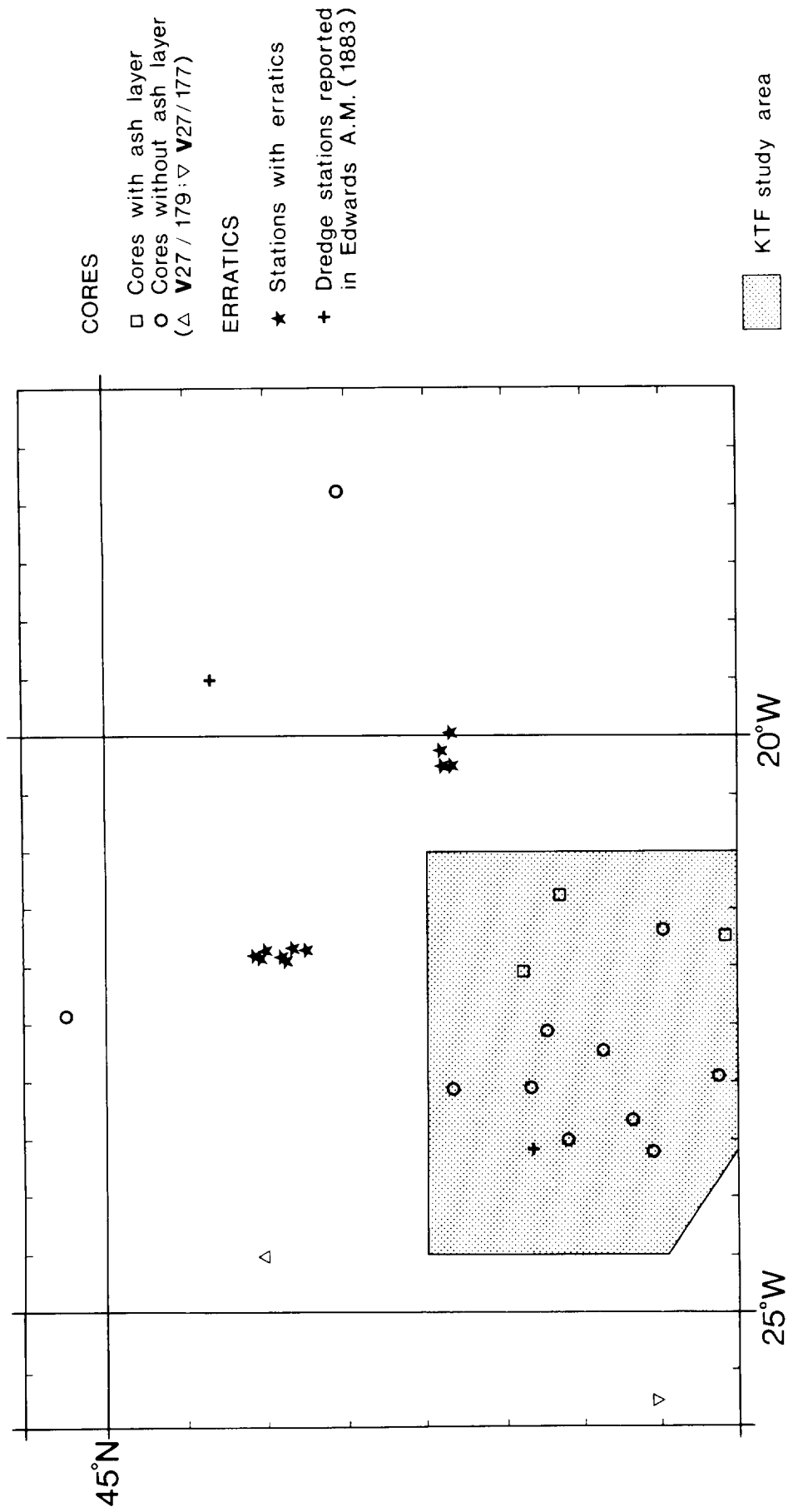
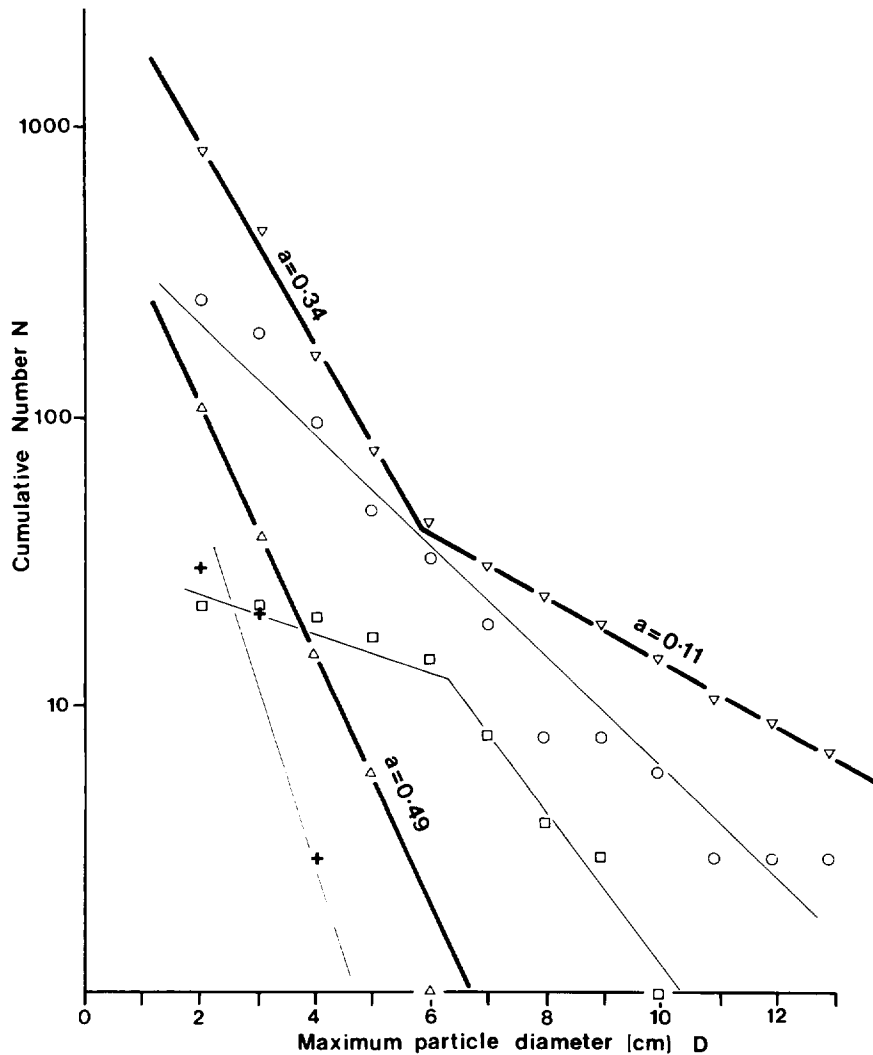


Figure 34. Locations of stations used in the study of ice-rafted material.

TABLE 4 - Location of dredge and core stations used in the study of glacial erratic and ice-rafted sand distributions.

STATION NO.	POSITION		WATER DEPTH (m)
	Latitude	Longitude	
A. Rock dredge collections containing glacial erratics examined			
D5614	42°53'.0N	20°16'.0W	3890
D5979	42°50'.0N	20°16'.0W	4900
D5607	42°54'.0N	20°08'.0W	3288
D5610	42°51'.0N	20°16'.0W	4645
D5626	42°50'.0N	19°59'.0W	2646
D9563	43°54'.0N	21°57'.0W	3850
D9561	43°50'.0N	21°51'.0W	3700
D9562	43°54'.0N	21°55'.0W	3200
D9564	44°00'.0N	21°52'.0W	2550
D9565	43°53'.0N	21°57'.0W	4100
V27D8	43°44'.7N	21°51'.6W	unavailable
B. Glacial erratics reported in the literature			
T133	42°19'.0N	23°36'.0W	4000
T136	44°20'.0N	19°31'.0W	4255
D7285	44°08'.0N	22°17'.0W	2885
D7289	43°54'.0N	23°09'.0W	2850
D7290	43°58'.0N	23°08'.0W	3150
D7294	44°02'.0N	21°56'.0W	2275
D7296	44°03'.0N	21°55'.0W	2060
D7297	44°05'.0N	21°55'.0W	1675
C. Dredges from sites to the north, used for grain-size determinations			
D9825	45°55'.0N	19°57'.0W	4800
D9756/9	49°47'.0N	14°02'.0W	4050
D9756/14	50°04'.0N	13°56'.0W	3690
SMBA 27	54°40'.0N	12°16'.0W	2880
SMBA 140	54°40'.0N	12°16'.0W	2912
SMBA 144	57°13'.0N	10°20'.0W	2240
SMBA 26	56°35'.0N	09°08'.0W	573
D. Cores from Ruddiman (1977)			
V29-177	41°32'.0N	25°43'.0W	3391
V29-179	44°01'.0N	24°32'.0W	3331



LEGEND:

- ▽ D9825
- △ D9756^{#9}, D9756^{#14}, SMBA27, SMBA140
- SMBA 144
- SMBA 26
- + V27 Dr.8

The straight lines on this graph can be represented by the equation
 $\text{Log}_{10} N = \text{Log}_{10} M - aD$

where: 'a' is the gradient of the line
 'M' is the intercept on the y axis
 'N' is the number of particles with diameter greater than or equal to D

Figure 35. Grain-size data from rock dredges: log-normal plot of cumulative number of particles against grain size. The cumulative value decreases exponentially as grain size increases; thus the distribution is a negative exponential function: the change in gradient of the lines at 6-cm diameter indicates that there may be two populations being sampled in the same area. For the latitudes so far examined (45°-57°N) there is no change in the relative frequency of different grain sizes; however, the bulk quantity does vary. The two heavier lines denote the stations for which statistical control was good.

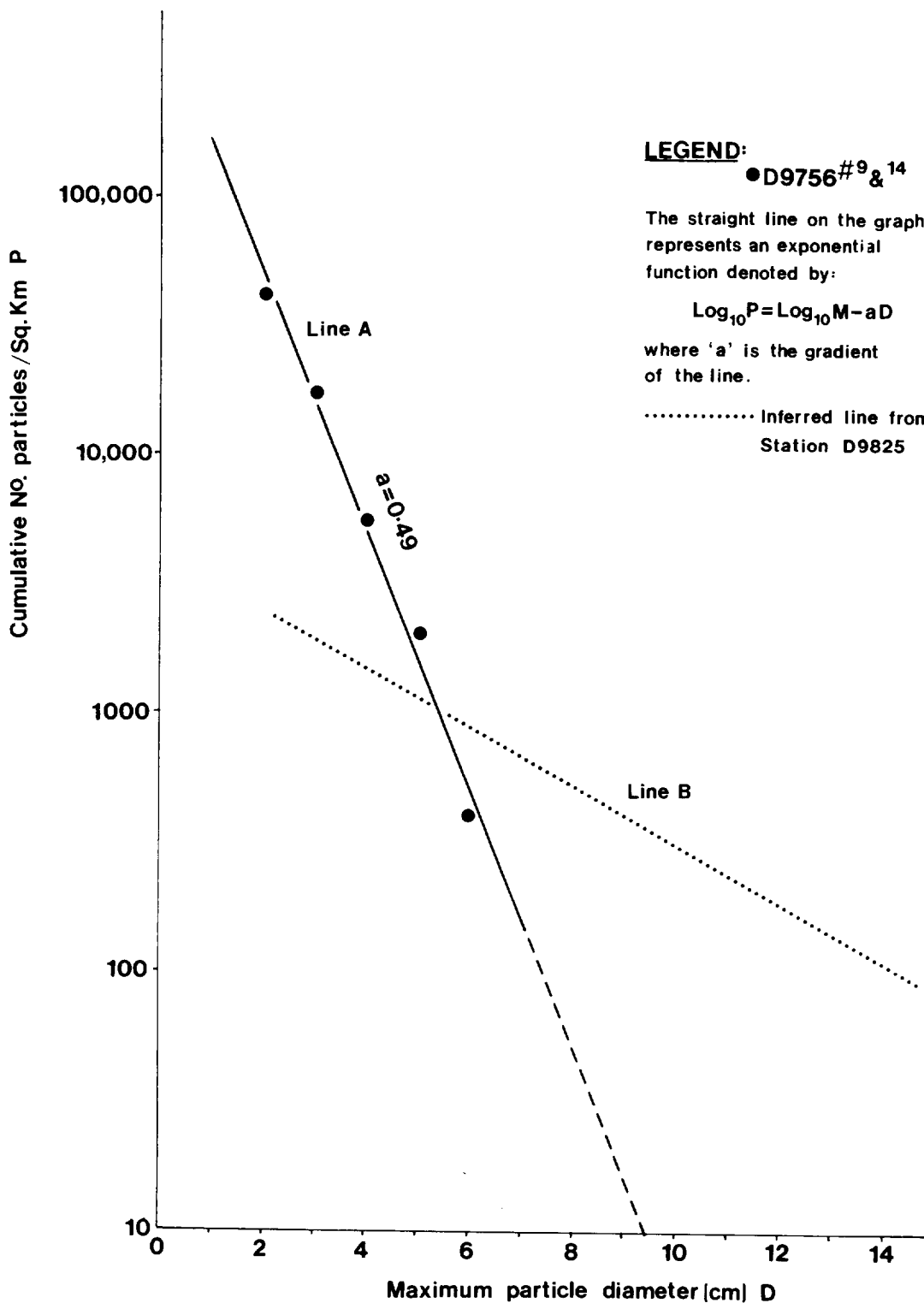


Figure 36. Normalised rock-dredge grain size data from stations D9756/9 and D9756/14; heavy line A is the cumulative frequency of particles/sq km. From this, estimates of the number of particles greater than 1.5 cm diameter per sq km can be made: for material >6 cm diameter, dotted line B should be used.

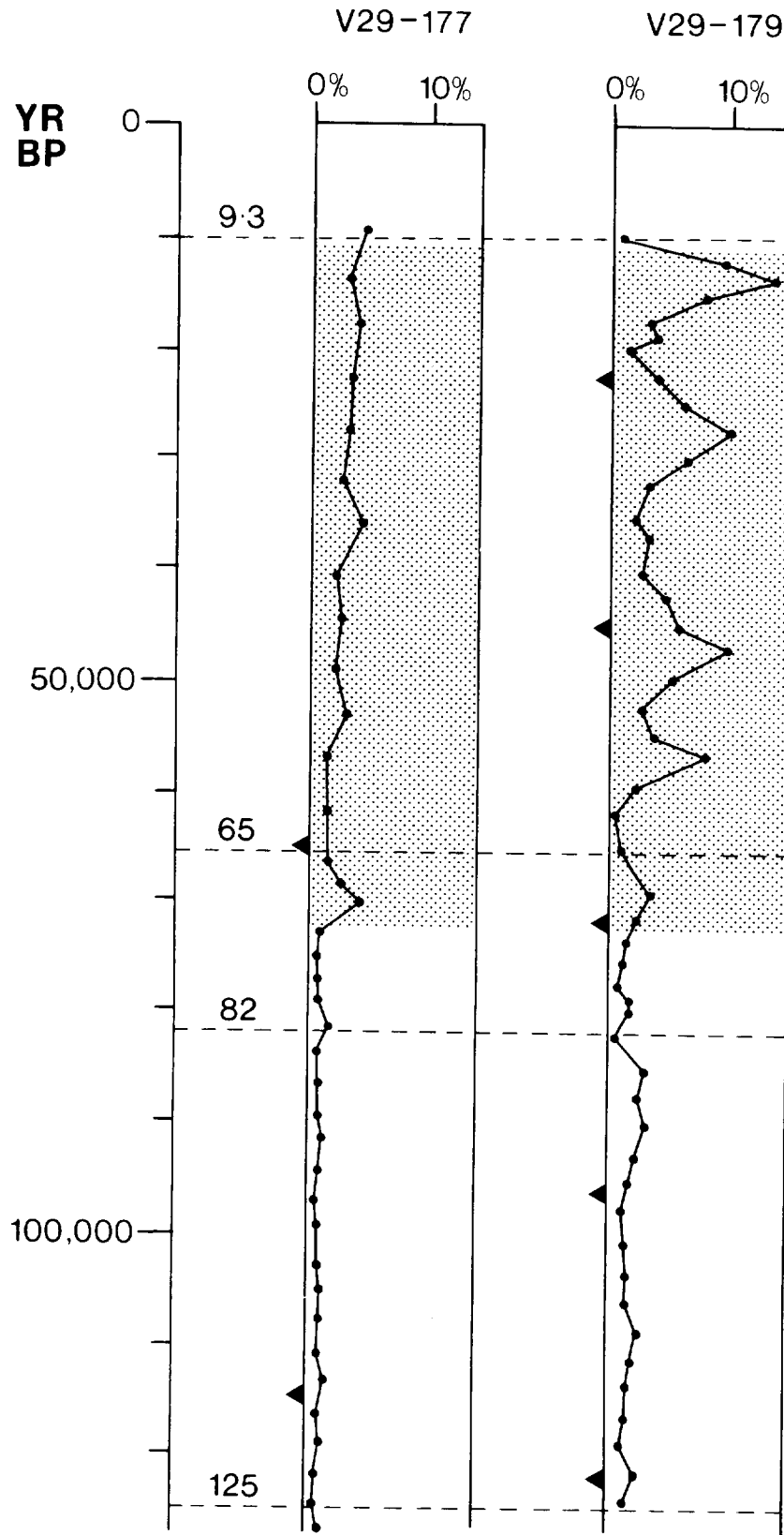


Figure 37. Downcore percentages of non-carbonate sand in cores V29/177 and 179 against time; stippled zone is the last glacial period; surface sediments were not recovered (after Ruddiman, 1977).

5. PHYSICAL PROPERTIES OF THE SEDIMENTS

5(a) CONSOLIDATION AND PERMEABILITY CHARACTERISTICS

A limited amount of physical properties data has been obtained from the King's Trough Flank study area. This has been obtained from the single Kastenlot core D10333 (15 cm square section) taken on Discovery cruise 118 in the southern part of the area (Figures 17 and 20, Table 1).

The consolidation and permeability characteristics of sediments composed predominantly of calcium carbonate microfossil debris have been studied relatively little compared with clay-rich sediments. Bryant *et al.* (1974), using consolidation data from a range of sediments, provided a clear discussion on the type of information that can be obtained from consolidation tests. It was concluded that fine-grained carbonate muds consolidate in a similar way to non-carbonate silty clays. The only difference observed was that under equal loads older carbonate sediments do not consolidate to as low a final void ratio as non-carbonate sediments. Miller and Richards (1969) observed marked differences in the void ratio/pressure relationships obtained from a laboratory consolidation test and from a sedimentation-compression computation on a short core of calcareous ooze. They concluded that laboratory consolidation tests on carbonate oozes should be interpreted with caution for geological and engineering purposes.

Six samples from core D10333 have been tested. Sample D10333/7 taken at a sub-bottom depth of 76 cm is used to illustrate their behaviour. The consolidation test is similar to that commonly used (Lambe and Whitman, 1979) except that the sample (75 mm in diameter, 20 mm in height) is subjected to a back pressure of 700 kPa to ensure complete saturation. Following each incremental load the permeability is measured assuming Darcian behaviour by applying a small hydraulic gradient and measuring the volume flow of water through the sample (Lambe and Whitman, 1979).

Figure 38 shows the results from sample D10333/7. The void ratio/vertical effective stress ($e \log p$) shows no obvious preconsolidation pressure, hence it is assumed to be normally consolidated. The slope of the $e \log p$ curve during the latter stages of the test defines the compression index, C_c , which in this case is 0.37. The compression index was found to vary between 0.2 and 0.63 in core D10333 depending on the carbonate content (higher values of C_c are obtained for lower carbonate values). These values are similar to data obtained by Buchan *et al.* (1971) on comparable North Atlantic sediments. The permeability/void ratio curve gives a permeability index (change in void ratio per logarithmic cycle of

SAMPLE : D10333/7
 SUB-BOTTOM DEPTH : 0.76m
 ORIENTATION : VERTICAL
 SEDIMENT TYPE : FORAM NANNO MARL

Initial void ratio e_0 --- 2.431

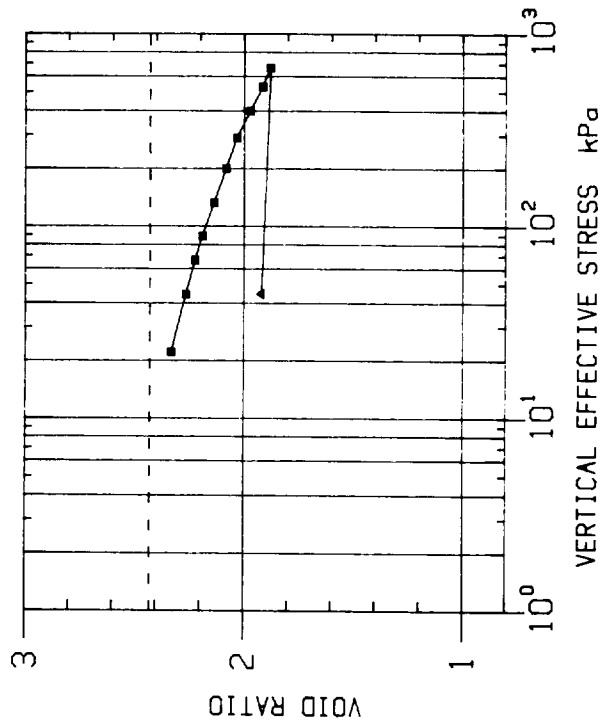
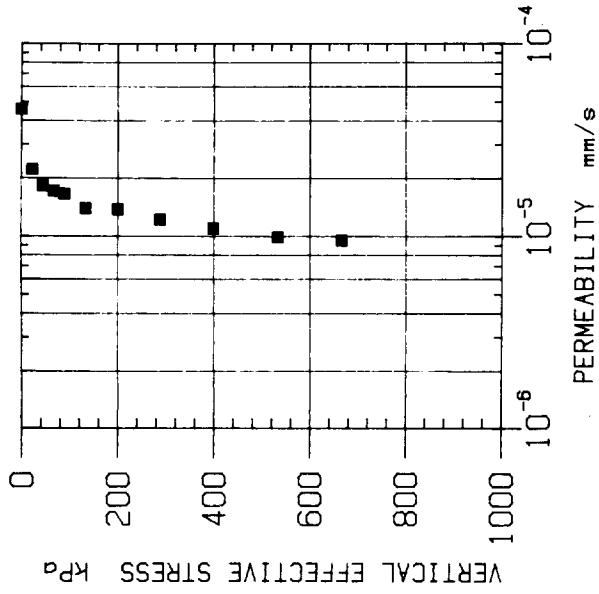


Figure 38. Permeability results of a consolidation test on a marl sample, D10333/7.

permeability) of 1.39. The extrapolated permeability at the initial void ratio ($e_0 = 2.431$) is 3×10^{-5} mm/s. The low value of C_c and the high value of the permeability index compared with other deep-sea sediments means that there is likely to be only a relatively small decrease in permeability with increasing depth as shown by the effective stress/permeability curve. For comparison purposes it is worth noting that 'red clays' have permeabilities around 2×10^{-7} mm/s at similar void ratios.

It is concluded, therefore, from the very limited data available that the surficial sediments in the KTF study area are probably normally consolidated (i.e. they exhibit no evidence of large-scale erosion or large excess pore pressures) and they have relatively high values of permeability ($\sim 10^{-5}$ mm/s). If confirmed by further sampling the higher values of permeability might make sediments of this type somewhat less attractive than deep sea clays as host media for shallow burial options of high-level radioactive wastes.

5(b) HEAT FLOW DATA

Three closely spaced measurements of sediment temperature and two of sediment conductivity were made at the location shown in Figure 17 (Station D10335). The instrument used was the model GR12 heat probe manufactured by Applied Microsystems Ltd., Victoria, British Columbia; shown schematically in Figure 39. The probe essentially comprises a 5m long, 5-cm diameter, solid steel strength member which acts as a support to a tubular steel, tensioned bowstring which houses the thermistors used for the temperature measurement. This arrangement minimises the effects of frictional heating by ensuring rapid attainment of thermal equilibrium of the sensors while also reducing the effects due to sediment disturbance. Temperatures are measured with a resolution of 0.008°C in terms of the thermistor resistances, and are logged on a reel-to-reel tape recorder every 15 seconds within the instrument head. Thermal conductivities were measured by observing the decay of a calibrated heat pulse created by passing a current through heater wires in the bowstring (Lister, 1979). The heat pulse is triggered by a seismometer circuit 7.5 minutes after probe penetration.

The temperature data were corrected for the effects of frictional heating according to the method of Bullard (1954) and the results are shown in Figure 40. For the first penetration (Figure 40a) the temperature profile is linear within the resolution of the instrument and the mean gradient is $7.69 \times 10^{-2}^\circ\text{C m}^{-1}$. The conductivity was not measured. The top thermistor recorded a temperature greater than the bottom water temperature thus confirming the complete burial of

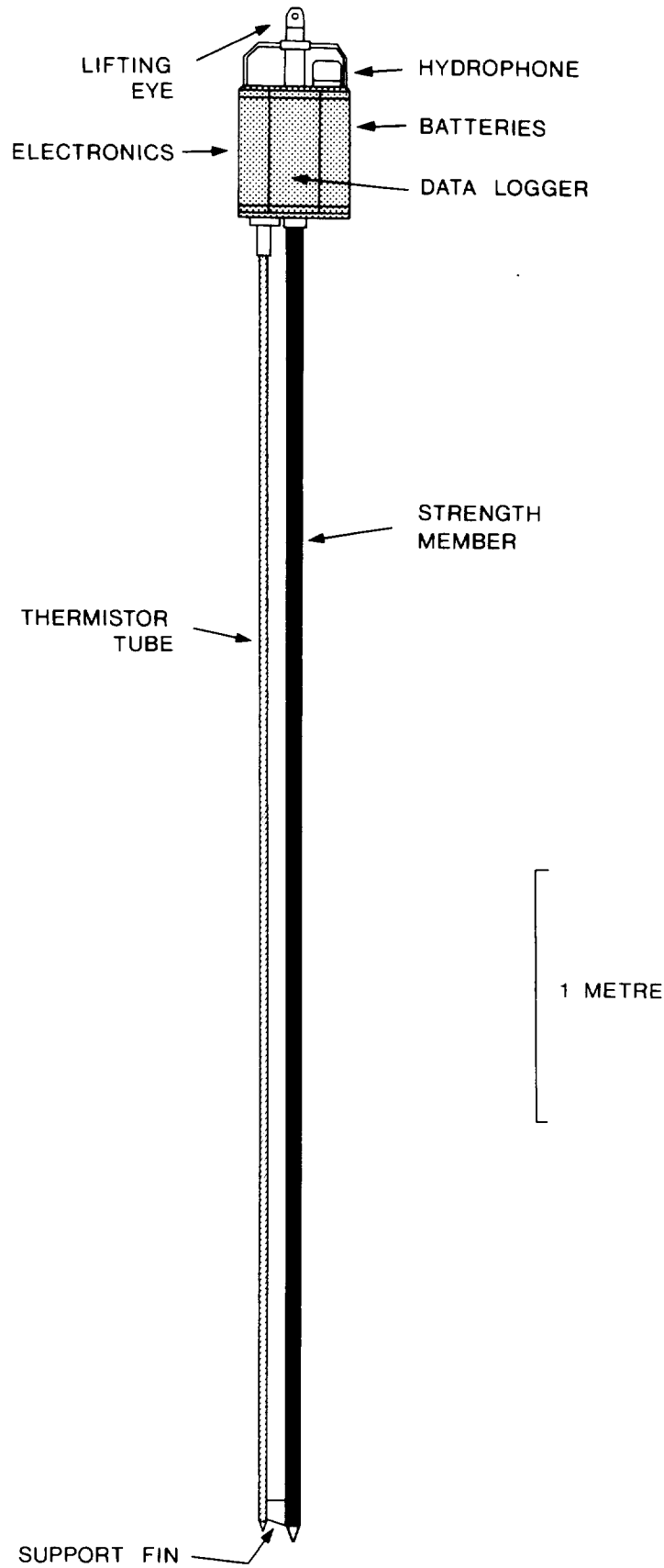


Figure 39. Schematic diagram showing the model GR12 Heat Flow Probe.

the probe. This also applies to the second penetration (Figure 40b) where the mean temperature gradient was $6.96 \times 10^{-2} \text{ }^\circ\text{C m}^{-1}$. This result excludes the value at 1.9 metres depth which is anomalous due to excessive thermistor drift. The temperature profile is again linear within the measurement resolution. The heat pulse decay gave a mean sediment conductivity of $2.1 \times 10^{-3} \text{ cal } ^\circ\text{C}^{-1} \text{ cm}^{-1} \text{ s}^{-1}$ which, when combined with the thermal gradient, gives a heat flow value of $1.46 \times 10^{-6} \text{ cal cm}^{-2} \text{ s}^{-1}$. This is slightly below the theoretical value of $1.67 \times 10^{-6} \text{ cal cm}^{-2} \text{ s}^{-1}$ for ocean crust of this age (~52 m.y.) according to the cooling model of Anderson et al., 1977).

On the third penetration (Figure 40c) the top thermistor did not enter the sediment which explains the discontinuity in the upper part of the profile. The temperatures between 0.9 metres and 4.9 metres depth exhibit a marked non-linearity which could not be explained by a conductivity change with depth. The computed heat flow (based on the mean gradient of $6.46 \times 10^{-2} \text{ }^\circ\text{C m}^{-1}$) is $1.36 \times 10^{-6} \text{ cal cm}^{-2} \text{ s}^{-1}$ which is similar to the previous value.

The curvature in this temperature profile can be explained in several ways (Noel, in press) viz.:

Changes in bottom water temperature: A sudden decrease in bottom water temperature prior to the measurement would cause a temperature wave to enter the sediment resulting in a gradient which increases with depth. However, this profile (Figure 40c) demands a sudden temperature drop of 0.17°C (120 days previously) which is in excess of the maximum temperature variation recorded by long-term deep current meters in the Northeast Atlantic (Müller, 1981). Similarly, the curvature is not likely to be due to any regular, seasonal changes in bottom water temperature which are only of importance in higher latitudes.

In-situ heat production: The curvature could be explained by a continuous heat production in the sediment. Possible mechanisms include exothermic chemical reactions due to diagenesis or biological activity, the conversion of potential energy to heat during compaction, the surface attenuation of seismic energy or the exothermic decay of radionuclides. The curvature in Figure 40c would require heat production at the rate of $0.1 \text{ cal cm}^{-3} \text{ y}^{-1}$. Although this rate appears to be low, the total heat demand per unit volume of sediment is greatly increased by the very slow oceanic deposition rate, thus reducing the likelihood of this being a viable mechanism.

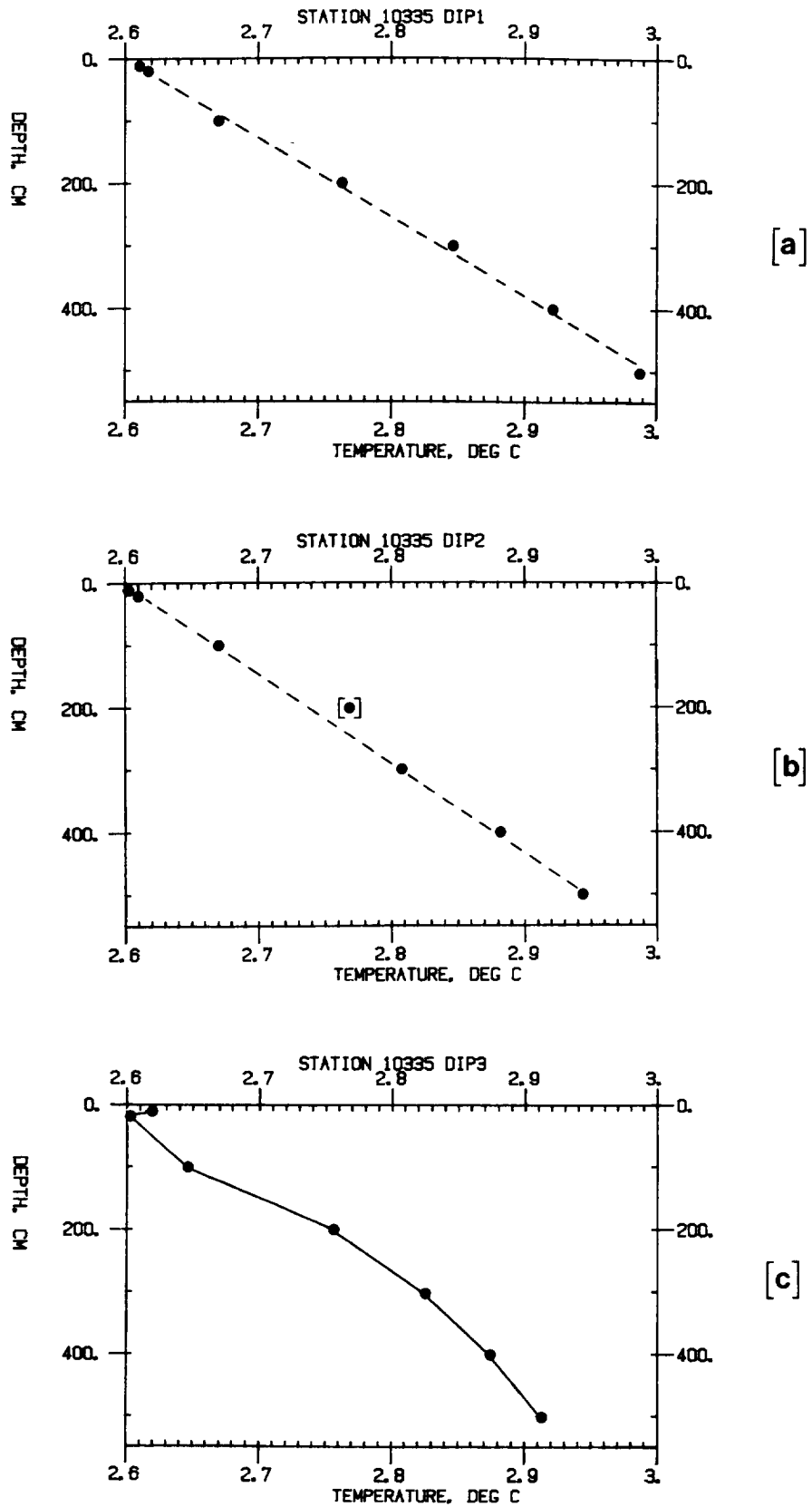


Figure 40. Results of three penetrations of the heat flow probe at station D10335; the temperature data are corrected for the effects of frictional heating; for explanation, see text.

Sedimentation Effects: A gradient increase with depth, such as seen here, could also be explained in terms of a disequilibrium profile following the removal of surface sediments (i.e. erosion). However, the probability of this observation occurring sufficiently soon (~1 year) after such a rare event must be regarded as very low.

Topographic effects: Irregular terrain can exert a major influence on the near surface temperature profile (Lachenbrach, 1968). This effect is particularly important where the topographic scale is similar to the probe length. It is, therefore, possible that the non-linearity seen here is due to the probe having penetrated near to a mound or ridge, several metres high, which could not be resolved by the ship's echo-sounder, whose beam width exceeds the scale of such surface irregularities.

Pore water advection: The vertical movement of pore water through the sediment column gives rise to curved temperature profiles (Bredehoeft and Papadopoulos, 1965). This effect can be used to model advection velocities from sediment temperature and conductivity measurements alone. The method has been applied to non-linear temperature profiles in deep sea sediments (e.g. Anderson et al., 1979).

The data of Figure 40 have been fitted by a conduction/advection model (Mansure and Reiter, 1979). The result implies an upward pore water flux with a velocity of 52 cm/y. If this velocity is genuine it would be sufficient to raise materials in solution at a depth of, say, 30m to the surface in only 58 years.

A search through the World Heat Flow Data Collection (Jessop et al., 1976) reveals no previous heat flow measurements in the KTF area. The data presented here are, therefore, the only thermal evidence to test the stability of the sediment pore water, albeit at only one station. The results from one temperature record show a marked non-linearity which may imply a rapid upward flux of sediment porewater. However, the influence of topography on the measurements may have been important in this case and it is, therefore, judged imperative to carry out further detailed sediment temperature measurements at this locality.

6. DISCUSSION

6(a) APPARENT CONFLICT BETWEEN THE GEOPHYSICAL SURVEY AND SEDIMENT CORE STUDIES

There appears to be a discrepancy between the geophysical interpretations of sedimentary processes in the KTF study area and the sediment core data.

To date our geophysical surveys have revealed a series of north-south scarps crossing the area with a 10-30 km separation, a series of rock outcrops at 40-50 km intervals often surrounded by steep (18-30°) slopes, and areas showing hyperbolic reflections on 3.5 kHz and 10-kHz profiles. All this evidence suggests considerable instability in the area and possibly also erosion of sediment. There are some areas of relatively smooth, and presumably more stable, seafloor: usually these are less than 35 km wide.

The twelve cores are well correlated across the area. Only two contain sediment slumps and two contain hiatuses. The hiatuses and one of the slumps represent no more than a couple of metres of missing or added sediment, whereas the other slump was not fully penetrated. Twelve cores in an area of 66,000 square kilometres, however, is a very low density, particularly when individual sediment disturbances may spread over no more than a hundred square kilometres. Four of the cores were taken in relatively smooth areas on the geophysical records and five cores were taken in areas showing hyperbolic reflections. There appears to be no obvious relationship between the areas of smooth seafloor, or the areas showing hyperbolae, with the occurrence of sediment slumping or hiatuses in the cores.

The hyperbolic reflections are thus proving to be enigmatic, in that, away from hills where they could be interpreted as side echoes, they are thought to be due to slumping or erosion, whereas the cores taken at these locations show no sedimentary evidence of such disturbances in their upper layers. Further detailed investigations involving coring, geophysical profiling and seabed photography are required to elucidate these problems.

To resolve the more general problem of the discrepancy between the sedimentology and the geophysical evidence in the KTF area it is necessary to obtain a series of extra cores. Particular locations to sample are 'smooth areas' that display hyperbolae on 3.5 kHz records and bright backscattering on sonographs; especially where they occur close to the bases of the scarps on steep slopes. Here the extent and frequency of mass sediment movement or current erosion might be determined.

It is clearly necessary to take longer cores than our present maximum lengths

(approximately ten metres) to obtain a more complete picture of sedimentation in the area and, more important, to provide a realistic assessment of the geology at the depths envisaged for disposal.

6(b) GENERAL SUITABILITY OF THE KING'S TROUGH FLANK AREA FOR DEEP OR SHALLOW DISPOSAL

In this section we assess our present geophysical and geological knowledge of KTF in comparison with the guidelines for the selection of sub-seabed disposal sites proposed by Searle (1979). At the outset, we note that these guidelines, and indeed others proposed at that particular time (e.g. Hollister et al., 1976), formed an assessment of factors which would probably need to be taken into account in selecting potential disposal sites. Their proposers recognised that information that was to come from generic study areas like KTF might require modification of some of the guidelines. One example might perhaps be the early suggestion that potential sites should lie below 4000-metres water depth (which clearly rules out most of the KTF area). Similarly, the requirement to avoid steep slopes because of potential sediment instability might be modified so that maximum acceptable slope angle would reflect sediment type, rate of sediment deposition, tectonic stability of the area, etc.

The information in this report relates primarily to the geological medium into which the waste might be emplaced. Thus, we discuss item by item below, the "desirable characteristics of the geological barrier" as outlined in Searle's (1979) guidelines, with particular emphasis on possible modes of failure of the barrier. We employ the numbering of characteristics as used in the 1979 report for ease of comparison. Some characteristics we are unable to comment upon from our present data set; for instance, geochemical studies of the sediments in the KTF area have yet to be made.

A1. The site should avoid areas near steep slopes where sediments may be unstable.

The area is a relatively rugged portion of the deep ocean floor with hills and scarps 10 to 30 km apart (but see Figure 41). Slopes around the hills range from 18° to 30° and the seafloor there is hummocky. Some of the scarps in the southwest represent sudden changes of seafloor depth of the order of 700 metres. Areas of relatively smooth seafloor with slopes of less than 2° do occur but in pockets, none more than 35 km wide. At present we are unable to fully assess the evidence of sediment stability on the slopes and have no relevant data close to

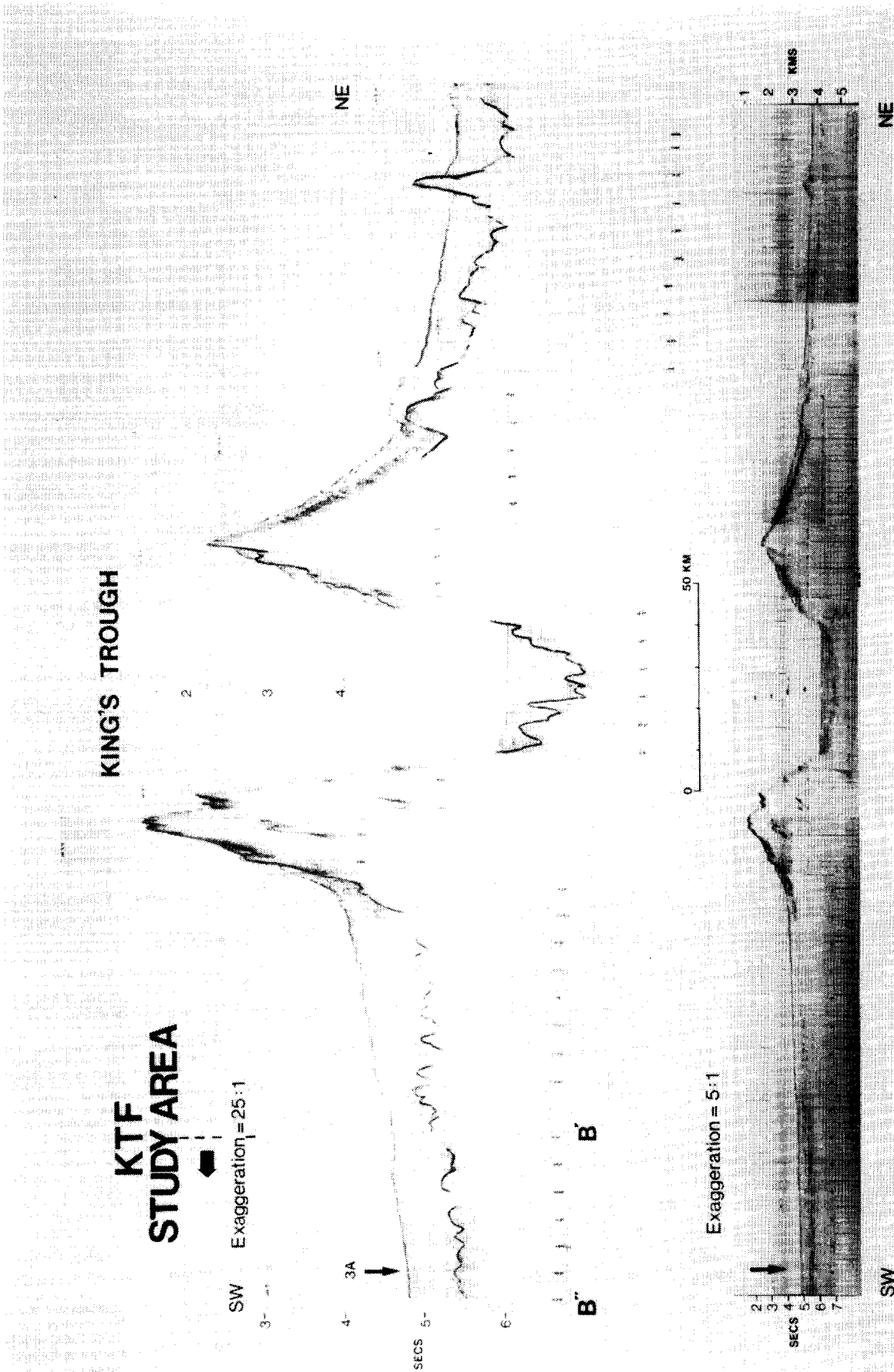


Figure 41. Discovery Cruise 54 seismic profile of the King's Trough Complex showing the proposed IPOD drill-site "NA-3A"; for location of the track see Figure 2. In the lower profile, the original (upper) record has been photographically reduced in one plane to remove some of its vertical exaggeration. The figure demonstrates that the apparent ruggedness of such seafloor terrains, compared to land areas, is partly a consequence of the scales used during shipboard recording of profiles.

the (fault) scarps.

- A2. The site should avoid areas of recent erosion, dissolution or mass movement of sediment, or the waste should be buried deep enough to be unaffected by such processes over a suitably long period.

EROSION - The generally weak bottom water circulation of the present day probably existed in the glacial periods also and could have been even weaker during pure ooze deposition in the late Neogene. At the present day, maximum current speeds around upstanding topography are probably sufficient for sediment erosion (Southard et al., 1971) and some of the hyperbolae detected during profiling could relate to erosional features. Core studies indicate periodic current erosion in the form of winnowing at the sediment surface and some hiatuses are present. More coring is needed to determine the scale and horizontal extent of erosion.

DISSOLUTION - The area is unaffected by significant dissolution; it has never been below the regional CCD and the CCD has not changed drastically. It has steadily deepened since the mid-Miocene, that is, approximately the last 12 million years (Van Andel, 1978; Kidd and Davies, 1978).

MASS SEDIMENT MOVEMENT - No large sediment slides have been interpreted from the geophysical profiles. Slumps do occur but, because of incomplete geophysical and core data, their magnitude and distribution are unknown. More coring is necessary to resolve this data gap.

- A3. The site should avoid areas of recent tectonic activity.

No major regional tectonic activity has affected the area since the formation of the King's Trough complex (around 16 million years ago). However, basement-controlled faults are widespread and one fracture zone is suspected. The height of the fault scarps (up to 700 metres high) and general ruggedness of the area might imply continuing recent tectonism. Even if the faults are no longer active they could form easy pathways for pore water migration. No evidence has so far come to light of compressive tectonics in this region that could bring about folding in the sediment sequences.

- A4. The site should avoid areas of recent volcanic activity.

No major volcanic ash horizons have been found in our cores but volcanoclastic strata are suspected at some hundreds of metres' depth in the regional sediment sequences. Intraplate volcanic activity appears to have ceased

around 30 million years ago. Volcanic horizons, therefore, are unlikely to present penetration problems to either shallow or deep disposal, but they may present modelling difficulties around deeply-buried waste.

A5. The site should be in a region of low seismic activity.

Historical records show the area to be characterised by low seismicity. However, one interpretation of the coincidence of a slump in one core with hiatuses in two others at about 190,000 years ago is that a regional earthquake occurred at that time that was capable of initiating sediment instability.

A6. The site should have adequate sediment thickness.

Acoustic basement, interpreted as igneous rock outcrop, occurs in patches at intervals of about 40 to 50 km. Most of the area, however, has an overlying sedimentary sequence at least 200 metres thick; the average thickness is 400 metres.

A7. The disposal medium should be laterally homogeneous.

Our present cores penetrate to a maximum depth of 10 metres below the seafloor so it is not possible to determine lateral sediment homogeneity at the presumed burial depth for shallow disposal. Calibration of our high-resolution seismic profiling is not sufficient at present to rely on this technique. Over the interval which we have sampled, the individual marl and ooze units are correlatable but, as outlined in Section 6(a), the geophysical data argues against lateral continuity of more than 35 km and the density of cores is insufficient to make any firm prediction. Should there be any large slumps in the area that have displaced 50 meters or more of sediment, then Pliocene chalks may crop out. These would be expected to have somewhat higher permeabilities than those measured in the Quaternary sediments. The widespread fault scarps, observed on the geophysical profiles, could also cause Pliocene chalk to crop out if they are reactivated. Even if inactive in recent geological time the fault zones that are observed could still provide easy pathways for pore water movement.

[A9 Diffusivity and A10 Adsorptivity - not dealt with in this report]

A11. The disposal medium should have a large active grain surface area to maximise nuclide adsorption.

In the Quaternary sediments, median grain diameters range from 2 to 8 microns

for both oozes and marls (see Appendix IV). In winnowed layers or the bases of graded layers, median grain diameters can reach 160 microns. Ice-rafted material can reach boulder size, although most is pebble or granule grade in the terminology of Inman (1952) (Figure 37). For the purposes of adsorption studies, however, the median grain sizes of the calcareous sediments at KTF should be regarded as lying in the "clay" and "very fine silt" grades (Inman, 1952) and thus individual particles do have large active grain surface areas. Grain sizes in the sediments at depth should be similar to those in the Quaternary oozes.

A12. The disposal medium should have low organic carbon content to minimise ion mobility.

No measurements of organic carbon have been made on these cores, taken for stratigraphic rather than geochemical purposes. The sediment types (pelagic marls and oozes) suggest that organic carbon will be a very minor constituent in this area, probably less than 0.2% (Lizitzin, 1972).

[A13 Strength of the disposal medium and A14 Plasticity of the medium - not dealt with in this report]

A15. The medium should contain no natural gases or gas hydrates.

Neither natural gas nor solid gas hydrate are likely to occur on the KTF study area which has throughout its geological history received pelagic ooze and marl sediments that are generally low in organic carbon.

A16. The site should be relatively free of obstructions on the seafloor.

The possibility of encountering glacial erratic pebbles or boulders on or in the sediments is probably higher in the KTF study area than in the other study areas. Further investigations are necessary to determine the extent of such obstructions.

A17. The thermal conductivity of the medium should be high enough to ensure acceptable in-situ temperatures.

In-situ measurements made by the heat probe show that the thermal conductivities of the near-surface sediments in the KTF area are similar to values recorded for carbonates elsewhere in the oceans. Due to consolidation, conductivity values will increase with depth. More data are thus needed on the conductivity of the deeply-buried sediments at likely waste burial depths.

[A18 Effects of the waste on the medium and A19 Pore water chemistry are not dealt with in this report]

6(c) FUTURE RESEARCH NEEDS

The above comments reflect the status of our knowledge of the KTF study area. Two cruises during 1983 greatly extend our knowledge of the area.

RRS Discovery cruise 134 will concentrate upon station work and extension of the 3.5 kHz profiling coverage. Clearly, precise sampling and near-bottom (profiler and camera) surveys are a priority over the areas of suspected slumping and/or erosion. More heat flow data are required, as are further cores for geotechnical studies. In addition to the camera studies over anomalous (sedimentary?) features, more information should become available from camera and deep-towed profiler stations on the extent of glacial boulder occurrences.

An IPOD drillsite, proposed site "NA-3A", is planned during the 1983 "Glomar Challenger" drilling transect in the North Atlantic (Figure 42). The drilling at "NA-3A" will examine (1) climatic fluctuations close to King's Trough over the past five to six million years; and (2) the tectonic history of the King's Trough complex for comparison with that inferred from dredge and rock core sampling. A great deal of information will emanate from the drilling of this site relevant to the KTF study area.

The site is to be located at 42°49.6'N; 23°03.8'W, at the location of gravity core S8/79/8. A complete sediment sequence is to be drilled to basement at around 600-metres depth. Potentially, the high-resolution stratigraphy such as has been derived from the gravity core (the last 190 thousand years) can be extended to the late Miocene, i.e. five million years, and a stratigraphy with less resolution will be available to the Eocene (~54 million years). The dating of reflectors at the site will enable calibration of our seismic profiles across the area. Samples for geotechnical and geochemical studies will become available from depths beyond the reach of our piston-coring and on to well over twice the anticipated burial depth for shallow disposal of ~30 metres.

Should the KTF study area remain under consideration for high-level radioactive waste disposal following these investigations, our major research need will still be to sample the most appropriate parts of the area at greater depth than is possible by conventional piston coring. Clearly, it is not possible to project easily many of our geological findings in the late Quaternary sediment cover even to the depth envisaged for shallow disposal.

7. CONCLUSIONS

Investigations of the suitability of the KTF study area for HLRW disposal have reached the stage where the 1983 field studies in the area could allow us to provide positive answers to many of the site selection requirements outlined in Searle, 1979.

Principally, an apparent conflict of the geophysical and sediment core data must be resolved, data on the distribution of ice-rafted material must be collected, and the cause of a non-linear temperature profile within the uppermost sediment cover must be investigated.

At this stage, the stability of the surface sediment cover is in question and sediment erosion by currents could be a possibility. Whether either is of a sufficient scale to affect seabed disposal options is at present unknown.

We are very conscious of our lack of sampling or measurement at the anticipated depth (possibly at least 30 metres) for shallow disposal. A drilling site planned in the IPOD programme for 1983 on the northern edge of KTF should increase our general knowledge of the total sediment cover, but many research needs relevant to the disposal studies will remain unfulfilled without further sampling below that possible with conventional piston coring.

8. ACKNOWLEDGEMENTS

We wish to acknowledge the persistent efforts of the Masters, officers, crew and other shipboard scientists aboard RRS "Shackleton", RRS "Discovery" and MV "Farnella" in helping us to obtain the data and samples that make up this report. Dutch colleagues at the Geological Survey of the Netherlands are thanked for collecting (aboard MV "Tyro") the piston cores and 3.5 kHz records. E.A. Hailwood and S. Robinson are acknowledged for providing some unpublished data from their palaeomagnetic studies and R. Dickson for unpublished current meter data.

N.J. Shackleton, L.M. Parson, T.J.G. Francis and S.G. Carlyle provided useful critical reviews. Amanda Bates, a cartographic student based at IOS for one year, drafted almost all of the figures presented here and Gabrielle Mabley patiently typed the many iterations of the text.

9. REFERENCES

- ANDERSON, R.N., LANGSETH, M.G. and SCLATER, J.G., 1977. The mechanisms of heat transfer through the floor of the Indian Ocean. *J. Geophys. Res.*, 82, 3391-3409.
- ANDERSON, R.N., HOBART, M.A. and LANGSETH, M.G., 1979. Geothermal convection through oceanic crust and sediments in the Indian Ocean. *Science*, 204, 828-832.
- ANONYMOUS, 1978. Oceanography related to Deep-Sea Waste Disposal. Institute of Oceanographic Sciences Report No. 77, 261 pp., unpublished manuscript.
- ANONYMOUS, 1982. Ocean Disposal of Radioactive Waste, an initial study into Penetrator shape and size for emplacement in Deep Ocean Sediments. Ove Arup and Partners - Report to Department of the Environment: No. DOE/RW/82-102.
- BATES, R.L. and JACKSON, J.A. (Editors), 1980. Glossary of Geology, 2nd edition. Amer. Geological Institute, Falls Church, Virginia, 749 pp.
- BARRON, E.J. and WHITMAN, J.M. Oceanic sediments in space and time. In: The Oceanic Lithosphere: The Sea, Volume 7, C. Emiliani (Editor), J. Wiley and Sons, New York, 689-731.
- BELDERSON, R.H., KENYON, N.H. and WILSON, J.B., 1973. Iceberg plough marks in the Northeast Atlantic. *Palaeogeography, Palaeoclimatology, Palaeoecology*, 13, 215-254.
- BOUMA, A.H., 1962. Sedimentology of some flysch deposits. Elsevier Publ. Co., Amsterdam, 168 pp.
- BOUMA, A.H., 1964. Notes on the X-ray interpretation of marine sediments. *Marine Geology*, 2, 278-309.
- BOUMA, A.H., 1969. Methods for the study of sedimentary structures. John Wiley, New York. 458 pp.
- BOUMA, A.H. and HOLLISTER, C.D., 1973. Deep Ocean Basin Sedimentation. In: "Turbidites and Deep Water Sedimentation". SEPM Short Course Lecture Notes, Anaheim, 79-118.
- BOYCE, R.E. and BODE, G.W., 1972. Carbon and carbonate analyses, Leg 9, Deep Sea Drilling Project. In: Hays, J.D. et.al., Initial Reports Deep Sea Drilling Project, Vol. IX, Washington (U.S. Government Printing Office) 797-816.
- BREDEHOEFT, J.D. and PAPADOPULOS, I.S., 1965. Rates of vertical groundwater movement estimated from the earth's thermal profile. *Water Resour. Res.*, 1, 325-328.

- BRYANT, W.R., DEFLACHE, A.P. and TRABANT, P.K., 1974. Consolidation of Marine Clays and Carbonates. In: Deep Sea sediments, physical and mechanical properties, Inderbitzen, A.L., (Editor), Plenum Press, N.Y., pp. 209-244.
- BUCHAN, S., DEWES, F.C.D., JONES, A.S.G., McCANN, D.M. and TAYLOR SMITH, D., 1971. The Acoustic and Geotechnical Properties of North Atlantic Cores. Univ. Coll. North Wales, Menai Bridge, Marine Science Labs., Geological Report No. 71-1, 200 pp.
- BULLARD, E.C., 1954. The flow of heat through the floor of the Atlantic Ocean. Proc. R. Soc., London, A222, 408-429.
- BURNS, R.E., 1963. A note on some possible misinformation from cores obtained by piston-type coring devices. J. Sediment. Petrol., 33, 950-952.
- CANN, J.R. and FUNNELL, B.M., 1967. Palmer Ridge: a section through the upper part of the ocean crust? Nature, 213, 661-664.
- CREAGER, J.S. and STERNBERG, R.W., 1963. Comparative evaluation of three techniques of pipette analysis. Jour. of Sed. Petrol., 33, 462-466.
- CROWLEY, T.J., 1981. Temperature and circulation changes in the eastern North Atlantic during the last 150,000 years: evidence from the planktonic foraminiferal record. Marine Micropaleontology, 6, 97-129.
- DAMUTH, J.E., 1980. Use of high-frequency (3.5-12 kHz) echograms in the study of nearbottom sedimentation processes in the deep sea: a review. Marine Geology, 38, 51-75.
- DUNN, D.A., 1980. Revised techniques for quantitative calcium carbonate analysis using the "Karbonat-Bombe" and comparisons to other quantitative carbonate analysis methods. Journ. Sed. Petrology, 50, 631-636.
- EDWARDS, A.M., 1883. L'expédition du Talisman faite dans l'Océan Atlantique. Bull. Ass. sci. Fr., (2) 7, 138-139 pp.
- EMBLEY, R.W., 1976. New evidence for the occurrence of debris flow deposits in the deep sea. Geology, 4, 371-374.
- EMBLEY, R.W., 1982. Anatomy of some Atlantic Margin sediment slides and some comments on ages and mechanisms. In: Marine slides and other mass movements, Saxov, S. and Nieuwenhuis, J.K. (Editors), Plenum Publishing Co., New York, 189-213.
- FLOOD, R.D., 1978. Studies of deep-sea sedimentary microtopography in the North Atlantic Ocean. Woods Hole Oceanographic Institution, Doctoral dissertation WHOI-78-64, unpublished manuscript, 395 pp.
- FRANCIS, T.J.G. et al., 1981a. Geology and geophysics in the Northeast Atlantic and on the Mid-Atlantic Ridge. Institute of Oceanographic Sciences Cruise

- Report No. 110, 9 pp., (unpublished manuscript).
- FRANCIS, T.J.G. et al., 1981b. Geophysics and sediment sampling in the North East Atlantic. IOS Cruise Report No. 117, 33 pp., (unpublished manuscript).
- GARTNER, S. and EMILIANI, C., 1976. Nannofossil biostratigraphy and climate stages of the Brunhes epoch. *Bull. Am. Assoc. Petr. Geol.*, 60, 1562-64.
- GRIMAUD, S., BOILLOT, G., COLLETTE, B., MAUFFRET, A., MILES, P.R. and ROBERTS, D.G., 1982. Western extension of the Iberian-European plate-boundary during the early Cenozoic (Pyrenean) convergence: a new model. *Marine Geology*, 45, 63-77.
- HOLLISTER, C.D., ANDERSON, D.R. and TALBERT, D.M., 1976. The first international workshop on seabed disposal of high-level wastes. Proceedings of the International Symposium on the Management of Wastes from the LWR Fuel Cycle, July 11-16, 1976, Denver, Colorado, 637-657.
- HOLLISTER, C.D., FLOOD, R. and McCAYE, I.N., 1978. Plastering and decorating in the North Atlantic. *Oceanus*, 21, 5-13.
- HSU, K., MONTADERT, L., et al., 1978. Initial reports of the Deep Sea Drilling Project, Vol. 42, Part 1. Washington (U.S. Government Printing Office), 1249 pp.
- INMAN, D.L., 1952. Measures for describing the size distribution of sediment. *Jour. Sed. Petrology*, 22, 125-145.
- JACOBI, R.D., 1976. Sediment slides on the north-western continental margin of Africa. *Marine Geology*, 22, 157-173.
- JESSOP, A.M., HOBART, M.A. and SCLATER, J.G., 1976. The world heat flow data collection - 1975. Geothermal Series No. 5. Energy, Mines and Resources, Ottawa, Canada.
- KIDD R.B., 1982. Long-range sidescan sonar studies of sediment slides and the effects of slope mass-sediment movement. In: Marine Slides and other mass movements, S. Saxov and J.K. Nieuwenhuis (editors), Plenum Press, New York and London, 289-303.
- KIDD, R.B. and DAVIES, T.A., 1978. Indian Ocean sediment distribution since the Late Jurassic. *Marine Geology*, 26, 49-70.
- KIDD, R.B. and ROBERTS, D.G., 1982. Long-range sidescan sonar studies of large-scale sedimentary features in the North Atlantic. *Bull. Inst. Geol. Basin d'Aquitaine, Bordeaux*, 31, 11-29.
- KIDD, R.B., SEARLE, R.C., RAMSAY, A.T.S., PRICHARD, H. and MITCHELL, J., 1982. The geology and formation of King's Trough, Northeast Atlantic Ocean.

- Marine Geology, 48, 1-30.
- KIDD, R.B. and SEARLE, R.C. Sedimentation in the southern Cape Verde Basin: regional observations by long-range sidescan sonar. In: Fine-grained sediments, D.A. Stow & D.J. Piper (Editors), Geological Society of London Special Publication, in press.
- KIPP, N.G., 1976. New transfer function for estimating past sea-surface conditions from sea-bed distribution of planktonic foraminiferal assemblages in the North Atlantic. Geol. Soc. Am. Mem., 145, 3-42.
- KOMINZ, M.A., HEATH, G.R., KU, J-L. and PISIAS, N.G., 1979. Brunhes time scale and the interpretation of climate change. Earth Planet. Sci. Lett., 45, 394-410.
- KRUMBEIN, W.C., 1936. Application of logarithmic moments to size frequency distribution of sediments. Jour. Sed. Petrology, 11, 64-72.
- KUIPERS, A., 1981. The sedimentology of two Northeast Atlantic Study Areas: the western Madeira Abyssal Plain and the area west of Great Meteor Seamount: Progress Report 1981. Rijks Geologische Dienst Internal Report, 61 pp.
- LACHENBRACH, A.M., 1968. Rapid estimation of the topographic disturbance to superficial thermal gradients. Rev. Geophys., 6, 365-400.
- LAMBE, T.W. and WHITMAN, R.V., 1979. Soil mechanics. John Wiley, N.Y., 553 pp.
- LAUGHTON, A.S., 1981. The first decade of GLORIA. Jour Geophys. Res., 86, 11511-11534.
- LAUGHTON, A.S., ROBERTS, D.G. and GRAVES, R., 1975. Bathymetry of the northeast Atlantic: Mid-Atlantic Ridge to southwest Europe. Deep Sea Research, Vol. 22, 791-810.
- LAUGHTON, A.S. and SEARLE, R.C., 1980. Tectonic processes on slow spreading ridges. In: Deep Drilling Results in the Atlantic Ocean crust, Talwani, M., Harrison, C.G. and Hayes, D.E. (Editors), Maurice Ewing series, Amer. Geophys. Union, Washington D.C., 2, 15-32.
- LILWALL, R.C., 1982. Intraplate seismicity and seismic risk in the Atlantic Ocean based on teleseismically observed earthquakes. Institute of Oceanographic Sciences, Report No. 136, 40 pp., (unpublished manuscript).
- LISTER, C.R.B., 1979. The pulse-probe method of conductivity measurement. Geophys. J., 57, 451-461.
- LIZITZIN, A.P., 1972. Sedimentation in the World Ocean. Soc. Econ. Paleontologists and Mineralogists. Spec. Publ., 17, SEPM, Tulsa, 218 pp.

- LOWRIE, W. and ALVAREZ, Z.W., 1981. One hundred million years of geomagnetic polarity history. *Geology*, 9, 392-397.
- McINTYRE, A., KIPP, N.G., BE, A.W.H., CROWLEY, T., KELLOG, T., GARDNER, J.V., PRELL, W. and RUDDIMAN, W.F., 1976. Glacial north Atlantic 18,000 years ago: A CLIMAP reconstruction. *Geol. Soc. Amer. Memoir.*, 145, 43-76.
- McINTYRE, A., RUDDIMAN, W.F. and JANTZEN, R., 1972. Southward penetrations of the North Atlantic Polar Front: faunal and floral evidence of large-scale surface water mass movements over the last 225,000 years. *Deep Sea Research*, 19, 61-77.
- MANSURE, A.J. and REITER, M., 1979. A vertical groundwater movement correction for heat flow. *J. Geophys. Res.*, 84, 3490-3496.
- MATTHEWS, D.H., LAUGHTON, A.S., PUGH, D.J., JONES, E.J.W., SUNDERLAND, J., TAHIN, M. and BACON, M., 1969. Crustal structure and origin of Peake and Freaan Deeps, N.E. Atlantic. *Geophys. J.R. astr. Soc.*, 18, 517-542.
- MILLER, D.G. and RICHARDS, A.F., 1969. Consolidation and sedimentation-compression studies of a calcareous core, Exuma Sound, Bahamas. *Sedimentology*, 12, 301-316.
- MÜLLER, G., 1961. Die Rezenten Sedimente im Golf von Neapel 2: Mineral-neeundumbildungen in den rezenten sedimenten des Golfes Pozzuoli. Ein Beitreig zur Umwandlung vulcanischer Gläser durch Hamyolyse. *Beiträge zur Mineralogie und Petrographie*, 8, 1-20.
- MÜLLER, G. and GASTNER, M., 1971. The Karbonate-Bombe: a simple device for the determination of the carbonate content in sediment soils and other materials. *N. Jhrb. Miner., Mk.* 10, 466-469.
- MÜLLER, T.J., 1981. Current and temperature measurements in the northeast Atlantic during NEADS. *Berichte aus dem Institut für Meereskunde. Christian-Albrechts-Universität, Kiel*, No. 90, 98 pp.
- NOEL, M., in press. Origins and significance of non-linear temperature profiles in deep-sea sediments. *Geophys. J.*
- OLAUSSON, E., 1960. Description of sediment cores from the North Atlantic. *Reports of the Swedish Deep Sea expedition 1947-1948. Vol. 7, part 5*, 229-286.
- PISIAS, N.G. and MOORE, T.C., 1981. The evolution of Pleistocene climate: a time series approach. *Earth Planet. Sci. Lett.*, 52, 450-458.
- PUJOL, C., 1980. Les foraminifères planctoniques de l'Atlantique nord au Quaternaire: ecologie - stratigraphie - environnement. *Memoires de l'institut de Geologie du Bassin d'Aquitaine*, No. 10, 1-254.

- RAMPINO, M.R., 1981. Revised age estimates of Brunhes Palaeomagnetic events: support for a link between geomagnetism and eccentricity. *Geophys. Res. Lett.*, 8, 1047.
- RAMSAY, A.T.S., 1970. The pre-Pleistocene stratigraphy and palaeontology of the Palmer Ridge area, N.E. Atlantic. *Marine Geology*, 9, 261-285.
- REES, A.I., 1965. The use of anisotropy of magnetic susceptibility in the estimation of sedimentary fabric. *Sedimentology*, 4, 257-271.
- RICHARDS, A.F., 1961. Investigations of deep-sea sediment cores. I: Shear strength, bearing capacity and consolidation. U.S. Navy Hydrographic Office Tech. Rept. No. 63, 70 pp.
- ROBERTS, D.G. and JONES, M.T., 1979. Magnetic anomalies in the north-east Atlantic. Sheets 1 and 2. Institute of Oceanographic Sciences Chart.
- ROBERTS, D.G. and KIDD, R.B., 1979. Abyssal sediment wave fields on Feni Ridge, Rockall Trough: long-range sonar studies. *Marine Geology*, 33, 175-191.
- RUDDIMAN, W.F., 1977. Late Quaternary deposition of ice-rafted sand in the sub-polar North Atlantic (Lat. 40° to 65°N). *Geol. Soc. Am. Bull.*, 88, 1813-1827.
- RUDDIMAN, W.F. and GLOVER, L.K., 1972. Vertical mixing of ice-rafted volcanic ash in North Atlantic sediments. *Geol. Soc. Am. Bull.*, 83, pp. 2817-2836.
- RUDDIMAN, W.F. and McINTYRE, A., 1976. Northeast Atlantic paleoclimatic changes over the past 600,000 years. In: Investigations of Late Quaternary Paleoceanography and Paleoclimatology, Cline, R.M. and Hayes, J.D. (Editors), *Geol. Soc. Amer., Memoir 145*, 111-146.
- RUDDIMAN, W.F. and McINTYRE, A., 1981. The North Atlantic Ocean during the last deglaciation. *Palaeogr., Palaeoclimatol., Palaeoecol.*, 35, pp. 145-214.
- SAUNDERS, P.M., 1982. Circulation in the Eastern North Atlantic. *Journ. Mar. Res.*, 40, 641-657.
- SCHULTHEISS, P.J., WEAVER, P.P.E. and PRICE, M.C. Electro-osmotic core cutting. In preparation.
- SCLATER, J.G., LAWYER, L.A. and PARSONS, B., 1975. Comparison of long-wavelength residual elevation free-air gravity anomalies in the North Atlantic and possible implications for the thickness of the lithospheric plate. *J. Geophys. Res.*, 80, 1031-1052.
- SEARLE, R.C., 1977. Geophysical studies of the Atlantic Seafloor near 40°N, 24°W and its relation to King's Trough and the Azores. *Marine Geology*, 25, 299-320.
- SEARLE, R.C., 1979. Guidelines for the selection of sites for disposal of

- radioactive waste on or beneath the ocean floor. Institute of Oceanographic Sciences, Report No. 91, 44 pp., (unpublished manuscript).
- SEARLE, R.C. and WHITMARSH, R.B., 1978. The structure of King's Trough, Northeast Atlantic from bathymetric, seismic and gravity studies. *Geophys. J.R. astr. Soc.*, 53, 259-287.
- SHACKLETON, N.J., 1969. The last interglacial in the marine and terrestrial records. *Proc. Roy. Soc. Lond.*, B, 174, 135-154.
- SHAW, A.B., 1964. *Time in stratigraphy*. McGraw-Hill, New York, 365 pages.
- SIBUET, J.C. and LE PICHON, X., 1971. Structure gravimétrique de Golfe de Gascogne et le fosse marginal nord-espagnol. In: Histoire Structural du Golfe de Gascogne, pp. VI.9.1 - VI.9.18. Technip, Paris.
- SIGURDSSON, H. and CAREY, S.N., 1981. Marine tephrochronology and Quaternary explosive volcanism in the lesser Antilles Arc. In: *Tephra Studies* (proceedings of the NATO advanced study institute "Tephra studies as a tool in Quaternary research" held in Lavgarvatn and Reykjavik, Iceland, 18-29 June 1980), D. Reidel Publishing Co., Dordrecht, Holland, pp. 255-280.
- SIMM, R.W. and KIDD, R.B.. Submarine debris flow deposits detected by long-range sidescan sonar 1000 km from source. *Geo-Marine Letts.* (in press).
- SOMERS, M.L., CARSON R.M., REVIE, J.A., EDGE, R.H., BARROW, B.J. and ANDREWS, A.G., 1978. GLORIA II: an improved long-range sidescan sonar. *Ocean. Int.*, 78, London, 16-24.
- SOUTHARD, J.B., YOUNG, R.A. and HOLLISTER, C.D., 1971. Experimental erosion of calcareous ooze. *Jour. Geophys. Res.*, 76, 5903-5909.
- STEBBINS, J. and THOMPSON, G., 1978. The nature and petrogenesis of intra-oceanic plate alkaline eruptive and plutonic rocks: King's Trough, Northeast Atlantic. *J. Volcanol. Geotherm. Res.*, 4, 333-361.
- SVERDRUP, H.U., JOHNSON, M.V. and FLEMMING, R.H., 1942. The Oceans, their physics, chemistry and general biology. Prentice-Hall, Engelwood Cliffs, N.J., 1987 pp.
- TRASK, P.D., 1932. *Origin and Environment of Source Sediments of Petroleum*. Amer. Petrol. Institute, Gulf Publ., Houston, Texas, 323 pp.
- U.S. NAVY OCEANOGRAPHIC OFFICE, 1968. Ice. Publication No. 700, 111 pp.
- VAN ANDEL, T., 1975. Mesozoic/Cenozoic Calcite Compensation Depth and the Global Distribution of Calcareous Sediments. *Earth Planet. Sci. Letts.*, 26, pp. 187-194.
- WEAVER, P.P.E., 1983. An integrated stratigraphy of the upper Quaternary of the

- King's Trough Flank area, N.E. Atlantic. *Oceanologica Acta*, in press.
- WEAVER, P.P.E. and SCHULTHEISS, P.J., 1983. Vertical open burrows in deep-sea sediments, 2m in length. *Nature*, 301, 329-331.
- WEAVER, P.P.E. and SCHULTHEISS, P.J., 1983. Detection of repenetration and sediment disturbance in open barrel gravity cores. *Jour. Sed. Petrology*, 53, 649-654.
- WHITMARSH, R.B., GINSBURG, A. and SEARLE, R.C., 1982. The structure and origin of the Azores-Biscay Rise, Northeast Atlantic Ocean. *Geophys. J.R. astr. Soc.*, 10, 79-107.
- ZIMMERMAN, H.B., 1982. Fine-grained sediment distribution in the late Pleistocene/Holocene, North Atlantic. *Bull. Inst. Geol. Bassin d'Aquitaine, Bordeaux*, 337-357.

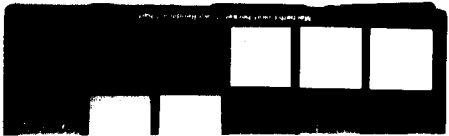
APPENDIX I - Geophysical data charts of the KTF study area held at IOS (to December 1982)

DATA	SCALE	COMMENTS
Contoured bathymetry	One to half million	To July 1982
Contoured bathymetry	One to quarter million	To July 1982
Soundings N. Sheet	One to quarter million	No "Farnella" 9 data included
Soundings S. Sheet	One to quarter million	No "Farnella" 9 data included
Soundings: All Discovery Cruises	One to half million	
Soundings from 'GEBCO' sheet	One to half million	
Tracks	One to half million	Includes "Farnella" and "Tyro" tracks.
Tracks	One to quarter million	22.5°-24.5°W, 41°-42.5°N
10 kHz profiles: Interpretation	One to half million	
2 kHz and 3.5 kHz profiles: Interpretation	One to half million	
Microtopography	One to half million	With locations of hyperbolae and GLORIA coverage
Sampling locations	One to half million	Including "Tyro" cores
Annotated sediment thickness N. Sheet	One to quarter million	
Annotated sediment thickness S. Sheet	One to quarter million	
Annotated sediment thickness	One to half million	
Contoured isopachs	One to half million	With GLORIA coverage and fault scarp interpretation
Annotated depth to basement	One to half million	
Contoured depth to basement	One to half million	With GLORIA coverage
Contoured depth to basement	One to quarter million	With GLORIA coverage
Master seismic reflection profile tracks	One to one million	Pre-"Farnella" 9 and "Tyro" cruises

APPENDIX I - continued

DATA	SCALE	COMMENTS
Digitised SRP profiles projected at 045°	One to quarter million	Two sheets
Digitised SRP profiles projected at 000°	One to quarter million	No "Tyro" data
Digitised SRP profiles projected at 270°	One to quarter million	" " "
Digitised SRP profiles projected at 315°	One to quarter million	" " "
Digitised SRP profiles projected at 000°	One to half million	No "Tyro" or "Farnella" 9 data
Digitised SRP profiles projected at 270°	One to half million	" " "
Farnella: GLORIA data, Fixed and AGC	One to quarter million	
Farnella: GLORIA data, Fixed and AGC: IPOD site survey	One to quarter million	
Farnella: GLORIA data, Interpretation	One to quarter million	
Farnella: GLORIA data, Interpretation	One to half million	
Annotated magnetic anomalies	One to half million	
Magnetic anomalies contoured	One to half million	After Roberts and Jones, 1979.
Magnetic anomalies profiles	One to half million	
Along-track presentation of "Farnella" 9; SRP, Magnetic Anomalies, Profiles and GLORIA		One sheet
Along-track presentation of Discovery 118; SRP, Magnetic Anomalies, Profiles and Grav profiles		Three sheets

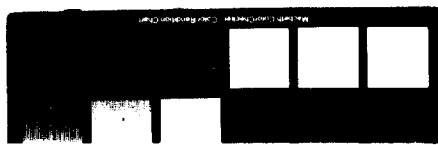
APPENDIX II - COLOUR PHOTOGRAPHS OF SPLIT SECTIONS OF THE KING'S TROUGH FLANK
PISTON CORES: 82PCS01, 02 and 04. Tapes laid alongside show a
centimetre scale. The top of the core begins with section one in
upper left of each photograph and the split sections are laid
sequentially left to right so that the base of core is lower right.

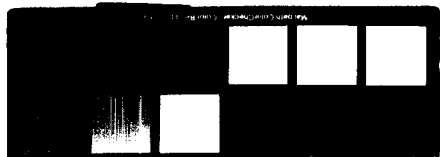


82 PCSO1



82 PCS02





APPENDIX III - Sub-samples taken from the KTF cores

	Grain Size	Oxygen Isotope	Forams	CaCO ₃	XRD	Mineral Magnetism	Magnetics (fabric)	Uranium Thorium	Coccoliths	Smear Slides
S8.79.1	8	25	23	25	6	125	-	11	21	18
S8.79.2	9	30	23	25	8	127	-	12	26	17
S8.79.3	13	40	28	36	12	107	-	-	48	27
S8.79.4	9	46	21	26	8	126	-	-	29	16
S8.79.5	10	49	28	25	8	123	43	-	24	11
S8.79.6	8	19	17	19	6	100	-	-	20	11
S8.79.7	10	29	21	26	9	140	-	-	30	31
S8.79.8	9	26	26	19	12	130	-	12	26	14
D9806	-	7	7	7	-	-	-	-	-	7
D9812	-	13	14	12	-	59	-	-	-	15
D10333	6	18	18	18	6	-	-	-	9	9
82PCS01	-	88	87	87	-	-	-	-	44	25
82PCS02	-	34	86	86	-	-	-	-	48	28
82PCS04	30	-	92	97	30	-	-	-	49	26
Total Samples	112	424	491	508	105	1037	43	35	374	255

APPENDIX IV - Grain Size Results from KTF gravity cores analysed at IOS Taunton.

Depth below top of core (cm)	% Sand*	% Silt*	% Clay*	Md ϕ ⁺
<u>Core 1 (S8.79.1)</u>				
26	21.40	25.60	53.00	8.25
56	21.79	25.20	53.01	8.25
86	20.20	21.00	58.80	9.00
116	22.78	23.45	53.77	8.25
145	27.30	22.70	50.00	8.00
176	16.04	29.04	54.92	8.63
206	13.14	72.96	13.0	5.75
236	20.75	24.47	54.78	8.37
<u>Core 2 (S8.79.2)</u>				
3	25.54	24.64	49.84	8.00
26	16.99	32.83	50.21	8.00
56	22.20	26.49	51.28	8.00
86	20.96	15.13	63.90	9.00+
116	23.44	24.82	51.72	8.25
146	26.00	18.03	55.97	8.86
176	13.62	29.61	56.77	8.65
200	25.68	21.73	52.61	8.25
236	22.32	20.54	57.14	9.00
<u>Core 3 (S8.79.3)</u>				
3	26.13	24.42	49.45	8.00
33	26.91	30.53	42.50	7.30
63	21.59	19.73	58.65	9.25
93	19.60	22.35	58.04	9.00
123	24.22	22.38	53.39	8.50
153	20.57	28.58	50.85	8.00
183	20.50	19.88	59.62	9.00
213	54.32	17.79	27.87	3.90
243	22.97	26.32	50.71	8.00
273	21.18	27.63	51.22	8.25
303	20.79	22.20	57.01	8.80
333	18.22	40.15	41.63	5.75
360	25.04	24.73	50.25	8.00
<u>Core 4 (S8.79.4)</u>				
6	30.02	28.94	41.06	7.50
36	19.07	28.78	52.16	8.25
66	19.69	27.92	52.39	8.25
96	27.02	17.26	55.72	8.50
126	25.71	22.85	51.43	8.25
156	22.59	25.04	52.37	8.25
186	22.96	24.49	52.55	8.25
212	20.67	23.46	55.87	8.75
245	23.52	26.29	50.19	8.00

* Size grade terminology after Inman (1952)

⁺ Md ϕ , a measure of central tendency of the size-frequency distribution (after Inman, 1952);

ϕ = $-\log D$, the particle diameter in millimetres (Krumbein, 1936)

APPENDIX IV - continued

Depth below top of core (cm)	% Sand*	% Silt*	% Clay*	Md ϕ Phi ⁺
<u>Core 5 (S8.79.5)</u>				
2	27.79	21.00	51.16	8.125
32	15.45	29.80	54.74	8.25
62	20.60	25.45	53.94	8.375
92	12.61	25.99	61.38	9.00
122	18.54	19.44	62.04	9.00
152	21.71	20.81	57.48	8.875
182	28.30	17.60	54.12	8.50
212	11.96	35.71	52.32	8.25
238	16.83	35.64	47.52	7.75
242	16.40	32.80	50.82	8.00
<u>Core 6 (S8.79.6)</u>				
4	20.02	29.93	50.05	8.00
14	27.33	23.67	48.96	8.00
44	19.63	27.58	52.80	8.25
74	14.81	29.62	55.54	8.40
104	22.93	30.35	46.72	7.80
134	27.72	21.19	51.09	8.10
164	25.77	19.59	54.63	8.50
194	19.77	30.35	49.87	8.00
<u>Core 7 (S8.79.7)</u>				
5	26.45	23.78	49.79	8.00
35	82.82	8.59	8.60	2.65
65	29.54	26.13	44.30	7.60
95	16.31	27.90	55.79	8.60
125	22.05	36.11	41.82	7.55
155	23.34	21.09	55.54	8.55
185	20.51	29.73	49.76	8.00
215	17.38	25.51	47.22	8.70
245	67.53	12.91	19.58	2.60
275	31.70	23.18	45.11	8.00
<u>Core 8 (S8.79.8)</u>				
20	27.20	28.60	44.20	7.50
50	26.80	26.20	47.00	7.75
80	27.00	20.10	52.90	8.25
108	26.75	29.82	43.43	7.50
140	21.05	27.64	51.31	8.15
170	30.80	40.60	28.60	7.25
200	29.90	23.10	47.00	7.75
230	20.40	17.90	61.70	8.50
260	29.50	20.70	49.80	8.00